

12-1-2014

Effect of Caliche on the Behavior of Drilled Shafts

Rouzbeh Afsharhasani
University of Nevada, Las Vegas, afsharha@unlv.nevada.edu

Follow this and additional works at: <https://digitalscholarship.unlv.edu/thesesdissertations>



Part of the [Civil Engineering Commons](#), and the [Geotechnical Engineering Commons](#)

Repository Citation

Afsharhasani, Rouzbeh, "Effect of Caliche on the Behavior of Drilled Shafts" (2014). *UNLV Theses, Dissertations, Professional Papers, and Capstones*. 2238.
<https://digitalscholarship.unlv.edu/thesesdissertations/2238>

This Dissertation is protected by copyright and/or related rights. It has been brought to you by Digital Scholarship@UNLV with permission from the rights-holder(s). You are free to use this Dissertation in any way that is permitted by the copyright and related rights legislation that applies to your use. For other uses you need to obtain permission from the rights-holder(s) directly, unless additional rights are indicated by a Creative Commons license in the record and/or on the work itself.

This Dissertation has been accepted for inclusion in UNLV Theses, Dissertations, Professional Papers, and Capstones by an authorized administrator of Digital Scholarship@UNLV. For more information, please contact digitalscholarship@unlv.edu.

EFFECT OF CALICHE ON THE BEHAVIOR OF DRILLED SHAFTS

By

Rouzbeh Afsharhasani

Bachelor of Science in Civil Engineering
Iran University of Science and Technology, Iran
2009

Master of Science in Civil Engineering
Sharif University of Technology, Iran
2011

A dissertation submitted in partial fulfillment
of the requirements for the

Doctor of Philosophy in Engineering - Civil and Environmental Engineering

Department of Civil and Environmental Engineering and Construction

Howard R. Hughes College of Engineering

Graduate College

University of Nevada, Las Vegas

December 2014

We recommend the dissertation prepared under our supervision by

Rouzbeh Afsharhasani

entitled

Effect of Caliche on the Behavior of Drilled Shafts

is approved in partial fulfillment of the requirements for the degree of

**Doctor of Philosophy in Engineering - Civil and Environmental
Engineering**

Department of Civil and Environmental Engineering and Construction

Moses Karakouzian, Ph.D., Committee Chair

Douglas Rigby, Ph.D., Committee Member

Donald Hayes, Ph.D., Committee Member

Mohamed Kaseko, Ph.D., Committee Member

Ashok Singh, Ph.D., Graduate College Representative

Kathryn Hausbeck Korgan, Ph.D., Interim Dean of the Graduate College

December 2014

ABSTRACT

The current design methodology for a drilled shaft foundation in cohesionless soil is primarily based on ultimate skin friction values of drilled shafts. In order to obtain these values for each soil type, load tests such as Osterberg test are designed and performed. The Osterberg test layout is designed to estimate the capacity of drilled shaft by applying an upward load during the test and then calculating the downward capacity assuming the upward and downward capacity are the same. This method is appropriate for soils not containing caliche layers because caliche layers bond to the shaft and prevent skin friction to reach its ultimate capacity during the load test. As long as ultimate skin friction is achieved, the location of O-cell with respect to any of existing soil layers is not an effective. Osterberg test results in soils containing caliche indicate that the ultimate skin friction is not achieved and shaft/caliche interaction is mostly elastic. In these cases, the behavior of the shaft when it is loaded from the bottom is different from when it is loaded from the top.

This study will show that, the location of O-cell with respect to the caliche layers will influence the interpretation of test results. The study will investigate the current interpretation method when O-cell is installed at a location far from caliche and will compare the equivalent top-down load from test results to when the shaft is loaded from the top. The reason for discrepancies between the behavior of the shaft in these two loading scenario will be explained. Additionally, the interpretation for tests when O-cell is installed close to caliche will be investigated and the behavior of the shaft will be compared for upward and downward loading. The procedure is performed by collecting 30 Osterberg load tests in soils containing caliche. The test

layouts with O-cell installed at identified locations are selected. The 2-D finite element software PLAXIS 8 is then used to simulate the Osterberg tests. The models are calibrated using field Osterberg tests and then loaded conventionally from the top. The behavior of the shaft during top-down loading is compared to interpreted test results from Osterberg test.

A test layout with O-cell at a location far from the caliche layers shown to have a higher capacity during conventional loading compared to interpreted test results from Osterberg load test. On the other hand when O-cell is installed close to caliche, the top-down loading shows a similar behavior to interpreted test results from Osterberg load test. In fact when O-cell and caliche layers are close to each other, the test layout is similar to the procedure performed to estimate rock socketed drilled shafts capacity.

The results of this study will help engineers to have better understanding of the drilled shafts behavior in soils containing caliche by introducing an appropriate test design and interpretation of the test results.

ACKNOWLEDGEMENTS

I would never have been able to finish my dissertation without the guidance of my advisor, help from friends, and support from my family. I would like to express my deepest gratitude to my advisor, Dr. Moses Karakouzian, for his excellent guidance, caring, patience, and providing me with an excellent atmosphere for doing research. I would like to thank Dr. Rigby, who guided me through this research selflessly and introduce me to practical issues beyond the textbooks. Special thanks go to who was willing to participate in my final defense committee including my friends and colleagues from KLEINFELDER.

I would like to thank Dr. Avishan Nasiri, my love. She has been supporting me the entire time I was working on this dissertation and helped me forget I was far away from home by creating a new home for me.

Last but not least, I am grateful for having an amazing family, my sister, Romina Afshar and my mom, Sheri Shahmalekpour. They have always been the inspiration of my life helping me through all my successes, as little as they may be.

This dissertation is dedicated to my mom and dad. They encouraged me to pursue a career in engineering and I am very thankful for their love and support. I love you!

Sincerely,

Rouzbeh Afsharhasani

TABLE OF CONTENTS

ABSTRACT	III
ACKNOWLEDGEMENTS.....	V
TABLE OF CONTENTS	VI
LIST OF TABLES.....	X
LIST OF FIGURES.....	XI
LIST OF SYMBOLS	XIII
1 INTRODUCTION.....	1
1.1 SCOPE OF RESEARCH PROJECT	3
1.2 RESEARCH OBJECTIVES	3
1.3 ORGANIZATION	4
2 GEOLOGY OF LAS VEGAS.....	6
2.1 LAS VEGAS CALICHE.....	6
2.2 CLASSIFICATION.....	7
2.3 CALICHE IMPACT ON FOUNDATION DESIGN.....	9
3 AXIAL CAPACITY OF DRILLED SHAFTS IN ROCK SOCKETS	10
3.1 SIDE RESISTANCE OF ROCK SOCKETS	10

3.1.1	ROCK/SHAFT JOINT STIFFNESS	15
3.2	BASE RESISTANCE OF ROCK SOCKETS	16
3.3	SUMMARY	18
4	LOAD TEST.....	19
4.1	CONVENTIONAL TOP-DOWN TEST	19
4.1.1	CONVENTIONAL LOAD TESTS IN CALICHE	21
4.2	BI-DIRECTIONAL LOAD TEST (OSTERBERG TEST).....	22
4.2.1	ELASTIC SHORTENING.....	26
4.2.2	DISADVANTAGEOUS OF OSTERBERG TEST METHOD	27
4.2.2.1	Current Practice for Interpretation of Osterberg tests.....	29
4.2.3	OSTERBERG TEST IN LAS VEGAS	32
4.2.4	OSTERBERG LOAD TESTS IN LAS VEGAS	32
4.2.4.1	O-cell above Caliche.....	34
4.2.4.2	O-cell between Caliche Layers.....	35
4.2.4.3	O-cell Under the Caliche (Close to Caliche)	35
4.2.4.4	O-cell Under the Caliche (Far from Caliche)	36
4.2.5	REFERENCE BEAM READINGS.....	38
4.3	VALIDITY OF LOAD TEST DATA.....	39
5	FINITE ELEMENT MODELING AND ANALYSIS.....	43
5.1	FINITE ELEMENT REPRESENTATION	43
5.2	CONSTITUTIVE MODELS	44
5.2.1	DRILLED SHAFT CONCRETE.....	44
5.2.2	SOIL LAYERS.....	45
5.3	INTERFACE MODEL	45

5.4	FINITE ELEMENT MATERIAL COLOR	46
5.5	THE EFFECT OF O-CELL LOCATION ON THE INTERPRETATION OF TEST	47
5.5.1	RESULTS AND DISCUSSION	50
6	CASE HISTORY ANALYSIS	51
6.1.1	CASE HISTORY I: CALICHE AT THE FURTHEST LOCATION FROM O-CELL.....	51
6.1.1.1	Step-1: Calibration and back analysis for Osterberg Test.....	53
6.1.1.2	Step-2: Material Properties and Soil Profile	56
6.1.1.3	Step 3: Conventional Loading	58
6.1.1.4	Load Transfer Curve.....	58
6.1.1.5	t-z Curve.....	60
6.1.1.6	Equivalent Load-Settlement Curve	62
6.1.2	CASE HISTORY II: CALICHE CLOSE TO O-CELL	63
6.1.2.1	Step-1: Calibration and back analysis for Osterberg Test.....	65
6.1.2.2	Step-2: Material Properties and Soil Profile	66
6.1.2.3	Step 3: Conventional Loading	68
6.1.2.4	Load Transfer Curve.....	69
6.1.2.5	t-z Curve.....	70
6.1.2.6	Equivalent Load-Settlement Curve	72
6.1.3	RESULTS AND DISCUSSION	73
7	CONCLUSIONS AND RECOMMENDATIONS.....	77
7.1	RECOMMENDATIONS FOR FURTHER RESEARCH.....	78
APPENDIX A	80

APPENDIX B.....	95
APPENDIX C	103
APPENDIX D	118
REFERENCE	122
CURRICULUM VITAE.....	128

LIST OF TABLES

Table 2-1 : Classification and Drilling/Sampling	8
Table 3-1: Unit Skin Friction Coefficients in Rock.....	12
Table 3-2: Adjustment of f_s for Presence of Soft Seams (M. O'Neill et al., 1996).....	14
Table 3-3: Base Resistance of Rock Sockets	17
Table 7-2: Reference Beam Movement	38
Table 5-1: Friction Angle for Mass Concrete against Soil (NAVFAC, 1982)	46
Table 5-2: Color Guide for PLAXIS material	47
Table 5-3: Material Properties for Sensitivity Case I	48
Table 6-1: PLAXIS Material Properties for I-215 and Airport Connector	57
Table 6-2: PLAXIS Material Properties for Palm	67

LIST OF FIGURES

Figure 1-1 Monolith Behavior of Deep Foundation System _____	2
Figure 3-1: Interface dilation of an unbounded rock-concrete _____	10
Figure 4-1: Conventional Static Load Test on a Drilled Shaft _____	20
Figure 4-2: O-cell Installation in a Drilled Shaft (Caltrans, 1998) _____	23
Figure 4-3: Osterberg Load Test _____	24
Figure 4-4: Typical bi-directional load test results after (J. O. Osterberg, 1998) _____	24
Figure 4-5: Equivalent top loaded settlement curve after (J. O. Osterberg, 1998) _____	25
Figure 4-6: Average Compressive Load in Shaft During Top Down and O-Cell Loading (Brown et al., 2010) _____	28
Figure 4-7: Load – Displacement Behavior for Interpreted test data from Osterberg test and conventional loading (Kwon et al., 2005) _____	30
Figure 4-8: Different Osterberg Test Layouts in Las Vegas _____	33
Figure 4-9: O-cell Load-Movement Curve _____	34
Figure 4-10: O-cell Load-Movement Curve _____	35
Figure 4-11: O-cell Load-Movement Curve _____	36
Figure 4-12: O-cell Load-Movement Curve _____	37
Figure 4-13: Net Unit Shear vs. Upward Average Zone Movement for Echelon TS-2 (LoadTest, 2007) _____	41
Figure 4-14: Load-Movement for Echelon TS-2 (LoadTest, 2007) _____	41
Figure 5-1: Interface Element in PLAXIS model _____	45
Figure 5-2: Osterberg Test with 10 ft. Caliche close to O-cell _____	48
Figure 5-3 Osterberg Test with 10 ft. Caliche far from O-cell _____	49
Figure 5-4: O-cell Location and Comparison of Upward and Downward Settlement _____	50
Figure 6-1: Schematic Section of Test Shaft _____	52
Figure 6-2: PLAXIS Simulations for I-215 and Airport Connector Load Test _____	53

Figure 6-3: Osterberg Test Load- Movement Curve _____	55
Figure 6-4: PLAXIS Simulation for Conventional Head-Down Loading _____	58
Figure 6-5: Load Transfer _____	59
Figure 6-6: t-z Curve between 20 -50 ft. _____	61
Figure 6-7: t-z Curve between 50 -80 ft. _____	61
Figure 6-8: Equivalent Load Settlement Curve for Traditional Method and Proposed Method _____	62
Figure 6-9: Schematic Section of Test Shaft _____	63
Figure 6-10: PLAXIS Simulations for Palm Load Test _____	64
Figure 6-11: Osterberg Test Load- Movement Curve _____	65
Figure 6-12: PLAXIS Simulation for Conventional Head-Down Loading _____	68
Figure 6-13: Load Transfer _____	69
Figure 6-14: t-z Curve between 10 – 20 ft. _____	70
Figure 6-15: t-z Curve between 20-30 ft. _____	71
Figure 6-16: t-z Curve between 30 -40 ft. _____	71
Figure 6-17: Equivalent Load Settlement Curve for Traditional Method and Proposed Method _____	73
Figure 6-18: Developed Side Shear Resistance _____	74
Figure 6-19: Unit Side Resistance and Load-settlement Comparison for O-cell test and Conventional Test (Case I) _____	75
Figure 6-20: Unit Side Resistance and Load-settlement Comparison for O-cell test and Conventional Test (Case II) _____	76

LIST OF SYMBOLS

<u>Symbol</u>	<u>Units</u>	<u>Meaning</u>
C	ksf or psf	Cohesion
C'		Centroid of side resistance
C increment	klb/ft ²	The increase of cohesion per unit depth
C _u	klb/ft ²	Undrained shear strength
D	foot	Diameter of shaft
E	klb/ft ²	Young's modulus
E increment	klb/ft ²	The increase of Young's modulus per unit depth
E _r	klb/ft ²	Mass modulus of rock
FEM		Finite Element Method
f _s	klb/ft ²	Interface shear stress
f _{su}	klb/ft ²	Ultimate skin friction
g		Aperture of the discontinuities
L		Socket length
N _c		Modified bearing capacity factor
OCR		Over consolidation ratio
P _a	klb/ft ²	Atmospheric pressure
q _t	klb/ft ²	Splitting tensile strength of rock core
q _u	klb/ft ²	Unconfined compression strength of core
Q	Kips	Total Load
R _{inter}		Interface Strength Reduction factor
RQD		Rock quality designation
s	inches	Spacing of discontinuities
γ _{unsat}	klb/ft ³	Unsaturated unit weight of soil
γ _{sat}	klb/ft ³	Saturated unit weight of soil
γ _w	klb/ft ³	Unit weight of water
δ		Movement of shaft head
ε		Vertical Strain
ε _{ij}		Cartesian normal strain component
φ	Degree	Friction angle
ψ	Degree	Dilatancy angle
σ _c		Unconfined strength of intact rock

1 Introduction

The general design procedure for drilled shaft foundations in soils is primarily based on ultimate values of drilled shaft skin friction and end bearing capacity. The basic load transfer mechanisms were identified through early research on drilled shafts (O'Neil & Reese, 1973). This method is appropriate for soils in conventional geological settings not containing caliche layers. Caliche is the hard lithification of both fine-grained sediments and sand and gravel through secondary cementation by calcium and magnesium carbonate.

Federal Highway code of design (Brown, Turner, & Castelli, 2010) suggests that, caliche can be treated as sedimentary rock for the purpose of foundation design. Therefore, the design parameters for drilled shafts in rocks are suggested for caliche.

However, the load test results in Las Vegas indicate that the shaft and the caliche layers may act as a continuous plate attached monolithically to the shaft as shown in Figure 1-1. The shaft/caliche bond is very strong and in order to be broken a large amount of load is needed. Caliche layers are usually underlain by weak soils. The strength of caliche/shaft bond and the unconventional geological setting may cause the caliche to sustain the load by an additional strength parameter beside side resistance and end bearing. Caliche layers will also bend when loaded and an additional flexural strength may need to be considered for the competent caliche layers in the soil profile.

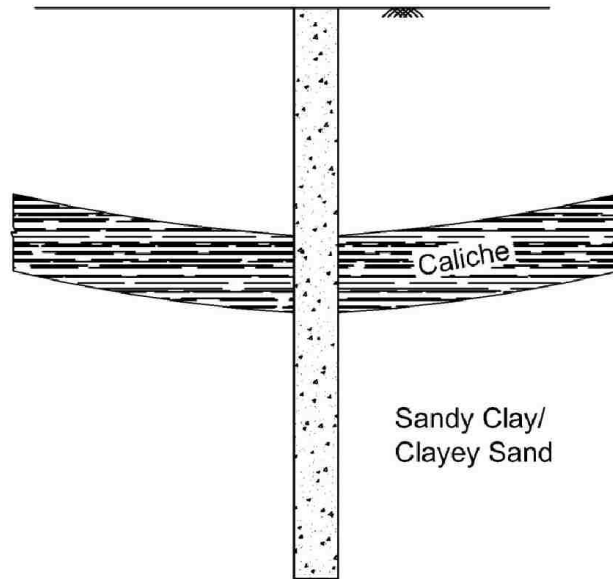


Figure 1-1 Monolith Behavior of Deep Foundation System

Additionally, bi-directional load test results in soils containing caliche indicate that the ultimate skin friction is not achieved and shaft/caliche interaction ultimate side resistance is not achieved through the tests. Due to limited slippage between the shaft and the surrounding soil layers, the ultimate side resistance may not be achievable. Traditional interpretation method for this type of test is appropriate when the ultimate side resistance value is achieved.

The presence of caliche layers will enforce limitations on the traditional method of test and design for drilled shafts. These limitations may mislead the engineers into unnecessarily conservative designs.

This study investigates the effect caliche layers on the behavior and design of drilled shafts in soils containing caliche. The current load test approach will be investigated and recommendations are suggested for soil profiles containing caliche.

1.1 Scope of Research Project

The research reported herein is concerned with the behavior of drilled shaft foundations constructed in soils containing caliche. The study focuses on competent caliche layers underlain by a weak geomaterial. The scope of these investigations is limited to the following:

1. Investigating the behavior of drilled shafts foundations subjected to axial loading only
2. Full-scale load tests on drilled shafts in predominantly sandy clay/clayey sand with caliche layers.
3. The load test was performed in general accordance with ASTM D-1143 "Quick Load Test Procedures" (2013)

1.2 Research Objectives

The overall objective was to verify the current Osterberg test interpretation for testing drilled shafts in soil profiles containing caliche. The objective was achieved in the following steps:

1. Acquiring full-scale O-cell and conventional test data for drilled shafts in soil containing caliche along with their associated boring log and laboratory test data.
2. Analyzing the validity of collected data.

3. Investigating the effect of caliche on the load tests in Las Vegas using finite element software PLAXIS 8.
4. Identify the difference between upward and downward mobilization of the shaft in Las Vegas
5. Introducing a step-by step procedure to design the drilled shafts properly in Las Vegas.

1.3 Organization

This dissertation consists of eight chapters. The detail of each chapter presents below:

Chapter 1 provides an introduction, background history of drilled shafts in Las Vegas caliche, problem statements explaining the significance of the project, research objectives, and organization to provide a framework of the completed research.

Chapter 2 describes the geology of Las Vegas Valley and the caliche layers. This chapter explains the potential impact of caliche layers on the design of drilled shaft and deep foundations.

Chapter 3 presents a literature review on drilled shaft design in rocks, their side resistance and end bearing capacity. The information is used for the design of test drilled shafts in practice

Chapter 4 provides background information on load test methodology for both conventional and bi-directional load test methods. The limitation and advantageous of each method is described. Additionally, the collected bi-directional test are evaluated in this chapter for further analytical purposes.

Chapter 5 focuses on modeling of Osterberg tests for a simplified soil profile with caliche. In this chapter an axisymmetric PLAXIS model is designed to compare the equivalent top-down load with a conventional load. The location of the O-cell with respect to caliche changes and the effect of this distance on the results will be explained.

Chapter 6 focuses on modeling two cases where in the first one O-cell is installed far from caliche and in the second scenario O-cell is installed under the caliche layer. The models are created using finite element software PLAXIS 8. The models are calibrated using the field measurements from the tests. The calibrated models are loaded from the top and the equivalent top-down behavior is compared to the analytical top-down behavior from PLAXIS results. This chapter also explains the reason why O-cell location may change the results when the soil profile contains caliche layers

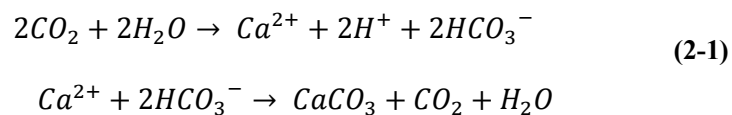
Chapter 7 presents recommendations for appropriately designing the O-cell test to minimize the discrepancies between top-down behavior from analytical results and load test results. A step-by-step method is introduced to appropriately design the test shaft in soil profiles containing caliche layers.

2 Geology of Las Vegas

Las Vegas is bounded on the west, south and east by mountains. The mountains to the west and east of Las Vegas are composed primarily of limestone and dolomite, while the mountains to the south consist of tertiary volcanics. Unconsolidated sediments of sand, silt, and clay, thousands of meters thick, are found in the center of the valley (Rodgers, Tkalcic, McCallen, Larsen, & Snelson, 2006). Cemented soils are found in most parts of the Las Vegas valley. These materials consist of sand and gravel particles cemented by calcium carbonate, or a finer-grained material consisting primarily of calcium, locally known as Caliche.

2.1 Las Vegas Caliche

Caliche is considered to be the hard lithification of both fine-grained sediments and sand and gravel through secondary cementation by calcium and magnesium carbonate (Cibor, 1983). Lattman (1973) divides carbonate cementation in the valley into six categories according to its occurrence and origin. The mechanism of caliche formation is described by (Schlesinger, 1985) and others (Marion, Schlesinger, & Fonteyn, 1985; McFadden, Wells, & Dohrenwend, 1986). The caliche formation in the Valley is shown in



Researchers agree that most thick caliches form under aggrading conditions and climatic reversals which cause extensive solution and redeposition (Frye & Leonard, 1967). deposition by rising artesian ground water (Blake, 1901), deposition by capillary rise of ground water (W. T. Lee, 1905), deposition by a regionally rising water table (Theis, 1936). Thus accretions of caliche could

accumulate above and below a lithified layer. Along the southern apron, lithification can be attributed to Aeolian transport of cementing agent from the Spring Mountains. The term “caliche” loosely applies to any cemented soils encountered in the Valley. Yet, this material varies considerably in the degree of cementation, its thickness and lateral continuity, and strength characteristics. Caliche can be found in the semi-arid and desert regions of the western U.S., in Florida, and along the banks of the lower Mississippi River. These deposits are widespread and important bearing units for both shallow and deep foundations. The cemented zone can be several inches to five or more feet in thickness.

2.2 Classification

(Cibor, 1983) classifies the caliche layers in the Las Vegas, NV area based on their nomenclature and drilling characteristics. A summarization of drilling/sampling characteristics of caliche is brought in Table 2-1. Table 2-1 explains the wide variety of material characteristics of cemented soils and suggests approaches for categorizing cemented soils and sampling strategies based on the categorization.

There is no simple approach for establishing the strength or deformation characteristics of caliche due to the extensive variation in properties and behavior of this material. A common sense approach is usually used, as follows. A simple unit weight can help to determine whether the material is as dense as the high blow count responses indicate. It may be possible to either submerge a sample in water or simply add water to a piece of the intact sample to assess whether the cementing agent is soluble or if the material softens when inundated with water.

Table 2-1 : Classification and Drilling/Sampling
Characteristics of Caliche, Las Vegas Valley (Cibor, 1983)

Cemented coarse-grained deposits	Cemented fine-grained deposits	Hardness Classification	Drilling Rates minutes/ft		Description of Material and Drill Cuttings
			Without pulldown	With pulldown	
Sand and gravel with scattered cementation	Decomposed caliche with silt and clay	Very Hard to lightly hard	-	-	Variable matrix of uncemented soil and cemented zones. Samples obtained with split-spoon or thick-walled sampler. Can be crumbled with fingers.
Partially cemented sand and gravel	Decomposed caliche	Moderately hard	< 5	< 3	Cemented to varying degrees. Fine-grained deposits sampled with thick-walled sampler; coarse-grained samples cannot be obtained with thick-walled sampler. Drilling produces large, rounded cuttings. Cuttings can be broken with difficulty with hands or easily when hammered.
Cemented sand and gravel	Weathered caliche	Hard	6 to 30	3 to 6	Visible chemical alterations from fresh deposits. Compressive strength similar to fresh deposits. Slight secondary porosity. Samples obtained by coring techniques. Drill cuttings less than 1/2 inch in diameter. Fragments can be broken with difficulty by hammering.
	Fresh caliche	Very hard	700	70	No visible signs of chemical alteration. Non-porous. Resembles metamorphic or sedimentary rock. Drill cuttings less than 1/8 inch in diameter. Samples obtained by coring techniques. Fragments cannot be broken by hammering.

If either of these responses is identified, a careful assessment must be made of whether the service conditions will result in the introduction of (and the effect of) water. If so, the strength of the soil should be evaluated for the uncemented state. Moreover the caliche can be fractured or competent, interbedded with uncemented soils or contain secondary solution cavities. There are a few in-situ and laboratory tests that can help understand if the caliche layers is competent enough for proposed engineering practice or not. Cemented material classified as very stiff or dense, and slightly to moderately hard can be excavated with conventional equipment and use of

ripper tooth. Caliche termed hard to very hard usually requires use of heavy excavation equipment such as a Ho-ram or headache ball. Blasting techniques are also employed for extensive excavation located away from developed areas.

2.3 Caliche Impact on Foundation Design

Cibor (1983) believed conventional methods of estimating settlement, which do not account for cementation, overestimate movement of foundations. The recent load tests and construction monitoring that were performed for a few projects in the Valley showed his assumption to be correct as the drilled shafts tend to displace a very small amount during the test and construction. The overestimated designs resulted in redundantly large and deep foundations for many projects in town. Recently a new approach was taken by Stone (2009) which account for the capacity of the caliche as a cemented material. The new foundation type consisting of a short pile system bonded to shallow cemented layers. The bonding of caliche layers together with short piles forms a caliche stiffened pile (CSP) foundation. This study indicates that increasing the pile length by 100 percent reduces the settlement by only 10 percent. The results show that caliche layers in Las Vegas Soil profile may interfere with the load distribution through the shaft length by sustaining majority of applied load.

3 Axial Capacity of Drilled Shafts in Rock Sockets

FHWA suggests that, caliche can be treated as sedimentary rock for the purpose of foundation design (Brown et al., 2010). Uniaxial (unconfined) compressive strength should be measured in laboratory tests and design equations for nominal resistances given for rock can be applied to drilled shaft design.

3.1 Side Resistance of Rock Sockets

Side resistance in rock sockets develops in one of three ways: (1) through shearing of the bond between the concrete and the rock that develops when cement paste penetrates into the pores of the rock (bond); (2) sliding friction between the concrete shaft and the rock when the cement paste does not penetrate into the pores of the rock and when the socket is smooth (friction); and (3) Interface dilation of an unbonded rock-concrete as shown in Figure 3-1.

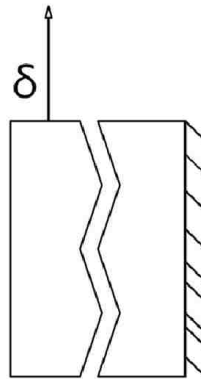


Figure 3-1: Interface dilation of an unbonded rock-concrete

The asperities shear off with increases in effective stresses in the rock asperities around the interface. Dilational behavior is also accompanied by frictional behavior. These phenomena occur simultaneously, with one being dominant. Rock that does not have large pores or in which the action of the drilling tool forces fine

cuttings into the pores (or in which drilling mud plugs the pores), thus limiting filtration of the cement paste into the formation, will not exhibit the bond condition. Instead, rock-concrete interfaces will exhibit either the friction condition or the dilation condition. This behavior may be more characteristic of argillaceous rock such as clay-shale than of carbonaceous or arenaceous rock, such as limestone or sandstone (Nam, 2004). Caliche or Calx is the Latin translation for limestone. For caliche the behavior may be similar to the second type of rocks where the friction and dilation are the dominant elements of skin friction.

Researchers have been working on approximating the ultimate side resistance for shafts in rock for a long time. Typically, the ultimate side resistance value may be evaluated on the basis of mean uniaxial compressive strength of the rock as follow:

$$\frac{f_{su}}{P_a} = C \left(\frac{q_u}{P_a} \right)^n \quad (3-1)$$

Where, q_u = mean value of uniaxial compressive strength for the rock layer; P_a = atmospheric pressure; C = constant and n =exponent

Regression coefficient used to analyze load test results. Many researchers have worked on the regression analysis of unit side resistance. A chronological summary of various researchers' work are shown in Table 3-1.

There is no simple approach for establishing the strength or deformation characteristics of caliche due to the extensive variation in properties and behavior of this material. A common sense approach is usually used, as follows. A simple unit weight can help to determine whether the material is as dense as the high blow count responses indicate. It may be possible to either submerge a sample in water or simply add water to a piece of the intact sample to assess whether the cementing agent is soluble or if the material softens when inundated with water.

Table 3-1: Unit Skin Friction Coefficients in Rock

Reference	C	n	Notes
Rosenberg & Journeaux (1976)	1.09	0.52	
Horvath (1978)	1.04	0.5	
Horvath and Kenney (1979)	0.65	0.5	B > 400 mm
Meigh and Wolski, (1979)	0.55	0.6	q _u / p _a between 4 and 7, they recommended a constant lower bound at f = 0.25 q _u .
Williams, et al. (1985)	1.84	0.37	
Rowe and Armitage, (1984)	1.42	0.5	
Carter and Kulhawy, (1988; 1992a; 1992b)	1.42	0.5	C=0.63, n=0.5 for lower bound
Reese and O'Neill, (1988)	0.65	1	q _u / p _a > 19
Reese and O'Neill, (1988)	0.15	1	17 < q _u / p _a < 19
Reese and O'Neill, (1999)	0.65	1	q _u / p _a > 50
Zhang and Einstein (1999)	1.26	0.5	
Kulhawy, Prakoso, & Akbas (2005)	1	0.5	

Most of the authors in Table 3-1 recommend the use of Equation (3-1) with C= 1.0 for design of “normal” rock sockets. A lower bound value of C= 0.63 was proven to cover 90% of the load test results (Brown et al., 2010). The term “normal” as used above applies to sockets constructed with conventional equipment and resulting in nominally clean sidewalls without resorting to special procedures or artificial roughening. Rocks that may be prone to smearing or rapid deterioration upon exposure to atmospheric conditions, water, or slurry, are outside the “normal” range and may require additional measures to insure reliable side resistance. O’Neill and Reese (1999) also applied an empirical reduction factor α_E to account for the degree of rock fracturing. The resulting expression is:

$$\frac{f_{su}}{P_a} = 0.65\alpha_E \sqrt{\frac{q_u}{P_a}} \quad (3-2)$$

Where, the coefficient α_E is determined as a function of the estimated ratio of rock mass modulus to modulus of intact rock $\left(\frac{E_m}{E_R}\right)$. This ratio is estimated from the RQD

Artificial roughening of rock sockets through the use of grooving tools or other measures can increase side resistance compared to normal sockets. Regression analysis of the available load test data by Kulhawy and Prakoso (2007) suggests a mean value of $C= 1.9$ and $n=0.5$ with use of equation (3-1) for roughened sockets. It is strongly recommended that load tests or local experience be used to verify values of C greater than 1.0. However, the advantages of achieving higher resistance by sidewall roughening often justify the cost of load tests of the rock. McVay, Townsend, & Williams (1992) also found that the best predictive results for Florida limestone resulted when the unconfined compressive strength was combined with the tensile strength from splitting tension tests.

$$f_{su} = \frac{1}{2} \sqrt{q_u} \sqrt{q_t} \quad (3-3)$$

Where, q_t is splitting tensile strength. McVay also claims that the ultimate bond strength is in close proximity to the rock's cohesion value.

A limited amount of data is reported on measured strength of the caliche. Cibor (1983) reports a range of 576 ksf to 1,440 ksf (4,000 to 10,000 psi) for compressive strength of competent caliche in the Las Vegas Valley.

O'Neill et al. (1996) focused on predicting the resistance-settlement behavior of individual axially loaded drilled shafts in intermediate geomaterials (IGM's). The design model included the variables described earlier and has a sound analytical basis. Its appropriate use, however, requires high-quality, state-of-the-practice sampling and testing and attention to construction details. The method is based on the finite element model of Hassan (1994). The authors give a simple method for estimating f_s in the referenced report. If the interface shear strength parameters are not known, the following approximation could be used:

$$f_s = \frac{q_u}{2} \quad (3-4)$$

O'Neill et al. (1996) recommend using a series of tables from Carter and Kulhawy (1988; 1992a; 1992b) However, those tables can be included under one table, Table 3-2, which gives adjusted apparent values of f_{max} .

Table 3-2: Adjustment of f , for Presence of Soft Seams (M. O'Neill et al., 1996).

RQD (%)	f_{max}/f_s	
	Closed Joints	Open Joints
100	1	0.84
70	0.88	0.55
50	0.59	0.55
20	0.45	0.45
<20	--	--

Rowe and Armitage (1984) provided theoretical solutions from which a comprehensive design method was developed to estimate rock socket settlement and to assure safety against bearing failure. Rowe and Armitage (1987) outline a specific design method for soft rock, based on the LRFD concept. The design values for unit side resistance and mass modulus of the rock are estimated from equations (3-5) and (3-6).

$$f_{max}(MPa) = 0.7\alpha[q_u(MPa)]^{0.5} \quad (3-5)$$

$$E_r(MPa) = 0.7\{215[q_u(MPa)]^{0.5}\} \quad (3-6)$$

$\alpha = 0.45[q_u(MPa)]^{0.5}$ for clean sockets, with roughness R1, R2 and R3 (Pells, Rowe, & Turner, 1980) and $\alpha = 0.6[q_u(MPa)]^{0.5}$ for clean sockets, with roughness R4 (Pells et al., 1980).

Kulhawy and Phoon (1993) developed expressions for the unit side resistance for drilled shafts in soil and for rock sockets from the analysis of 127 load tests in soil and 114 load tests in rock. On the basis of the load test data, Kulhawy and Phoon also suggest that peak unit side resistance, f_{\max} , be computed in general for rock sockets from

$$\frac{f_{su}}{P_a} = \psi \left(\frac{q_u}{2P_a} \right)^{0.5} \quad (3-7)$$

Ψ is quantitative roughness factor for design, the Ψ value for when the borehole is very rough (e.g., roughened artificially) is 3, 2 for normal drilling conditions, and 1 for conditions that produce “gun-barrel-smooth” sockets.

3.1.1 Rock/Shaft Joint Stiffness

In a socket, the normal stresses against the geomaterial at the interface that are generated by dilation depend on the radial stiffness of the rock, which can crudely be characterized by its Young’s modulus (Nam, 2004). It may therefore be expected that rocks with low RQD’s will result in sockets with lower side resistance than rocks with higher RQD’s, for the same strength of intact rock.

The observation is made that side shear failure does not always occur through the rock asperities. If the rock is stronger than the concrete, the concrete asperities, rather than the rock asperities, are sheared off. This effect is not likely to occur in the soft rock formations; however, in harder rock, the side resistance should be checked

considering both possibilities. This is often done at the design level by using both the q_u of the rock and the f'_c of the concrete in the design formulae for side resistance.

3.2 Base Resistance of Rock Sockets

Base resistance in rocks is more complex than in soil because of the wide range of possible rock mass types. Many failure modes are possible depending upon whether rock mass strength is governed by intact rock, fractured rock mass or structurally controlled by shearing along dominant discontinuity surfaces. Discontinuities can have a significant influence on the strength of the rock mass depending on their orientation and the nature of material within discontinuities (Pells & Turner, 1980).

It is common to have information on the uniaxial compressive strength of intact rock (q_u) and the general condition of rock at the base of a shaft. Empirical relationships between nominal unit base resistance (q_{BU}) and rock compressive strength can be expressed in the form:

$$q_{bu} = N_c^* \sigma_c \quad (3-8)$$

Where, The value of N_c^* is a function of rock mass quality and rock type, where rock Mass quality, in essence, expresses the degree of jointing and weathering. Analogous to the ultimate side shear resistance, many attempts have been made to correlate the end bearing capacity, q_{bu} to the unconfined strength, σ_c of intact rock. Some of the suggested relations are shown in Table 3-3.

Table 3-3: Base Resistance of Rock Sockets

Reference	N_c^*	Notes
Teng (1962)	5-8	
Coates (1966)	3	
Rowe and Armitage(1987)	2.7	
ARGEMA (1992)	4.5	$q_{bu} < 10MPa$

Kulhawy and Goodman (1980) presented the following relationship originally proposed by Bishnoi (1968):

$$q_{bu} = JcN_c^* \quad (3-9)$$

Where J =correction factor depending on normalized spacing of horizontal joints (spacing of horizontal joints/shaft diameter); c =cohesion of the rock mass; and N_c^* = modified bearing capacity factor, which is a function of the friction angle ϕ of the rock mass and normalized spacing of vertical joints.

The Canadian Foundation Engineering Manual (1985) proposed that the ultimate bearing pressure can be calculated using the following equation

$$q_{bu} = 3\sigma_c K_{sp} D \quad (3-10)$$

In which:

$$K_{sp} = \frac{3 + \frac{s}{B}}{10 \left(1 + 300 \frac{g}{s}\right)^{0.5}} \quad (3-11)$$

s = spacing of the discontinuities; B = socket width or diameter; g = aperture of the discontinuities; $D = 1 + 0.4 \left(\frac{L}{B}\right) \leq 3.4$ = depth factor; and L = socket length. In general the method will apply only if $\frac{s}{B}$ ratios lie between 0.05 and 2.0 and the values of $\frac{g}{s}$ is between 0 and 0.02.

It is common to design for frictional capacity and neglect end-bearing effects in shafts socketed into rocks. This is due to the need for inspection and cleaning of the pile base if an end-bearing load effect is included; however, the shaft bottom should always be partially cleaned of loose rock/soil (M. W. O'Neill & Reese, 1999).

3.3 Summary

A few published design methods for the estimation of the performance of drilled shafts in rocks have been reviewed. The most important parameters that affect the capacity of a drilled shaft socket in soft rock are the compression strength of the rock, the Young's modulus of the rock, the pattern of roughness that develops on the interface due to construction (possibly a function of drilling tool and rock formation), the diameter of the socket, the presence or absence of smear on the socket walls, and the size, orientation and infill characteristics of the rock joints. The most important characteristics that influence the side resistance appear to be strength of the rock mass and the roughness of the sides of the borehole.

site-specific field loading tests reduce some of the variability associated with predicting performance, the use of larger resistance factors are justified when loading tests are performed at the project site (Brown et al., 2010). Loading tests are performed for two general reasons:

- 1) to obtain detailed information on load transfer in side and base resistance to allow for an improved design ("load transfer test").
- 2) to prove that the test shaft, as constructed, is capable of sustaining a load of a given magnitude and thus verifying the strength and/or serviceability requirements of the design ("proof test").

4 Load Test

In spite of the most thorough efforts to correlate drilled shaft performance to geomaterial properties, the behavior of drilled shafts is highly dependent upon the local geology and details of construction procedures. This makes it difficult to accurately predict strength and serviceability limits from standardized design methods such as those given in this manual. Site-specific field loading tests performed under realistic conditions offer the potential to improve accuracy of the predictions of performance and reliability of the constructed foundations. Because site-specific field loading tests reduce some of the variability associated with predicting performance, the use of larger resistance factors are justified when loading tests are performed at the project site.

The predominant methods used for static load testing of drilled shafts include conventional top-down static loading tests with a hydraulic jack and reaction system, bi-directional testing using an embedded jack, Each of these methods has advantages and limitations in certain circumstances and experienced foundation engineers (like mechanics) know how to use all the tools in their toolbox. A brief description of each of these methods is provided below.

4.1 Conventional Top-Down Test

The most reliable method to measure the axial performance of a constructed drilled shaft is to apply static load downward onto the top of the shaft in the same manner that the shaft will receive load from the structure. The most common reaction system used with a conventional static load test is comprised of a reaction beam with an anchorage system, as shown in Figure 4-1.

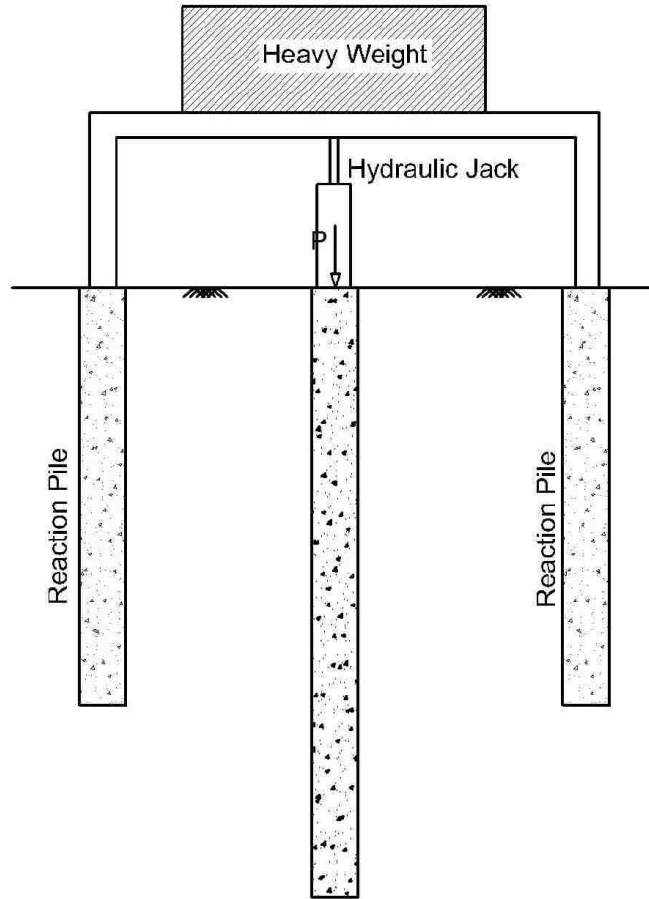


Figure 4-1: Conventional Static Load Test on a Drilled Shaft

The recommended loading procedure for static testing follows the ASTM D1143 “Procedure A: Quick Test” loading method. This procedure requires that the load be applied in increments of 5% of the “anticipated failure load” which should be interpreted as the nominal axial resistance of the shaft. Each load increment is maintained for at least 4 minutes but not more than 15 minutes, using the same time interval for all increments. After completion of the test, the load should be removed in 5 to 10 equal decrements, with similar unloading time intervals. Load, displacement, strain, and any other measurements should be recorded at periods of 0.5, 1, 2, and 4 minutes and at 8 and 15 minutes if longer intervals are used. Periodic measurements of the movements of the reaction system are also recommended in order to detect any

unusual movements which might indicate pending failure of an anchor shaft or other component.

4.1.1 Conventional Load Tests in Caliche

The purpose of the test program was to determine ultimate failure parameters for the upper caliche deposit, the soil zone immediately below the upper caliche deposit, and the load distribution and settlement of a full scale pile at the design load of 1,500 tons (Stone Jr, 2009). The upper caliche deposit included a 2 foot thick soil layer from 14 to 16 feet below grade. A second layer of caliche was encountered at a depth of about 40 feet below grade, which was 7.5 feet in thickness. The water level at the time of the boring was recorded at a depth of 19 feet. The upper 2.5 feet of the cemented deposit is logged as a cemented sand and gravel material which usually has a lower strength than the caliche.

From the first test, it was concluded that less than 10 percent of the applied top load was actually being applied to the test section due to friction in the upper soils and caliche. Following the air drilling process to isolate the pile from the upper caliche, second test pile showed a geotechnical failure in friction of the soil below the upper caliche deposit. The peak unit side shear resistance was about of 5 ksf. An ultimate load transfer value of 25 ksf was obtained in the upper caliche zone following fracturing by pre-drilling,

The study also showed that, the settlement for the introduce foundation system is mostly controlled by caliche layers that bond the drilled shaft. 2-D and 3-D finite element software are utilized to predict the behavior and settlement of introduced foundation system.

4.2 Bi-directional Load Test (Osterberg Test)

The method of bidirectional load test on bored piles was modified by Osterberg (1984) with the use of a loading device called an O-cell placed on or near the bottom of the pile, which when internally pressurized applies an equal upward and downward load and, thus separately determining the side shear and end-bearing. Osterberg cell (O-cell) bi-directional testing method enables relatively low-cost, high-capacity static load testing of bored piles that were otherwise prohibitively expensive or technically impractical. The genius behind the innovation is a specially designed hydraulic jack (O-cell assembly) cast directly into the pile at a predetermined location shown in Figure 4-2. After curing or set-up, the O-cell is hydraulically pressurized from the surface, simultaneously loading the pile section above the O-cell and the pile section below it. By loading the pile internally, the pile component above the O-cell acts as reaction for loading the pile component below the O-cell, and vice-versa. As the load is applied during testing, electronic sensors measure the displacement of both pile sections. In this way, the O-cell simultaneously tests the end bearing and skin friction and quantifies their resistances individually, thereby maximizing the information obtained.



Figure 4-2: O-cell Installation in a Drilled Shaft (Caltrans, 1998)

The O-cell method improves safety and saves time and money because of the reduced effort required to prepare for testing. While the O-cell test has become the premier method for static load testing of bored piles and auger cast in place piles. A schematic load test layout is show in Figure 4-3.

The O-cell is bounded between two steel plates and the reinforcement cage is tack-welded to the steel plates to be able to carry the cage easily. During the load test tack-welds break and the two sections are loaded in opposite direction.

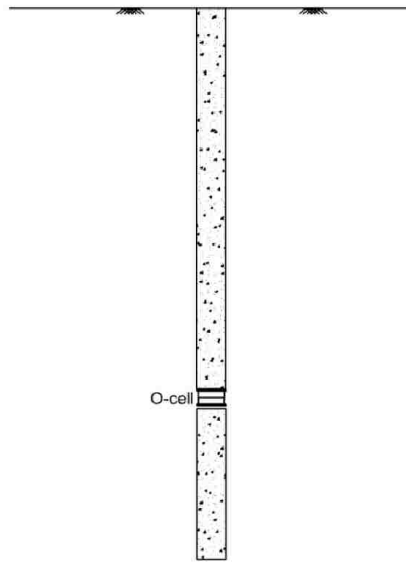


Figure 4-3: Osterberg Load Test

The side resistance and end bearing capacity of the drilled shaft is measured easily using this method. The test is performed by O-cell expansion moving the upper and lower part of the shaft in opposite directions. An example of the produced results is brought in Figure 4-4.

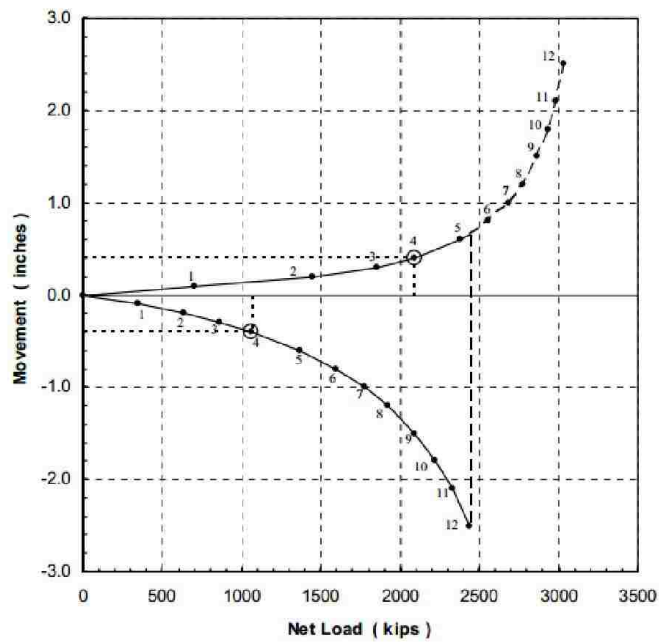


Figure 4-4: Typical bi-directional load test results after (J. O. Osterberg, 1998)

The results from bi-directional load test should be converted to results from a head-down test. The succeeding assumptions are followed in order to convert the results:

- 1- The shaft is considered rigid.
- 2- The side-shear deflection curve for upward displacement of the shaft in a bidirectional test is the same as the downward side-shear deflection component of a conventional top-down test when tested in rock.
- 3- The end-bearing load-deflection curve obtained from an O-cell test is the same as the end-bearing load-deflection curve of a conventional top-down test.

Pick an arbitrary point on the side shear curve (Upper Section). Find another point on the measured end bearing curve (Lower Section) which has the same deflection. Since the shaft is assumed incompressible, the top of the shaft moves down the same as the bottom in a head-down curve. Since the deflections at both points are the same, the load for a head-down test is the sum of side shear and end bearing. By repeating the process for several points, the equivalent top down curve equivalent to the measured side resistance and measured end bearing curve is determined as shown in Figure 4-5.

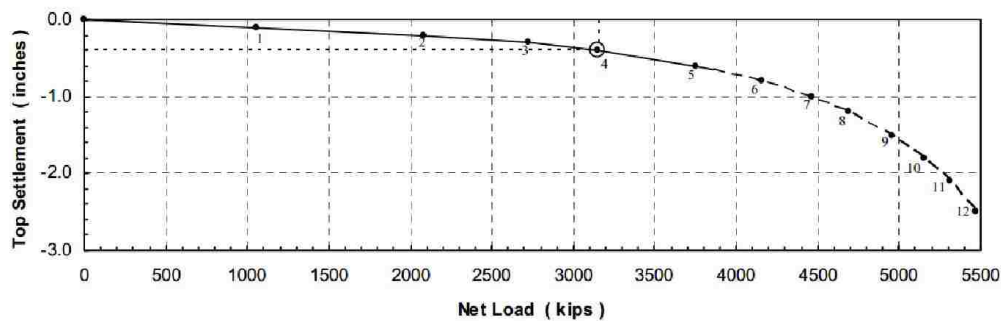


Figure 4-5: Equivalent top loaded settlement curve after (J. O. Osterberg, 1998)

4.2.1 Elastic Shortening

The elastic behavior of any column is clearly additional to any settlement in the soil. In general, the elastic shortening depends on the development of load transfer between the pile and the soil along its length, as well as on any free length or nearly friction free length at the pile head, and on the load being transferred at the pile base. Elastic shortening is not (as suggested) in general, a linear function for materials like concrete, but it may be assumed to follow an elastic function within the usual range of testing piles. A simplified method can be used, such as that proposed by Fleming (1992). The effect of duration of load needs to be taken into consideration. In most materials the creep effect can be significant and is particularly so for large movements (England, 1993). Russo et al. (2003) completed numerical simulations and showed that the original method is satisfactory when the pile slenderness ratio is less than approximately 20. Other researchers (Hossain, Omelchenko, & Haque, 2007; J. Lee & Park, 2008; Qudus, Osterberg, & Waxse, 2004; Zuo, Drumm, Islam, & Yang, 2004), however, reported that the equivalent top-loaded displacement curve that does not consider elastic shortening of the pile are stiffer than conventional top-down load-displacement curves. These approaches neglects that the upward movement starts by mobilizing the stiffer shaft resistance at the depth of the cell, whereas the head-down test starts by mobilizing the less stiff load-movement response near the pile head and vice versa. A new approach have been presented by Kim and Mission (2010) presented a modified method for evaluating the elastic shaft shortening from the skin-friction load component in a head-down test by using the measured data of the upward displacement curves in a bottom-up load test of a pile. Fellenius et. al (1999) has made several finite element method (FEM) studies of an OLT in which he adjusted the parameters to produce good load-deflection matches with the OLT up and down

load-deflection curves. According to Fleming (1992), the total elastic compression is the summation of the elemental shortening. Theoretical elastic compression in top loaded test based on pattern of developed side shear stress is calculated using Equation (A- 2).

$$\delta_{\downarrow} = [(C_1)Q'_{\downarrow} + (1 - C_1)P] \frac{L}{EA} \quad (4-1)$$

And to model the elastic compression of the upper section of the pile above the point of application of load, is calculated using

$$\delta_{\uparrow} = [(C_1)Q'_{\uparrow}] \frac{L}{EA} \quad (4-2)$$

To estimate the top down elastic behavior, it is possible to subtract from the total for the section, as in equation (4-1), the elastic compression integrated already in the measured upward response, as in equation (A- 2). Alternatively, it can be recomputed, but now the friction is effective from the top.

4.2.2 Disadvantageous of Osterberg Test Method

There is little evidence that drilled shafts deriving axial resistance in soil exhibit any significance difference in behavior associated with direction of loading. Although not proven theoretically, the side-shear deflection curve for upward displacement of the shaft in a bi-directional test is the same as the downward side-shear deflection component of a conventional top-down test when tested in rock (J. O. Osterberg, 1998). The assumption may be correct when the ultimate skin resistance is reached in the test.

McVay et. al (1994) performed a numerical study to understand the different between upward and downward load distribution behavior in drilled shafts. They have pointed out differences between O-cell test conditions and top loading conditions in

rock that may require interpretation. The most significant difference is that compression loading at the head of a shaft causes compression in the concrete, outward radial strain (Poisson's effect), and a load transfer distribution in which axial load in the shaft decreases with depth as shown in Figure 4-6.

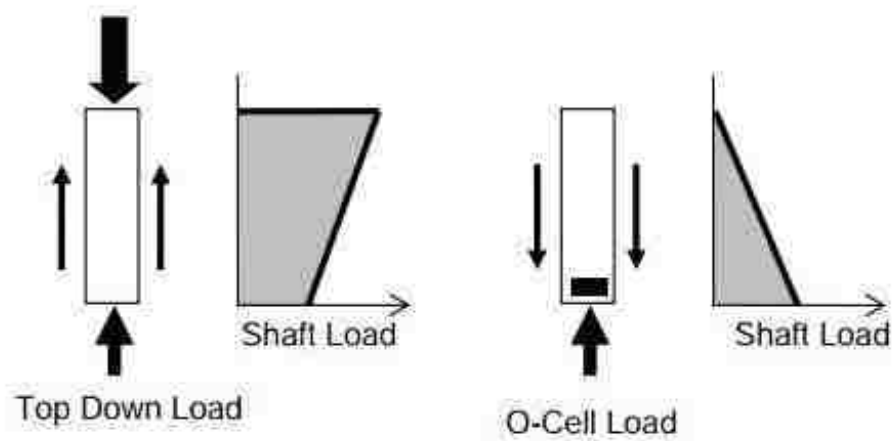


Figure 4-6: Average Compressive Load in Shaft During Top Down and O-Cell Loading (Brown et al., 2010)

Dilatancy at the shaft/rock interface adds to the effect, with the result that the normal stress at the shaft/rock interface may be less in the O-cell test than in a top-down load test. Loading from an embedded O-cell also produces compression in the concrete but a load transfer distribution in which axial load in the shaft decreases upward from a maximum at the O-cell to zero at the head of the shaft. It is possible that different load transfer distributions could result in different distributions of side resistance with depth and, depending upon subsurface conditions, different total side resistance of a rock socket.

Additionally, in shallow rock sockets under bottom-up (O-cell) loading conditions, a potential failure mode is by formation of a conical wedge-type failure surface (“cone breakout”). Obviously, this type of failure mode would not yield results equivalent to a shaft loaded in compression from the top. A construction detail

noted by Crapps and Schmertmann (2002) that could potentially influence load test results is the change in shaft diameter that might exist at the top of a rock socket.

4.2.2.1 Current Practice for Interpretation of Osterberg tests

Because of the different mechanisms of loading in a bidirectional test from those of a conventional top-down static load test a curve equivalent to applying the load at the top of a pile has to be constructed from the upward displacement side-shear curve and downward displacement end-bearing curve. Osterberg's (1998) original method for constructing the equivalent top-down load displacement curves assumes the pile to be rigid, in which the top and bottom are assumed to move the same amount and have the same displacement but different loads. The equivalent top-down load-displacement curve is constructed by adding the side shear to the end-bearing in the same deflection. Osterberg (1998) and Peng et al. (1999) reported that the equivalent top-loaded displacement curves from the bidirectional load test results were in reasonable agreement with the conventional top-down test results when the pile deformations were small.

Kim and Mission (2010) suggested that the current practice neglects that the soil profile may include a very strong material close to the surface and at a significant distance from the O-cell. The upward movement starts by mobilizing the less stiffer material, whereas the head-down test starts by mobilizing the stiffer material. The results would be different load-movement response near the pile head. The opposite of this scenario may also happen but this time the O-cell starts mobilizing the stiffer material. The second case is very similar to what happens in Drilled shafts socketed into rocks.

(Kwon, Choi, Kwon, & Kim, 2005) performed a bi-directional load test using Osterberg method and the conventional top-down load were executed on 1.5-m diameter cast-in-place concrete piles at the same time and site. The top-down equivalent curve constructed from the bidirectional load test results predicted the pile head settlement under the pile design load to be approximately one half of that predicted by the conventional top-down load test. However, after adding the elastic shortening of the pile the interpreted top-down curve shows similar results to conventional top-down test as shown in Figure 4-7.

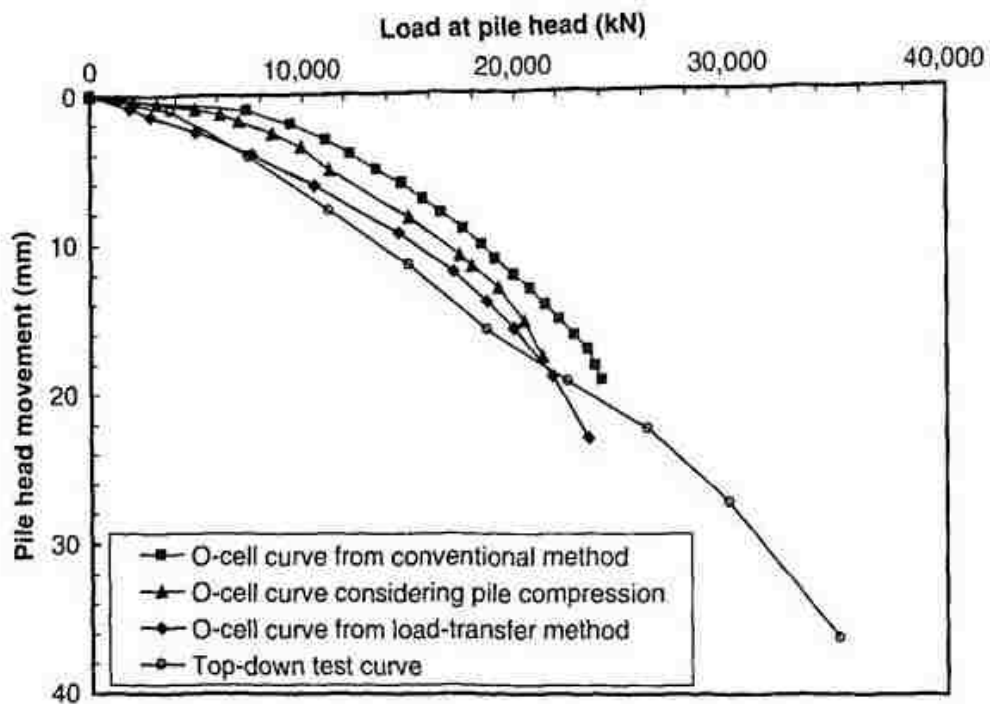


Figure 4-7: Load – Displacement Behavior for Interpreted test data from Osterberg test and conventional loading (Kwon et al., 2005)

The test during the study by Kwon et. al. (2005) was performed in a rock socketed drilled shaft in a highly weathered rock. The strain gauges in these two tests are installed at different locations and the strain gauge zones do not reach their ultimate capacity limit.

Paikowsky et al. (2006) believes that differences between O-cell test conditions and top loading conditions that may require interpretation. The most significant difference is that compressional loading at the head of a shaft causes compression in the concrete, outward radial strain (Poisson's effect), and a load transfer distribution in which axial load in the shaft decreases with depth. Loading from an embedded O-cell also produces compression in the concrete, but a load transfer distribution in which axial load in the shaft decreases upward from a maximum at the O-cell to zero at the head of the shaft. It is possible that different load transfer distributions could result in different distributions of side resistance with depth and, depending on subsurface conditions, different total side resistance of a rock socket. In shallow rock sockets under bottom-up (O-cell) loading conditions, a potential failure mode is by formation of a conical wedge-type failure surface ("cone breakout"). This type of failure mode would not yield results equivalent to a shaft loaded in compression from the top.

Paikowsky et al. (2006) reviewed the available data that might allow direct comparisons between O-cell and conventional top-down loading tests on drilled shafts. Three sets of load tests reported in the literature and involving rock sockets were reviewed. FEM reported by Paikowsky et al. (2006) suggests that differences in rock-socket response between O-cell testing and top-load testing may be affected by (1) modulus of the rock mass, E_M , and (2) interface friction angle, ϕ_i . Paikowsky first calibrated the FEM model to provide good agreement with the results of O-cell tests on full-scale rock-socketed shafts. In the FEM, load was applied similarly to the field O-cell test; that is, loading from the bottom upward. The model was then used to predict behavior of the test shafts under a compression load applied at the top and compared with the equivalent top-load settlement curve determined from O-cell test

results. Their study suggested that the equivalent top-load settlement curve derived from an O-cell load test may underpredict side resistance for higher displacements; that is, the O-cell derived curve is conservative.

4.2.3 Osterberg test in Las Vegas

The presence of caliche in Las Vegas soil profile requires a carefully designed Osterberg test. The most Competent caliche layers are usually located at 10 to 20 feet under the ground surface. Their thickness varies between 5 to 15 feet. Caliche is a very hard material and when loaded it shows great load bearing capacity. Therefore, it is important to test the caliche layers properly for a good estimation of shaft capacity.

4.2.4 Osterberg Load Tests in Las Vegas

A data base of 30 load tests is built for Las Vegas. The database is collected for purposes described below:

- 1) Identifying different load test layouts in Las Vegas and determining the most appropriate test layout when caliche layers are present.
- 2) Studying the load distribution behavior of the drilled shafts in caliche

A total of 31 bidirectional load tests are summarized in APPENDIX D, which gives general information about the load tests, including test location, caliche thickness, shaft geometry and the maximum load applied during the test. Since the performance of drilled shafts in rock varies depending upon its geologic formations, load test data for drilled shafts in caliche were acquired from different locations in Las Vegas.

The load test data were classified into four categories based on the location of O-cell during the test and distribution of caliche layers. Four different

scenarios are identified in Las Vegas. Different test layouts are described below:

- 1) O-cell is installed above competent caliche layers
- 2) O-cell is installed between competent caliche layers or in the caliche zone.
- 3) O-cell is installed under the caliche very close to caliche.
- 4) O-cell is installed under the competent caliche layer and far from caliche.

Different test layouts can be seen in Figure 4-8

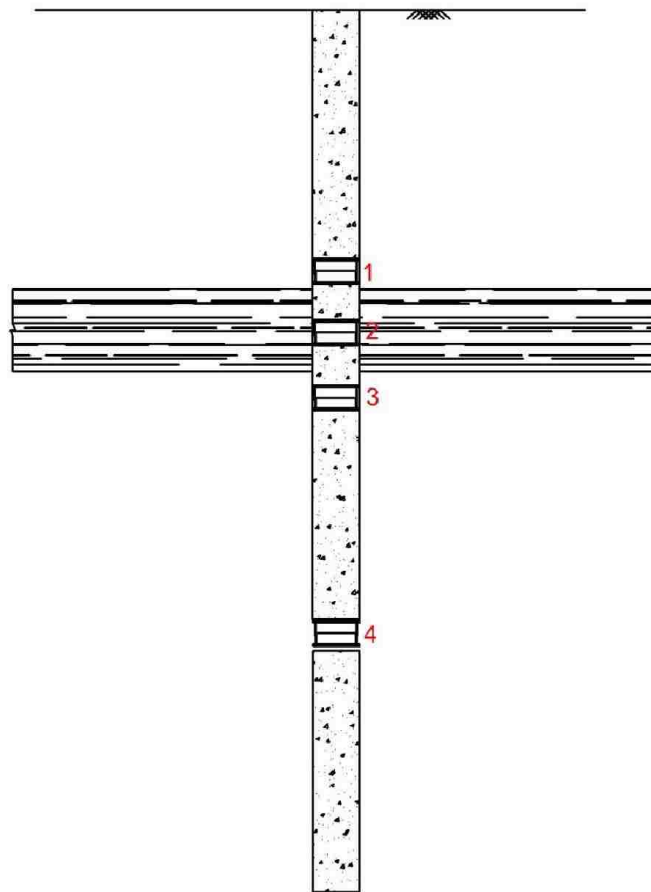


Figure 4-8: Different Osterberg Test Layouts in Las Vegas

4.2.4.1 O-cell above Caliche

Caliche layers usually show a great strength during the load tests and drilled shafts usually require a significant amount of load to be mobilized in soil profiles that have caliche layers. The most competent caliche layers usually occur in the upper sections of the soil profile. If the O-cell is installed above caliche the soil above it may not produce enough side resistance to fully mobilize the caliche layer. The result will be limited movement of the caliche in the downward mobilization of the lower part of the shaft and failing the upper section of the test shaft as shown in Figure 4-9.

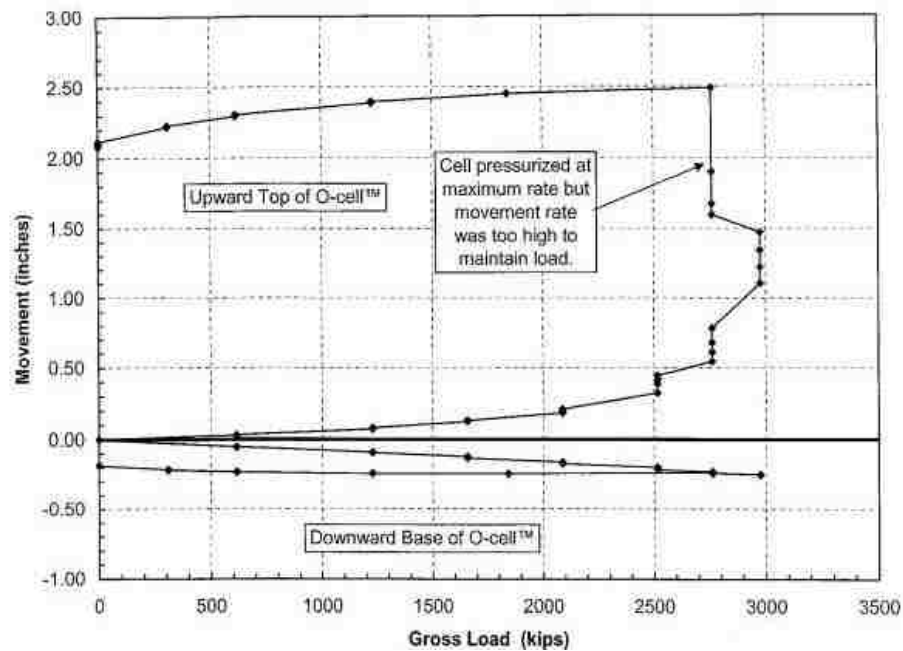


Figure 4-9: O-cell Load-Movement Curve

The applied load from O-cell is enough to fail the upper part of the test shaft but it is not close enough to mobilize the lower part as expected. The test did not provide the engineer with good measurements for caliche capacity. The results may be an unnecessary long shaft.

4.2.4.2 O-cell between Caliche Layers

If the O-cell is installed between caliche layers or in the caliche zone, both upper and lower part of the shaft will develop enough resistance to measure the capacity of both caliche layers. The test results are expected to show limited to fully mobilization of upper and lower section of the shaft. The Load- Movement curve for this scenario is shown in Figure 4-10.

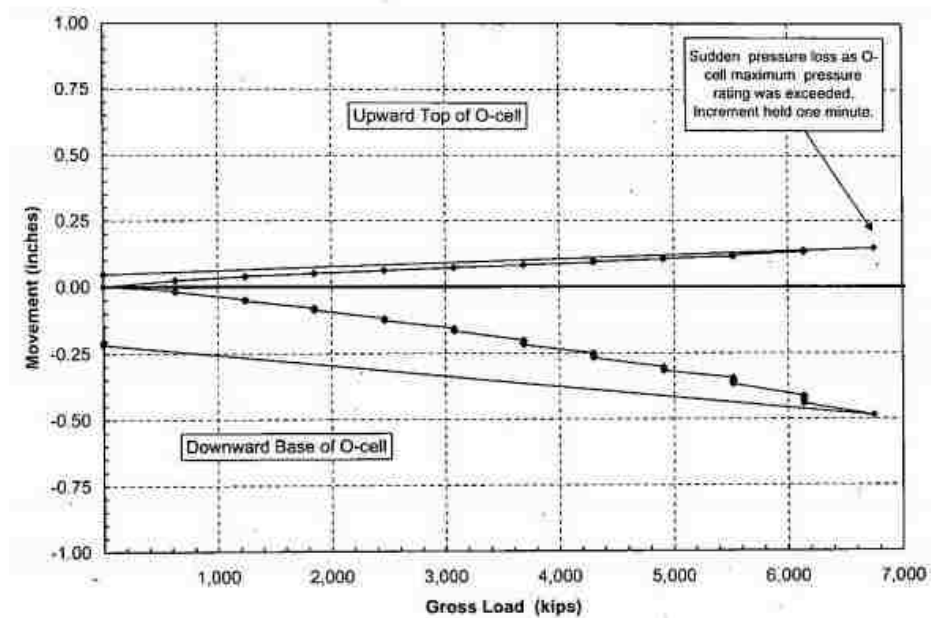


Figure 4-10: O-cell Load-Movement Curve

4.2.4.3 O-cell Under the Caliche (Close to Caliche)

One of the appropriate load test layouts is when the O-cell is installed underneath the caliche layer and the lower shaft sections extends to a lower depth. The extension into lower depths provides enough resistance in the lower section of the shaft to mobilize the caliche in the upper section. Since caliche is stronger than typical soil layers in order to mobilize it larger amount of load needed compared to a general soil profile. In order to generate that load and prevent the early failure in the opposite

direction (lower section of the shaft), this section is extended into lower depths to provide the system with the counter resistance to balance out the resistance from caliche. The test layout results in failure of both lower section and upper section at the same time as shown in Figure 4-11.

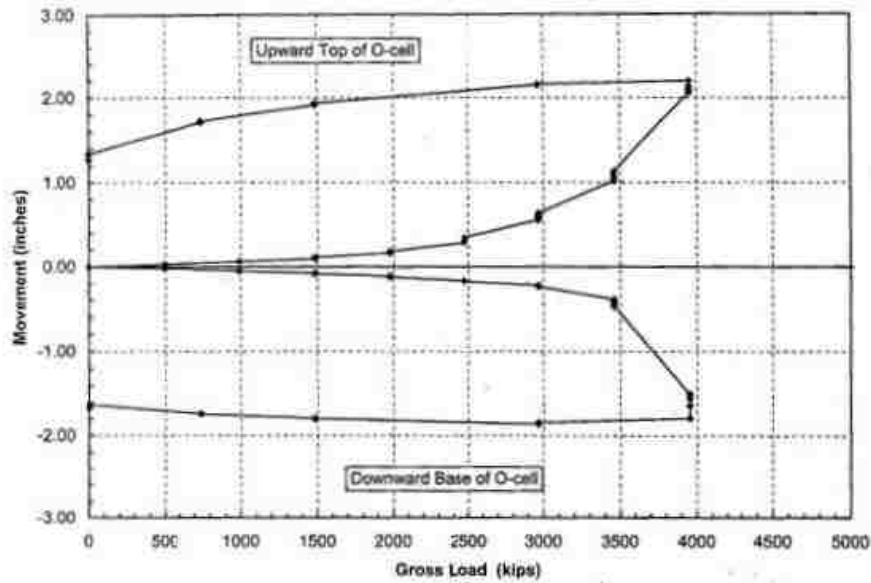


Figure 4-11: O-cell Load-Movement Curve

Traditionally, Osterberg test is designed in a way that ideally, the resistance from lower section of the shaft stays in balance with the resistance of the upper section of the shaft. In this layout this expectations are met.

4.2.4.4 O-cell Under the Caliche (Far from Caliche)

Unlike Previous scenario when the O-cell is installed far from caliche competent caliche layers, the lower section of the shaft may not provide enough resistance to withstand the reaction from the upper section. This scenario is the reverse of first scenario where the soil failed before mobilizing caliche layers except this time the lower part of the shaft fails before the upper section of the shaft. The test

layout results in failure lower section and limited mobilization of upper section is shown in.

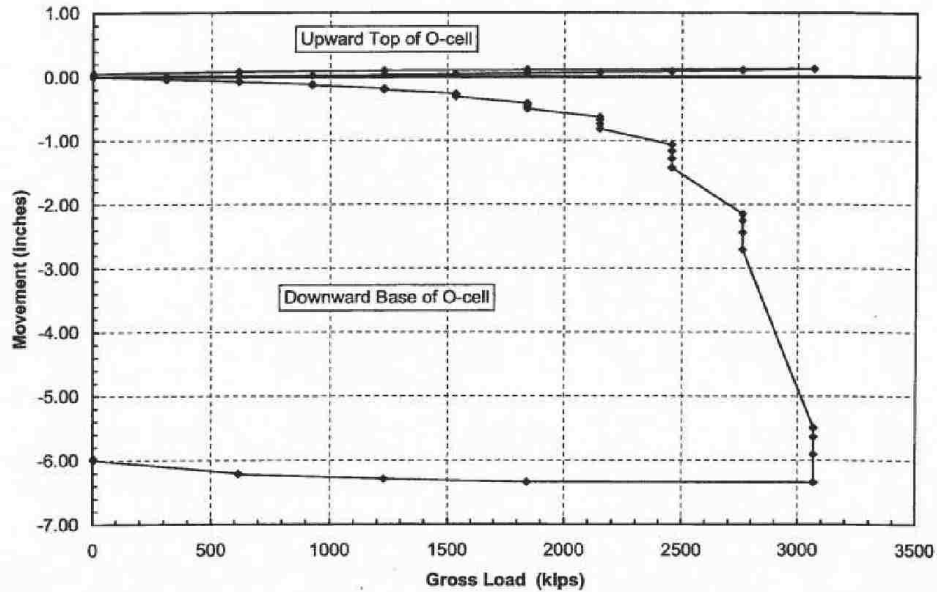


Figure 4-12: O-cell Load-Movement Curve

The first and fourth scenario could both result in unnecessarily conservative designs since the measurements were not able to provide ultimate values in one of the shaft sections.

Four different scenarios for load tests in caliche are introduced. By experience local engineering firm stopped designing the tests similar to the first scenario since the test results are more or less worthless. The second scenario where the O-cell is installed between two competent caliche layers may be a good layout to measure the capacity of both caliche layers in one test. Also, the results from the third scenario show that this test layout is a good way of measuring the capacity of upper and lower section of the shaft. The fourth scenario as well as the first scenario could result in an unnecessarily long shaft. The third and fourth scenario are the most used test layouts

in Las Vegas and the author decided to simulate these two scenarios and study the effect of O-cell location on the interpretation of test results.

4.2.5 Reference Beam Readings

The Osterberg test results are investigated for one of the projects at which the caliche layer is very close to the ground surface. Reference beam reading for the test performed on this site is presented in Table 4-1. The readings are for the maximum applied load by the O-cell and after unloading. The values shown in this table indicate there is reversible or elastic movement in the reference beam during the test.

Table 4-1: Reference Beam Movement

Project	Reference beam	
	Max	After Unloading
Desert Inn	0.037	0.006

Reference beam values are usually affected by the soil heave during the test when the body of the soil moves as the test shaft is driven upward. This value in a normal geological setting where no caliche exists is an irreversible value. During unloading it has been observed that the reference beam readings decrease significantly and will get close to zero. The reference beam reading indicates, there is another resisting element beside side resistance which behaves elastically. It could be perceived from the test results that the existing caliche layer might have been bent during the test and since the flexural behavior was completely elastic the reference beam readings decrease to zero after unloading.

If the readings from reference beam remained the same during unloading it could be concluded that caliche does not bend during the loading and all the deformation is caused by sliding between the shaft and caliche but the value of

reference beam movement drops during unloading meaning the ground heave that occurred during the test is reversible. In conclusion if there is significant difference in the reference beam movement during the test and after unloading it means there is a reversible movement as a result of caliche presence that causes heaving during the test.

As caliche occurs in deeper locations in the soil profile, the overburden soil resist the flexural deflection of caliche during the test. The reference beam readings when caliche is at a deeper location are usually irreversible meaning the deflection is mostly due to sliding between the shaft and soil/caliche layers.

4.3 Validity of Load Test Data

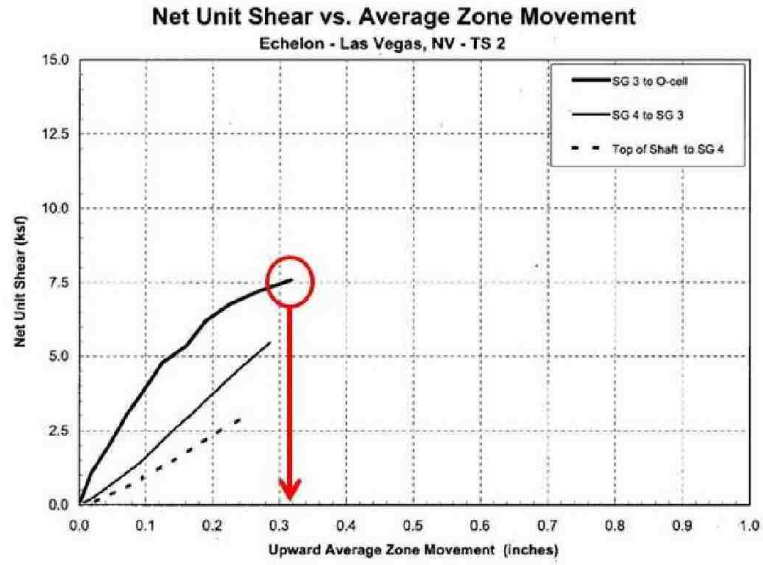
The gathered database includes all the Osterberg load tests in Las Vegas. One of the common problems that occur during the O-cell load test in soil profiles with caliche is the unrealistic readings from the strain gauges. In the provide data base the strain gauge readings have been studied carefully and any results that were to some extent unrealistic, were reported and eliminated before numerical calibration and analysis. The evaluation criteria are listed below:

- 1) The strain gauges readings should be positive
- 2) Strain gauges readings should be less than the maximum applied load by O-cell
- 3) The strain gauge zone average movement should be less than the maximum movement of the drilled shaft in any direction.
- 4) Load test that experienced local crushing in the shaft concrete should be identified.

- 5) If the total length of the shaft does not fall within the depths that contain caliche, that test report is eliminated.

Following the mentioned criteria a few of the load test reports were set aside for the analysis purposes and the rest are eliminated from this study.

- 4 of the tests are eliminated only because the average strain gauges zone movement exceeds the maximum shaft movement. Figure 4-13 shows the strain zone unit shear stress vs. average movement which has a maximum of 0.32 in. On the other hand, Figure 4-14 shows the upward and downward shaft movement with the gross applied load from O-cell. It can be observed that the maximum upward movement of the shaft is less than the strain gauge zone average movement. The strain gauge zones average movement should be less than the shaft movement at all time. The incorrect calculation of conversion factors for strain gauge readings results in incorrect stiffness of the shaft and hence, the average movement values turn out to be incorrect. In order to use these four important test, these values should be fixed by reevaluating the stiffness of the shaft and recalculating the strain gauge zone movements.



LOADTEST, Inc. Project No. 9277-2

Figure E-1

Figure 4-13: Net Unit Shear vs. Upward Average Zone Movement for Echelon TS-2 (LoadTest, 2007)

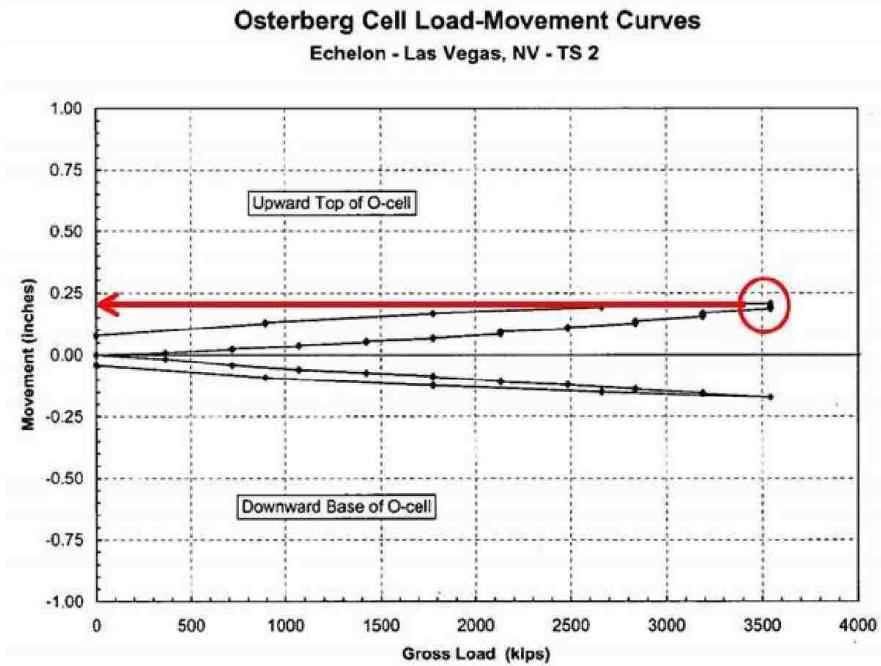


Figure 4-14: Load-Movement for Echelon TS-2 (LoadTest, 2007)

- 3 other tests are eliminated because the total length of the shaft does not fall within the depths that contain caliche. The tests are basically performed in a clayey to sandy type of material without any cemented layers present.

Total of six tests are eliminated from the total numbers. The test for I-215 Airport Connector project matches the criteria for the fourth extreme case where caliche is at a distance from the O-cell. The test for Palm resort matches the criteria introduced for the third case where caliche and O-cell are very close to each other and O-cell is installed under the caliche. The two selected tests are used individually to help calibrate the finite element model that simulates two of the most used test layouts.

5 Finite Element Modeling and Analysis

In this chapter, finite element method (FEM) is performed by using PLAXIS 8 program to simulate the drilled shaft under bi-directional (O-Cell) load test. The main objectives of this analysis are to study behavior of drilled shafts under bidirectional load, compare results with the field monitoring results and investigate force/stress distributions from shaft to surrounding soil and caliche layers. The test procedures of these three kinds of methods are simulated by the FEM model.

The respective results of the tests are compared in the following sections and to check on the validity of the first Osterberg's assumptions which was that the shaft resistance-movement curve for upward movement of the pile is the same as the downward side-movement component of a conventional head-down test.

Furthermore, the results of the finite element analyses are used to determine the parameters involved in the approximate design model. The modeling and analyses associated with the tests are performed using the commercially available software; PLAXIS 8 Professional version 8.2.1 (PLAXIS, 2004). The software provides potent capabilities of modeling geomaterial behavior and interface interaction.

5.1 Finite Element Representation

Different parts of the finite element modeling are individualized in this section by explaining the logic behind any selection in the model. Fifteen-node triangle axisymmetric elements were used to represent the concrete shaft, soil layers and caliche, which provide a second order interpolation for displacements. The element stiffness matrix was evaluated by numerical integration using a total of three Gauss stress points (PLAXIS, 2004). The O-cell part of the shaft is simulated as a one foot

empty void. The O-cell load is applied at the bottom of the upper section of the shaft for upward loading as well as the top of the lower section of the shaft for downward loading. The width of the mesh is assumed to be 150 ft. from the center of the shaft and the depth of the mesh is twice the length of the shaft. This is approximately about 200 ft.

5.2 Constitutive Models

When the resolution of a geotechnical engineering problem is solved via Finite Element analyses, the most crucial step is the choice of the constitutive model for the soil. Constitutive model is what defines that if the soil model is created correctly and is in conformance with what happens in reality. For instance, within the elastic limits (working loading condition), the soil constitutive modeling have been based upon Hooke's law of linear elasticity and for describing soil behavior under collapse state Coulomb's law of perfect plasticity is used because of its simplicity in applications. The combination of the two is formulated in an elastic- perfectly plastic framework which is known as Mohr-Coulomb model. The abovementioned constitutive models will be used in the PLAXIS models to define the relationship between forces and displacements. For each individual part of the numerical model, the constitutive model is assigned as follows:

5.2.1 Drilled Shaft Concrete

The shaft concrete was assumed to be an isotropic, homogeneous and elastic solid with a Poisson's ratio $\nu = 0.15$, which is typical for drilled shaft (Hassan, 1994).

5.2.2 Soil Layers

Las Vegas soil stratigraphy consist of 7 to 8 significant soil types including, clayey Sand (SC), silty sand (SM), lean clay with traces of caliche or gravel (CL), fat clay (CH), sand and gravel (GP, GM, GC) and cemented layers such as cemented sand and gravel. The characteristic of each mentioned soil type could vary with depth or site location. A Mohr-Coulomb model used to represent the soil layers. The shear strength parameters of soil and caliche layers are provided in APPENDIX A. Finite element model is calibrated by varying these parameters to match the field load test results. Also calculation of Young's modulus for soil and caliche layers is provide in APPENDIX B.

5.3 Interface Model

The interface element between the shaft concrete and soil layers are modeled as shown in Figure 5-1. The element chose to be part of the soil layer with 0.1 ft length. Interface elements are selected for each individual soil and caliche type.

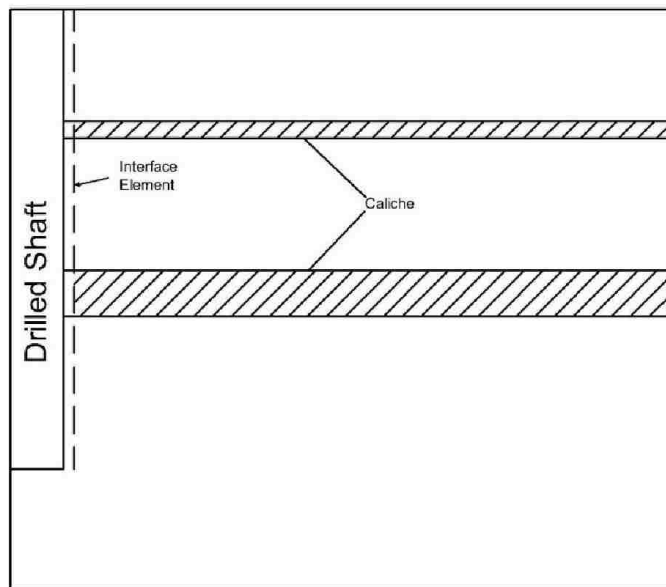


Figure 5-1: Interface Element in PLAXIS model

An elastic-plastic model using Mohr-Coulomb criterion was used to describe the behavior of interfaces for the modeling of mass concrete against soil layers presented in Table 5-1. These values are intended for mass concrete cast against the soil or rock foundation materials listed, and according to Brown, Turner, & Castelli (2010) should be suitable for cast-in-place drilled shafts as long as the concrete and soil interface was relatively rough.

Table 5-1: Friction Angle for Mass Concrete against Soil (NAVFAC, 1982)

Interface Materials	Friction Angle, δ°	Coefficient of Friction, $\tan \delta$
Clean sound rock	35	0.7
Clean gravel, gravel-sand mixtures, coarse sand	29 to 31	0.55 to 0.6
Clean fine to medium sand, silty medium to coarse sand, silty or clayey gravel	24 to 29	0.45 to 0.55
Clean fine sand, silty or clayey fine to medium sand	19 to 24	0.34 to 0.45
Fine sandy silt, nonplastic silt	17 to 19	0.31 to 0.34
Very stiff and hard residual or preconsolidated clay	22 to 26	0.4 to 0.49
Medium stiff and stiff clay and silty clay	17 to 19	0.31 to 0.34

The strength properties of interfaces are linked to the strength properties of a rock layer and each data set has an associated strength reduction factor, R_{inter} , for interfaces as following (PLAXIS, 2004):

5.4 Finite Element Material Color

A color is assigned to each material through this study. The material color is shown in Table 5-2.

Table 5-2: Color Guide for PLAXIS material

Hard Caliche	
Sandy Clay (CL)	
Cemented fine grained material (less strong caliche)	
Clayey Sand (SC)	
Stiff Clay (Usually Fat Clay)	
Sand and Gravel	
Gravelly Clay or Gravelly Sand	

5.5 The effect of O-cell location on the interpretation of Test

An Osterberg test is designed in a controlled soil environment to better understand the effect of O-cell distance to caliche layers on the interpretation of test results. A simple soil stratigraphy is selected with sandy clay soil type to perform this analysis. The soil profile includes a 10-ft. layer of caliche which at first is located at 50 ft. below the ground surface as seen in Figure 5-2. The O-cell is installed under the caliche layer. The test is performed using the material properties shown in Table 5-3.

The test results are converted into equivalent top-down load displacement behavior. The equivalent test results are then compared to normal displacement of the shaft under loading from the top. The loads in this scenario are similar to what is selected for Osterberg test model.

Table 5-3: Material Properties for Sensitivity Case I

Material Properties of Sensitivity Case 1				
Parameter	Unit	Concrete	Sandy Clay	Caliche
Material Model		Linear Elastic	M-C	M-C
Type of Behavior		Drained	Drained	Drained
Dry Unit Weight	kcf	0.15	0.12	0.16
Saturated Unit Weight	kcf	0.15	0.13	0.16
Young's Modulus	ksf	500,000	4000	280,000
Poisson's ratio		0.15	0.3	0.2
Cohesion	ksf	--	1	10
Friction Angle	Degree	--	28	35
Interface Material				
Material Model	Unit		M-C	M-C
Type of Behavior		--	Drained	Drained
Dry Unit Weight	kcf	--	0.12	0.16
Saturated Unit Weight	kcf	--	0.13	0.16
Young's Modulus	ksf	--	4000	280,000
Poisson's ratio		--	0.3	0.2
Cohesion	ksf	--	0.3	10
Friction Angle	Degree	--	23	35

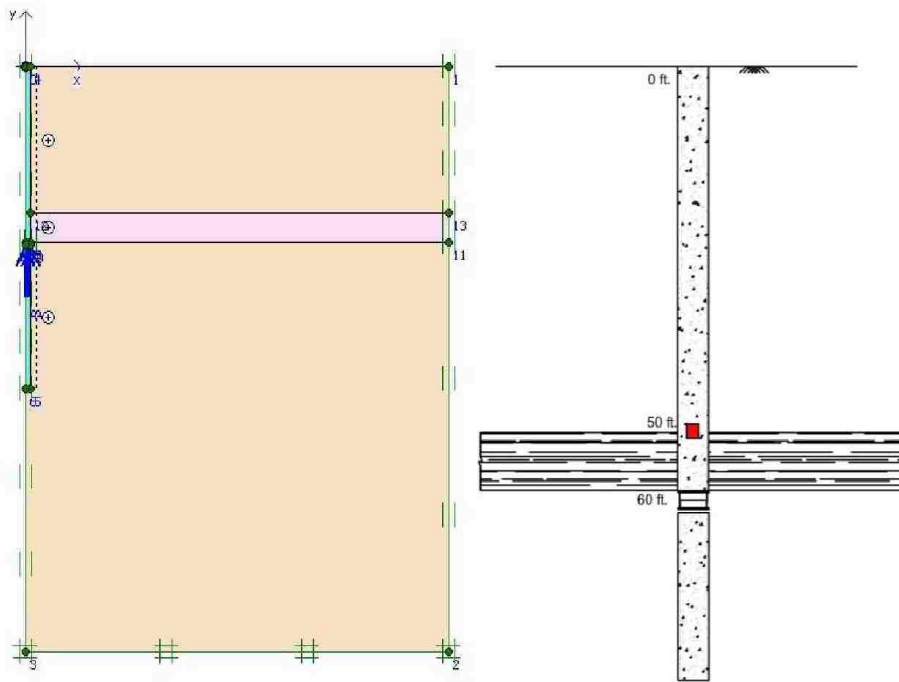


Figure 5-2: Osterberg Test with 10 ft. Caliche close to O-cell

The caliche layer is moved to higher elevations further from the O-cell location. The equivalent load-settlement from Osterberg interpretation and Top-down load are compared again and the results are saved. Caliche layer is moved to higher elevation in each analysis. In the final analysis the caliche layer is located at the furthest possible location from O-cell Figure 5-3. The Equivalent top-down behavior from Osterberg test is again compared to top-down loading.

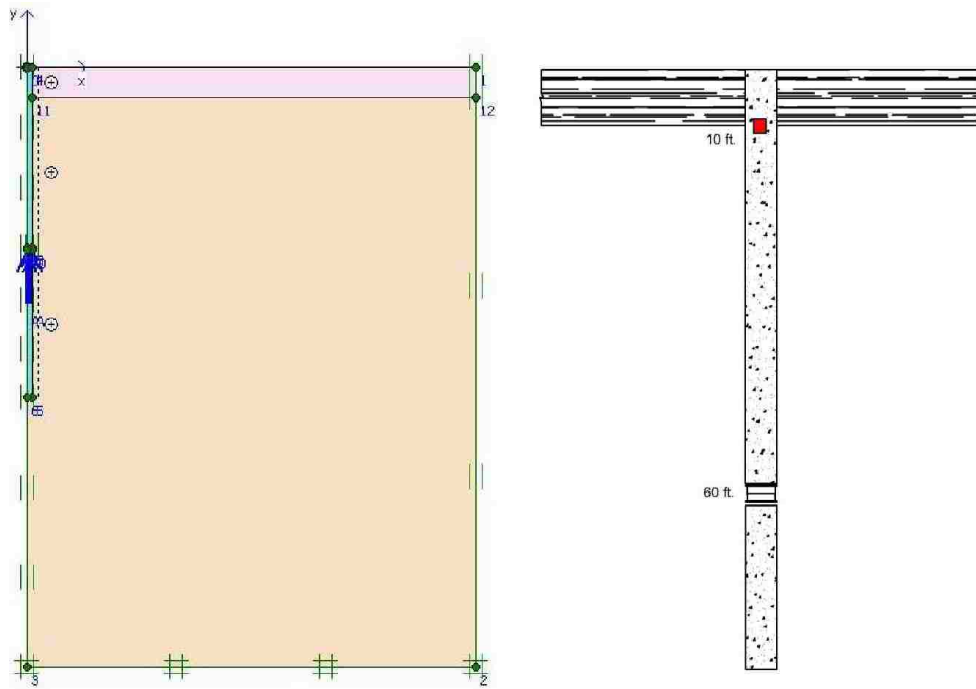


Figure 5-3 Osterberg Test with 10 ft. Caliche far from O-cell

Caliche and soil layer properties were kept the same for all the scenarios through this analysis. The only difference was the location of caliche with respect to O-cell.

5.5.1 Results and Discussion

The results of this analysis show that location of O-cell with respect to caliche layer can affect the interpretation of test results. As shown in Figure 5-4, by increasing the distance between O-cell location during the test and caliche layer, the settlement ratio calculated from Osterberg test results interpretation and conventional top-down results will decrease. This figure shows that for the least discrepancies between the Osterberg equivalent top-down results and an actual top-down loading scenario, the O-cell should be installed as close as possible to the caliche layer.

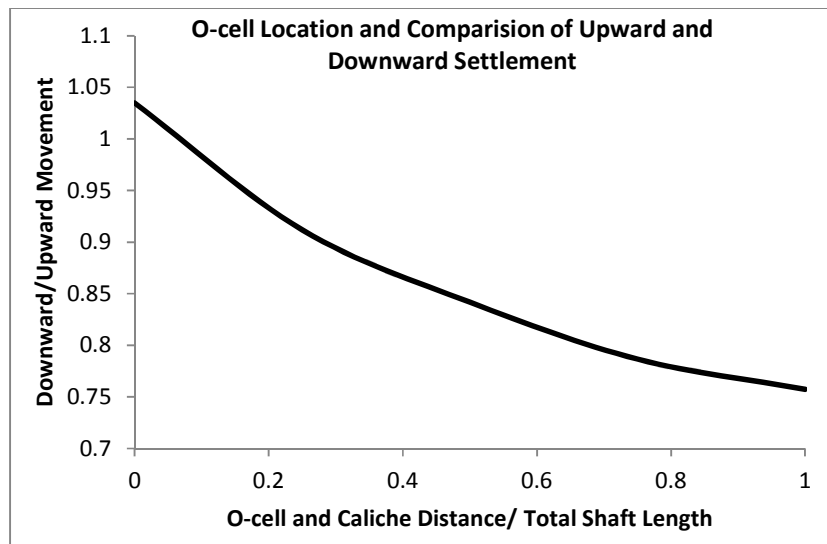


Figure 5-4: O-cell Location and Comparison of Upward and Downward Settlement

The caliche layer may not be mobilized enough for measuring its capacity when the O-cell is at a far distance from this layer. The load generated by O-cell dissipates through the soil layers and a small portion reaches the caliche layer close to the ground surface. When loaded from the top the same caliche layer is mobilized more and produced more resistance resulting in less settlement than what is expected from interpretation of the test results.

6 Case History Analysis

The analysis using PLAXIS consisted of the following two steps: The first step was to apply the initial stresses due to the self-weight of caliche and soil layers. The second step to apply the structural loads. The analysis was verified by comparing the predicted load-settlement and t-z curves with those measured in field load tests.

The analysis procedure is calibrated for three different cases depending on the location of caliche layers with respect to O-cell. To determine the difference between upward ultimate shaft resistance and downward ultimate shaft resistance in soils with caliche layers, two cases are designed and simulated using finite element software, PLAXIS 8.

6.1.1 Case History I: Caliche at the Furthest Location from O-Cell

The Osterberg test that was selected to be used for simulation purposes is for “I-215 Airport Connector” project. Caliche layers are concentrated very close to the ground surface and at the distant location from the O-cell as shown in Figure 6-1. Caliche layers are located at 18 and 30 feet and their thicknesses are 4 and 6 feet respectively. The boring log for this report is included in Appendix A. The O-cell is located at the depth of 80 ft. which is 50 ft. below the lower caliche layer and is loaded up to 3,316 kips. The one strain gauge used in the upper part of the shaft is located at 50 ft. deep.

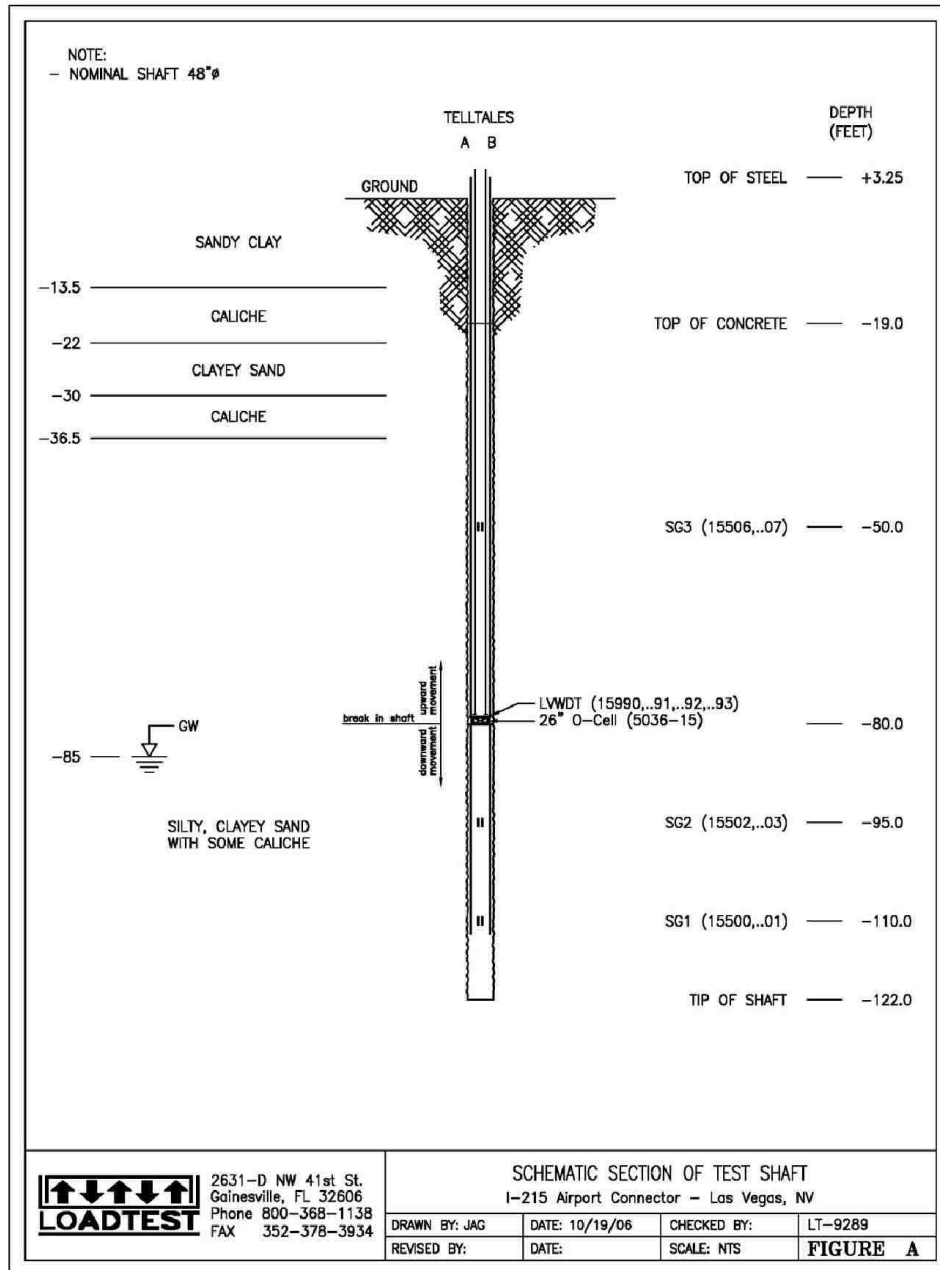


Figure 6-1: Schematic Section of Test Shaft

The PLAXIS model is created using the axisymmetric option which is the closest tool to a 3-dimensional analysis in this version. Dimensions and material properties are assigned to each element. The interface element is assigned to the soil-shaft interface. Very fine mesh is selected for the analysis purposes. The Osterberg test is performed in 15 loading stages up to 3316 kips. The same loading schedule is

applied to the PLAXIS model using the “Stage Construction” option. The water table is at 85 feet which is relatively low for Las Vegas soil profile. The PLAXIS model is shown in Figure 6-2.

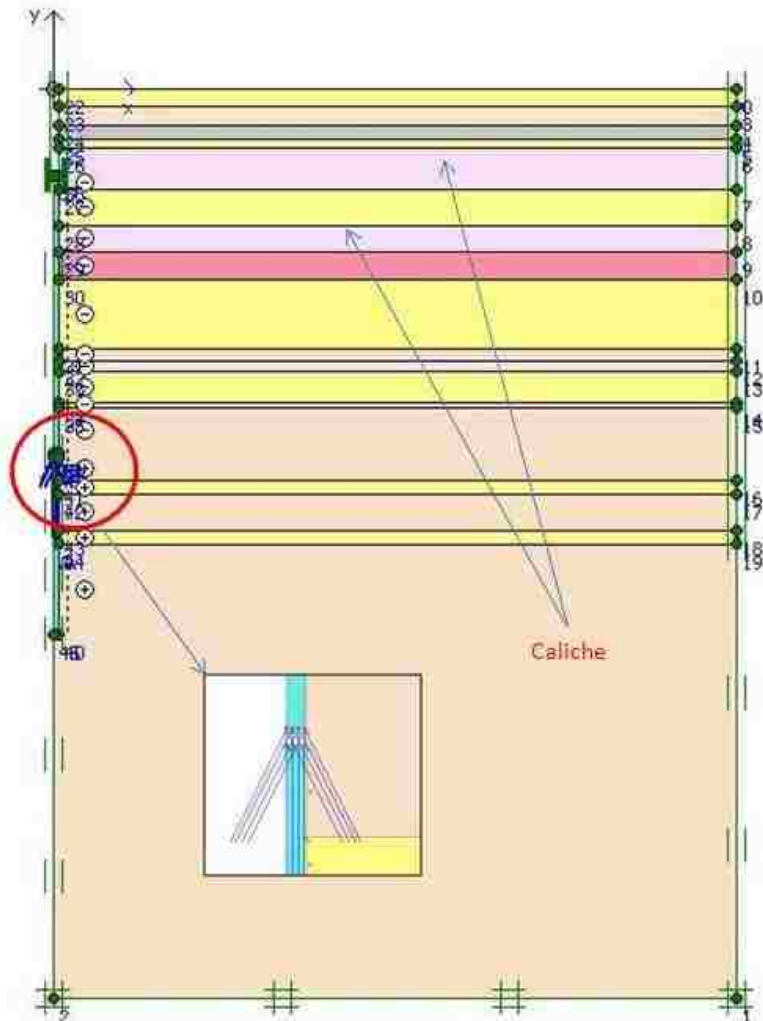


Figure 6-2: PLAXIS Simulations for I-215 and Airport Connector Load Test

6.1.1.1 Step-1: Calibration and back analysis for Osterberg Test

The Osterberg test for “I-215 Airport Connector” is simulated using PLAXIS 8 to determine the correct material properties. The strength properties of soil layers and caliche are subject to change within the allowable range from laboratory data to match the field measurements. In the analysis for both the O-cell test and

conventional head-down test, the following settings were assigned and some assumptions were made:

- 1) Axisymmetric model was adopted considering the boundary conditions of the pile load test.
- 2) Mohr Coulomb failure criterion was used for soil types and caliche layers.
- 3) Interface elements were incorporated along the shaft to simulate the soil-pile interaction and extend 0.1 ft. beyond shaft perimeter.
- 4) The O-cell is simulated with a 1-ft thick hollow space. For upward and downward loading scenarios the shaft is loaded in the hollow space provided.
- 5) According to the geotechnical description of the gathered borehole logs, all soils are sandy clay, clayey sand, stiff clay, cemented sand and gravel or caliche and behavior of all the soil strata can be assumed to be undrained since rapid loading method is used for Osterberg test.
- 6) Most of the soils can be regarded as normally consolidated according to the laboratory consolidation test result, although some overconsolidation of the stiffer soils may be possible.
- 7) No dilatancy effect of the soil was considered. For caliche the dilatancy of 1 degree is assumed.
- 8) The elastic compression of the pile is taken into account.

The calibrated PLAXIS model and actual Osterberg test Load-Movement curves are shown in Figure 6-3. There is a good match between the PLAXIS model and the actual test. The Calibration is only performed for the loading scenario unloading has not been addressed in this study.

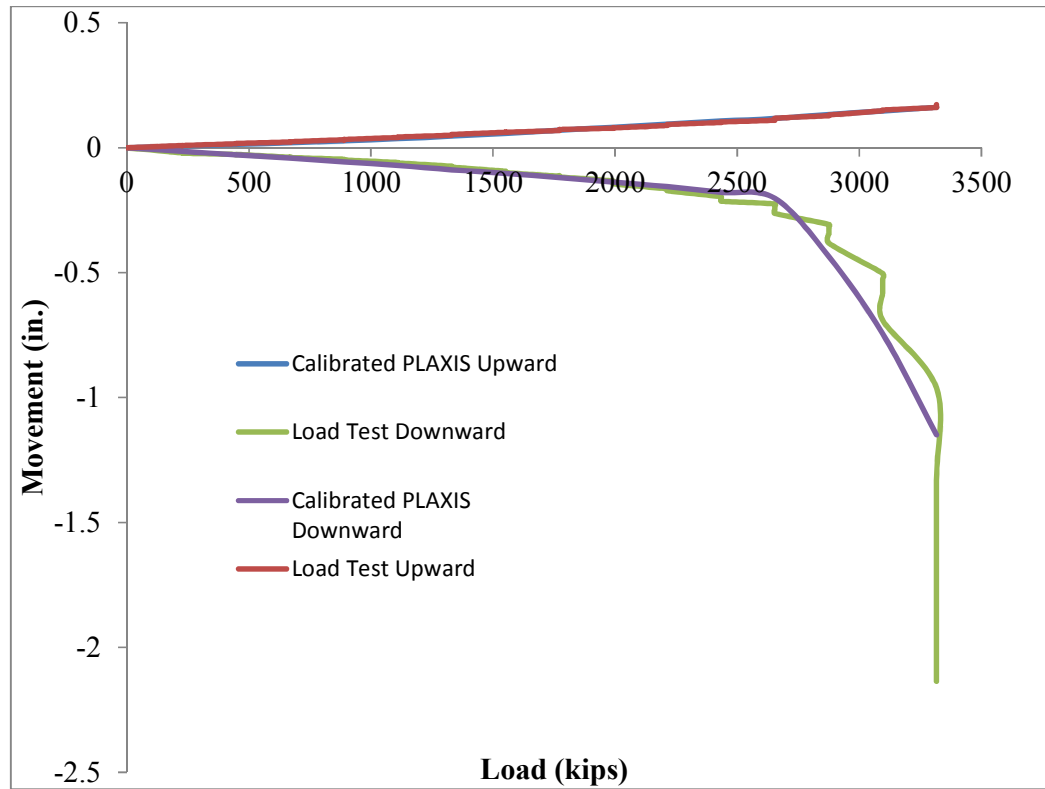


Figure 6-3: Osterberg Test Load- Movement Curve

6.1.1.2 Step-2: Material Properties and Soil Profile

The ACI formula ($E_c=57000\sqrt{f_c'}$) was used to calculate an elastic modulus for the pile concrete, in which f_c' was the concrete unconfined compressive strength and was reported to be 585,000 ksf. This combined with the area of reinforcing steel and nominal pile diameter, provided average pile stiffness (EA) of 7360000 kips in the upper cased portion of the shaft.

No field test data on the effective soil properties such as c' and ϕ' , undrained analysis with direct input of the undrained shear strength (C_u) and $\phi=\phi_u$ are available for the soil model. Drained soil parameters were used instead of undrained strength properties. The drained strength parameters are determined based on the field investigation and range of accepted correlations in local practice and lab results. The soil properties that were adjusted according to the comparison on back-analysis result and measured data to get the best fit are summarized in Table 6-1 together with the shaft concrete characteristics. In the material section a different material is assigned for the interface element. The interface has the elastic characteristics of the original material with less strength. The strength reduction is shown by decreasing the value of ϕ and c .

Table 6-1: PLAXIS Material Properties for I-215 and Airport Connector

Material Properties of I-215 and Airport Connector							
Parameter	Unit	Concrete	Clayey Sand	Sandy Clay	Cemented Sand and Gravel	Caliche	Stiff Clay
Material Model		Linear Elastic	M-C	M-C	M-C	M-C	M-C
Type of Behavior		Drained	Undrained	Undrained	Undrained	Undrained	Undrained
Dry Unit Weight	kcf	0.15	0.12	0.12	0.12	0.16	0.13
Saturated Unit Weight	kcf	0.15	0.12	0.13	0.13	0.16	0.13
Young's Modulus	ksf	445,600	1000	2000	4000	10,000	1000
Poisson's ratio		0.15	0.3	0.3	0.3	0.2	0.4
Cohesion	ksf	--	0.1	0.3	0.1	150	0.1
Friction Angle	Degree	--	35	28	45	35	28
Interface Material							
Material Model	Unit		M-C	M-C	M-C	M-C	M-C
Type of Behavior		--	Drained	Drained	Drained	Drained	Drained
Dry Unit Weight	kcf	--	0.12	0.12	0.12	0.16	0.13
Saturated Unit Weight	kcf	--	0.12	0.13	0.13	0.16	0.13
Young's Modulus	ksf	--	1000	2000	4000	10,000	1000
Poisson's ratio		--	0.3	0.3	0.3	0.2	0.4
Cohesion	ksf	--	0.1	0.3	0.1	150	0.1
Friction Angle	Degree	--	22	23	30	28	18

6.1.1.3 Step 3: Conventional Loading

The calibrated model is then used for conventional head-down loading scenario using the same amount of load applied by the O-cell except this time it is applied from the top shown in Figure 6-4.

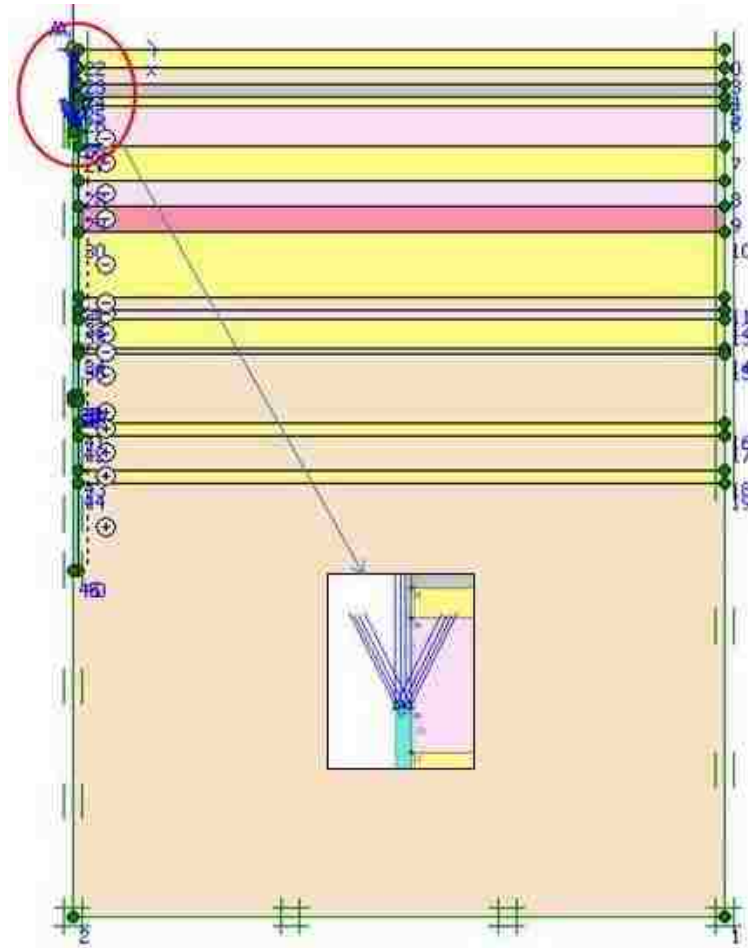


Figure 6-4: PLAXIS Simulation for Conventional Head-Down Loading

The results of both loading scenarios are compared in the following sections in form of load transfer, t-z curves and global load-settlement graph.

6.1.1.4 Load Transfer Curve

The load transfer curves for both Osterberg and conventional loading are displayed in Figure 6-5. The soil layers between caliche and O-cell are carrying more

loads in the upward loading compared to when the test is being performed from the top. Figure 6-5 shows that more load has been carried by caliche layers in the conventional loading scenario.

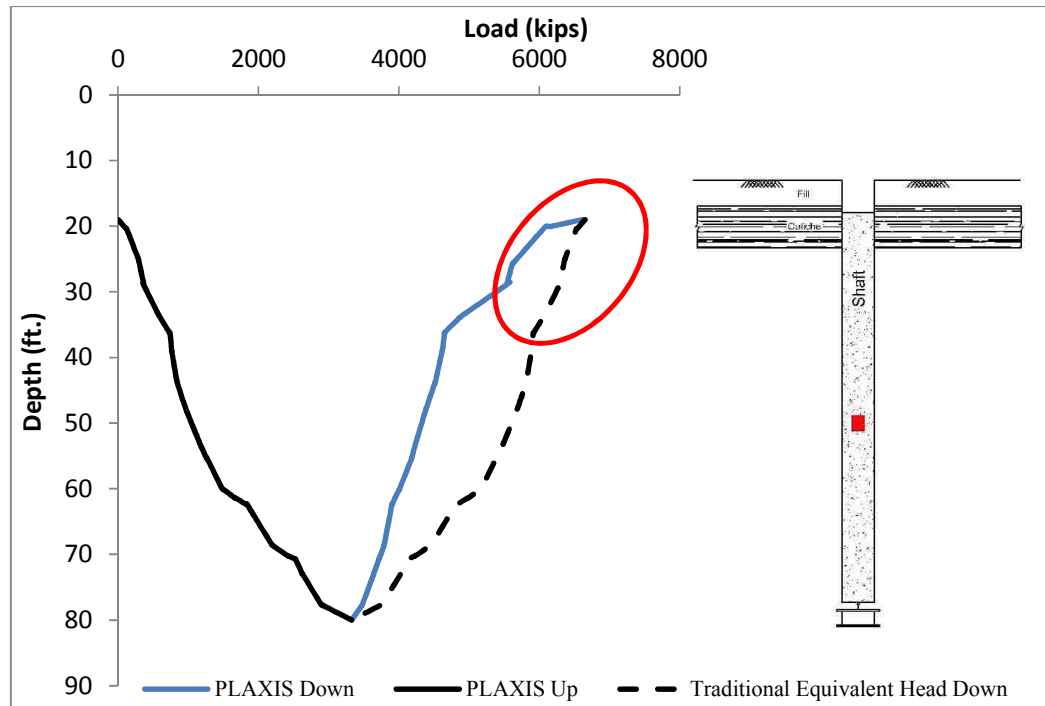


Figure 6-5: Load Transfer

The load transfer curve shows that the top load of 6400 kips is decreased to about 4500 kips from 19 to 36 ft. while the load transfer curves of O-cell tests shows only a decrease of 500 kips within the same length. The PLAXIS shows that the amount of dissipated load in the caliche from the conventional loading scenario is more than three times of what is calculated using the traditional method. Since caliche layer is at a distant location from to O-cell, it may not be fully mobilized during the Osterberg test. Therefore, the measured load bearing capacity of caliche is a fracture of its full capacity. Unlike Osterberg test, similar load from the top can mobilize caliche more and consequently more unit shear stress will be developed.

6.1.1.5 t-z Curve

The t-z curve from the Osterberg test result and calibrated model are compared to theoretical conventional loading. Figure 6-6 consists of t-z curve for points between strain gauge location at 50 feet and the top of the shaft at 20 feet. Figure 6-7 consists of t-z curve for the points between 50 and 80 ft. (O-cell location).

As depicted in Figure 6-6 and Figure 6-7, the calibrated PLAXIS model gives fairly close result to the O-cell test; the shaft shear resistance in between 50-80 ft. is reaches its ultimate capacity of about 6 ksf during the load test while the shear resistance of shaft between 20-50 ft. reaches 3 ksf at a relatively linear-elastic condition. The same load is applied from the top and the unit shear resistance between 20 to 50 ft. reaches to 6 ksf when the shear resistance between 50 and 80 ft barely gets close to 3 ksf. These results agree well with the assumption that the caliche layers located at a distant location from O-cell are not fully mobilized to develop their ultimate capacity.

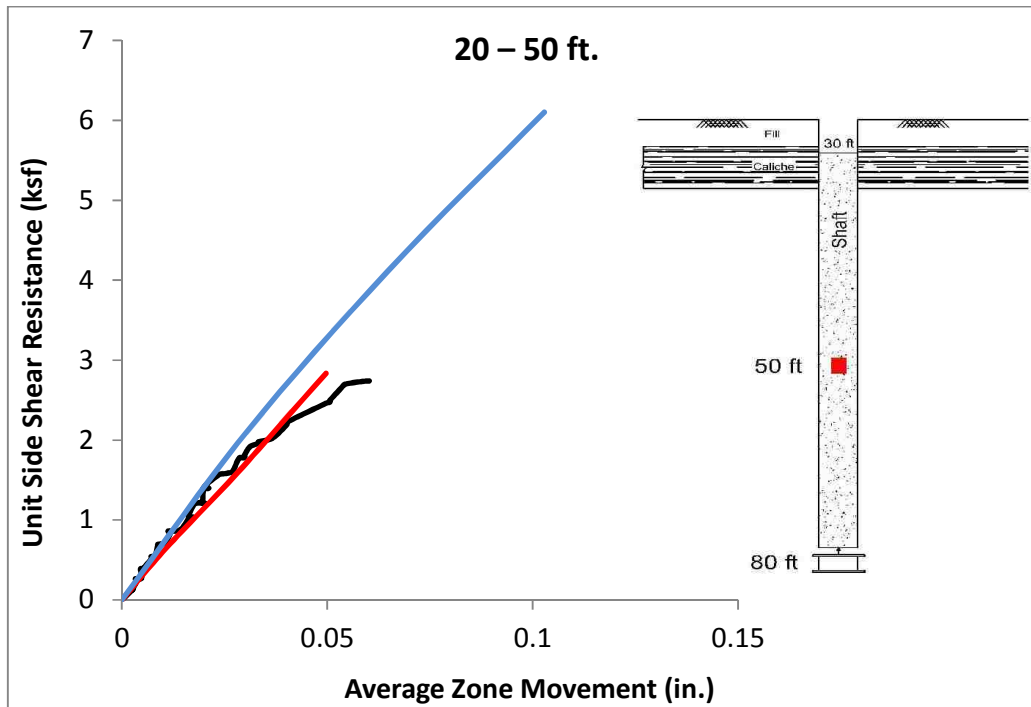


Figure 6-6: t-z Curve between 20 -50 ft.

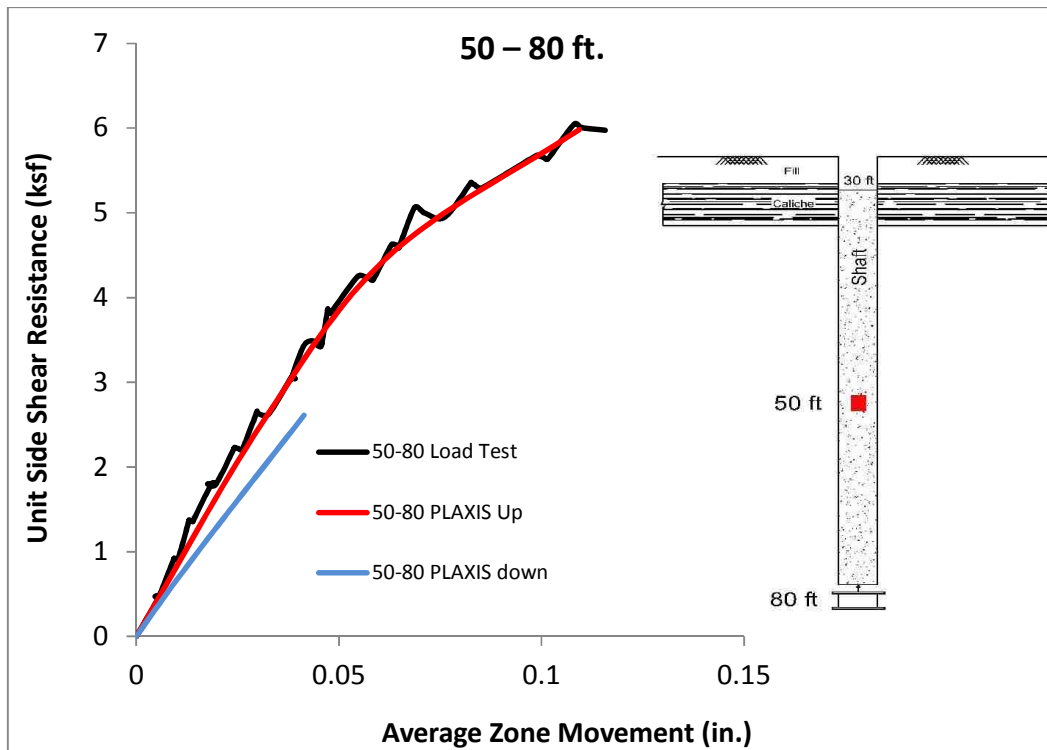


Figure 6-7: t-z Curve between 50 -80 ft.

6.1.1.6 Equivalent Load-Settlement Curve

The theoretical head-down load-settlement graph is re-constructed and compared with the equivalent load-movement curve traditionally obtained from O-cell test results. Figure 6-8 shows the load-settlement results for the traditional method and the new analysis. For a certain displacement the associated load is less in the new analysis compared to what it is being used traditionally.

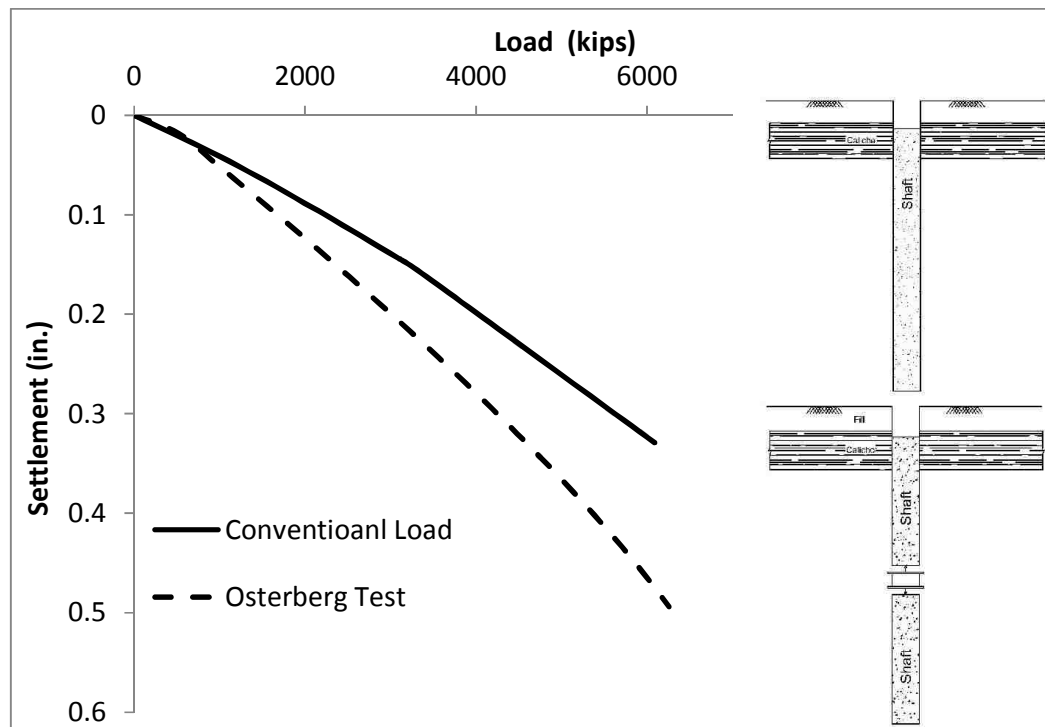


Figure 6-8: Equivalent Load Settlement Curve for Traditional Method and Proposed Method

6.1.2 Case History II: Caliche Close To O-Cell

The Osterberg test that was selected to be used for simulation purposes is for “Palm Resort” project. O-cell is installed closed to Caliche layers. There are 3 more drilled shaft tests in the database that have the same layout. PLAXIS 8 is used to simulate the Osterberg test. The O-cell is located at 40 ft. where the 15 ft. caliche ends. The strain gauges are located at 30 and 20 ft. in the shaft. The test layout can be seen in Figure 6-9. The O-cell is loaded up to 6128 kips during the test.

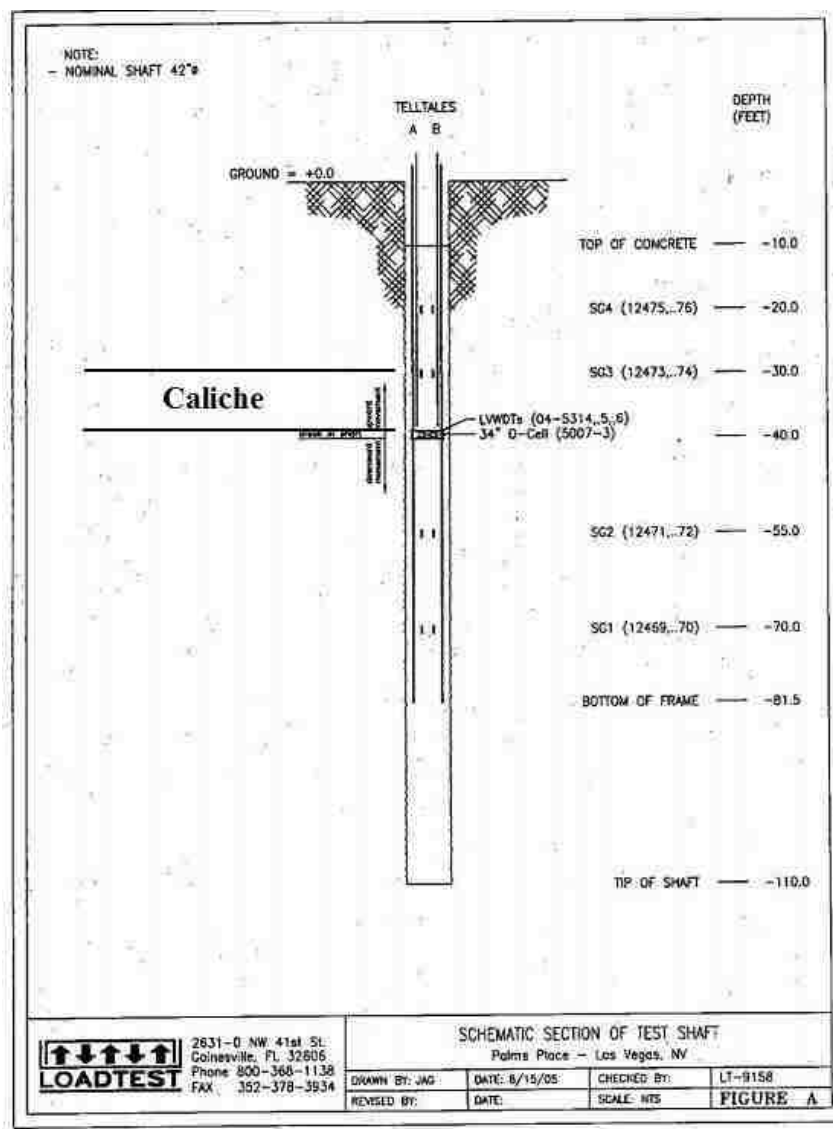


Figure 6-9: Schematic Section of Test Shaft

The PLAXIS model is created using the axisymmetric option which is the closest tool to a 3-dimensional analysis in this version. Dimensions and material properties are assigned to each element. The interface element is assigned to the soil-shaft interface. Very fine mesh is selected for the analysis purposes. The Osterberg test is performed in 10 loading stages up to 6128 kips. The same loading schedule is applied to the PLAXIS model using the “Stage Construction” option. The water table is at 22 feet which is right above the beginning of caliche layer. The PLAXIS model is shown in Figure 6-10.

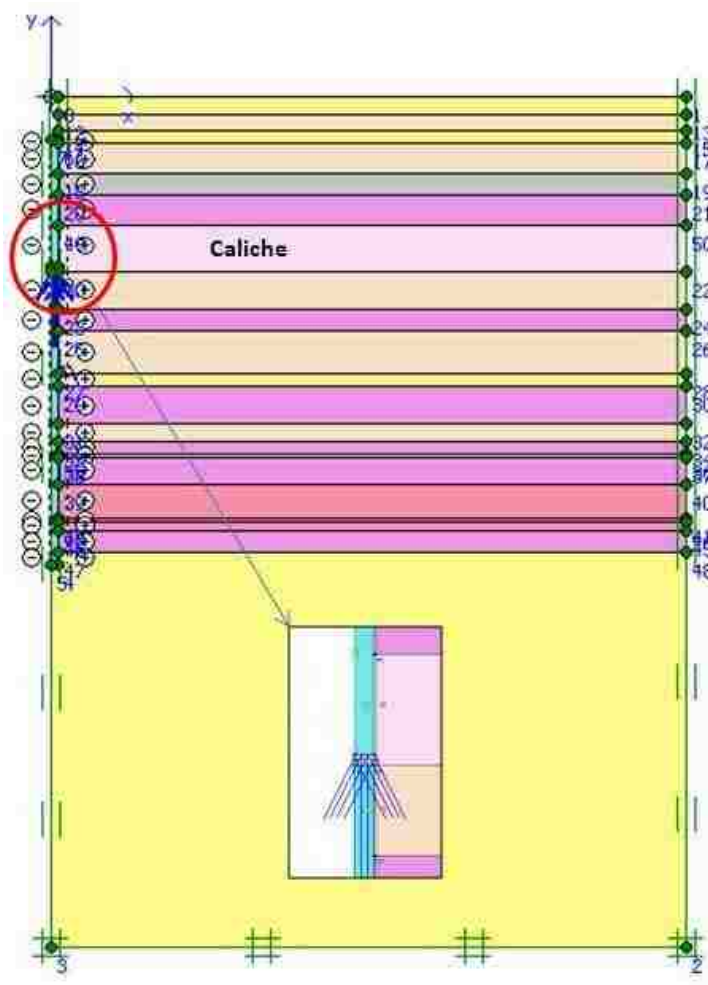


Figure 6-10: PLAXIS Simulations for Palm Load Test

6.1.2.1 Step-1: Calibration and back analysis for Osterberg Test

The Osterberg test for “Palm Resort” is simulated using PLAXIS 8 to determine the correct material properties. The strength properties of soil layers and caliche are subject to change within the allowable range from laboratory data to match the field measurements. In the analysis for both the O-cell test and conventional head-down test, the following settings were assigned and some assumptions were made:

In the analysis for both the O-cell test and conventional head-down test, the similar settings as the first case history were assigned.

The calibrated PLAXIS model and actual Osterberg test Load-Movement curves are shown in Figure 6-11. There is a good match between the PLAXIS model and the actual test. The Calibration is only performed for the loading scenario unloading has not been addressed in this study.

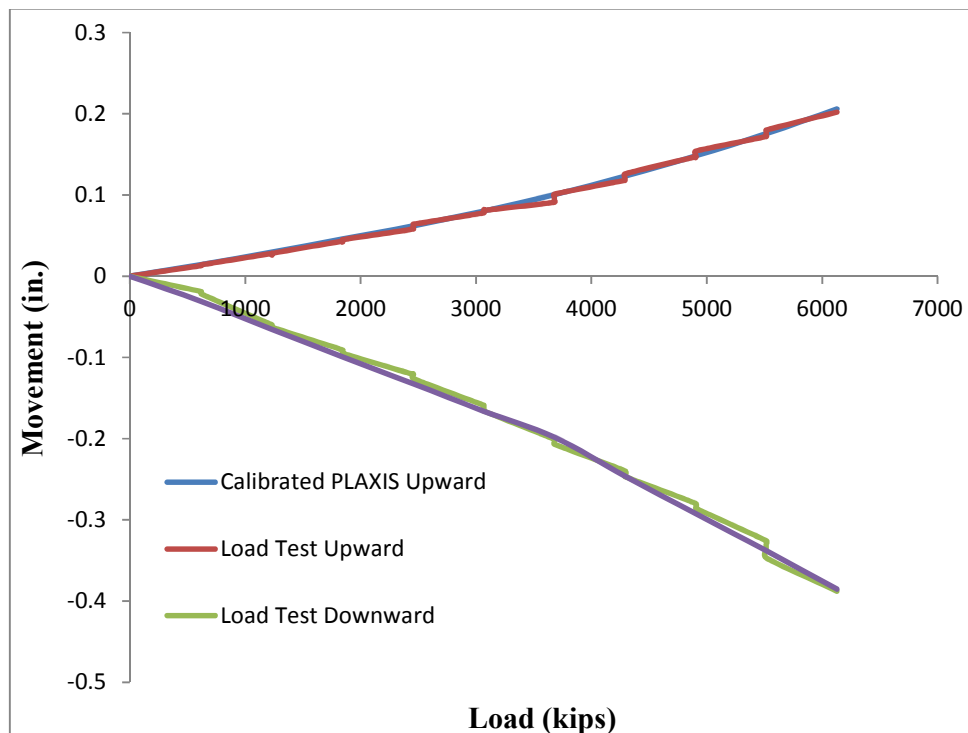


Figure 6-11: Osterberg Test Load- Movement Curve

6.1.2.2 Step-2: Material Properties and Soil Profile

The ACI formula ($E_c=57000\sqrt{f_c'}$) was used to calculate an elastic modulus for the pile concrete, in which f_c' was the concrete unconfined compressive strength and was reported to be 445,000 ksf. This combined with the area of reinforcing steel and nominal pile diameter, provided average pile stiffness (EA) of 5600000 kips in the upper cased portion of the shaft.

No field test data on the effective soil properties such as c' and ϕ' , undrained analysis with direct input of the undrained shear strength (C_u) and $\phi=\phi_u$ are available for the soil model. Undrained soil parameters were determined here according to the field investigation and range of accepted correlations in local practice and lab results which are mostly performed assuming a drained test environment.

The material properties used to calibrate the PLAXIS model are presented in Table 6-2. In the material section a different material is assigned for the interface element. The interface has the elastic characteristics of the original material with less strength. The strength reduction is shown by decreasing the value of ϕ and c based on the reduction factors introduced by NAVFAC (1982).

Table 6-2: PLAXIS Material Properties for Palm

Material Properties of Palm							
Parameter	Unit	Concrete	Clayey Sand	Sandy Clay	Cemented Sand and Gravel	Caliche	Stiff Clay
Material Model		Linear Elastic	M-C	M-C	M-C	M-C	M-C
Type of Behavior		Drained	Drained	Drained	Drained	Drained	Drained
Dry Unit Weight	kcf	0.15	0.12	0.12	0.12	0.16	0.13
Saturated Unit Weight	kcf	0.15	0.12	0.13	0.13	0.16	0.13
Young's Modulus	ksf	445,600	1000	1500	3000	560,000	1000
Poisson's ratio		0.15	0.3	0.3	0.3	0.2	0.4
Cohesion	ksf	--	0.8	1	0.1	20	0.2
Friction Angle	Degree	--	35	28	45	35	30
Interface Material							
Material Model	Unit		M-C	M-C	M-C	M-C	M-C
Type of Behavior		--	Drained	Drained	Drained	Drained	Drained
Dry Unit Weight	kcf	--	0.12	0.12	0.12	0.16	0.13
Saturated Unit Weight	kcf	--	0.12	0.13	0.13	0.16	0.13
Young's Modulus	ksf	--	1000	1500	3000	560,000	1000
Poisson's ratio		--	0.3	0.3	0.3	0.2	0.4
Cohesion	ksf	--	0.8	1	0.1	20	0.2
Friction Angle	Degree	--	22	23	30	28	18

6.1.2.3 Step 3: Conventional Loading

Similar to the first case, the calibrated model is used to model conventional head-down loading scenario using the same amount of load applied by the O-cell except this time it is applied from the top which is presented in Figure 6-12.

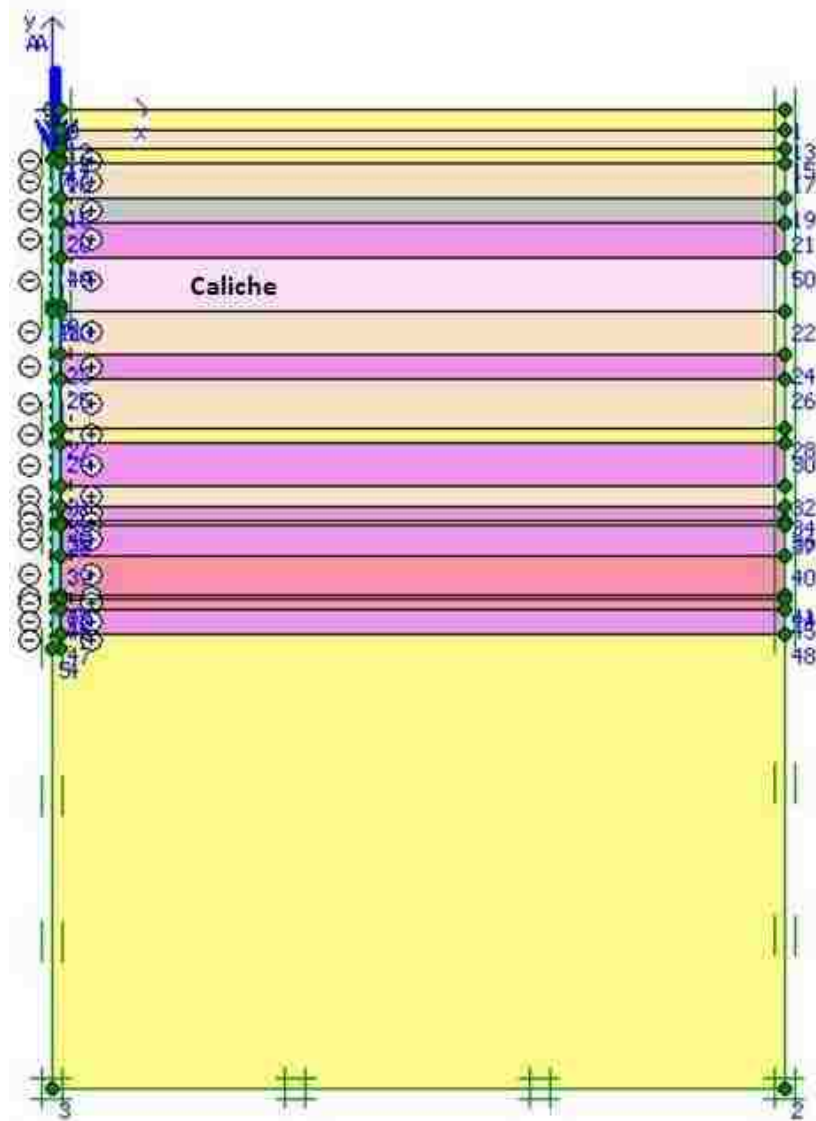


Figure 6-12: PLAXIS Simulation for Conventional Head-Down Loading

The results of both loading scenarios are compared in the following sections in form of load transfer, t-z curves and global load-settlement graph.

6.1.2.4 Load Transfer Curve

The load transfer curves for both Osterberg and conventional loading are displayed in Figure 6-13. The caliche and soil layers carry a relatively similar load during the conventional loading compared to when the Osterberg test is being performed.

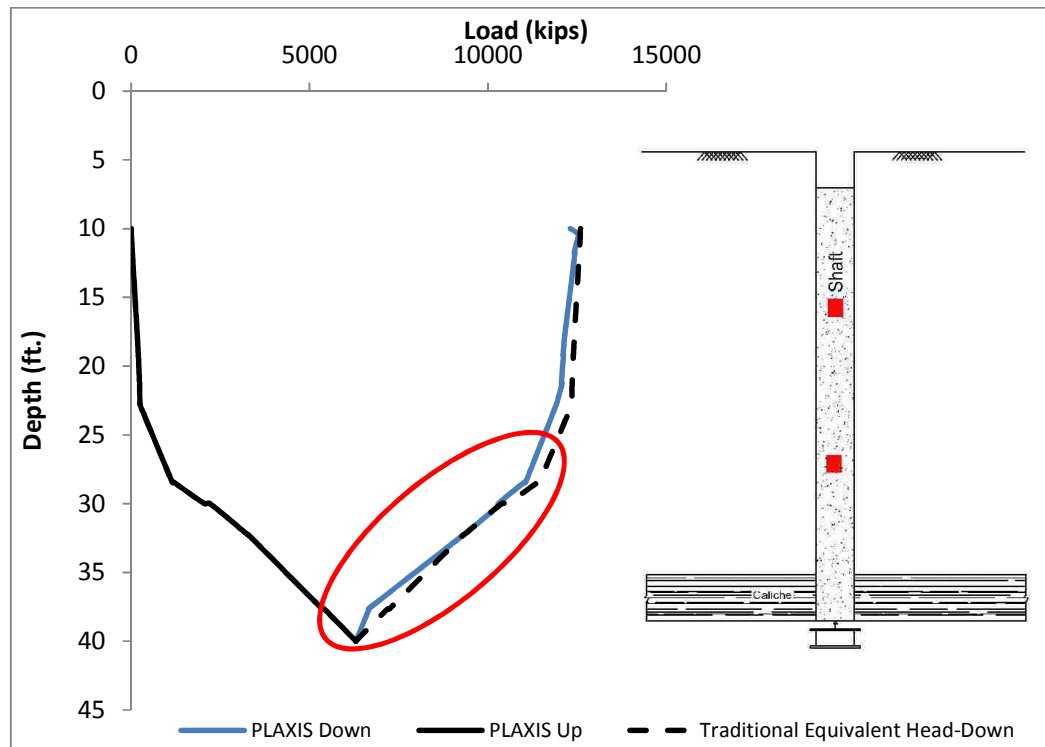


Figure 6-13: Load Transfer

The minor differences are coming from a few geometrical close to the ground surface that are mobilized further compared to when the O-cell test was being performed. Caliche is still the most dominant load carrying mechanism in this test layout. Additionally, the results are very similar to a rock socketed drilled shaft. The caliche shows almost the same bearing capacity whether it is loaded upward or downward. The major difference between this scenario and the first scenario is the fact the caliche is mobilized more during the Osterberg test when O-cell is close to the

caliche. Accordingly, when the load is being applied from the top, the load transfer mechanism stays close to the measurements. Unlike the first case, caliche does not show any excessive capacity due to further mobilization.

6.1.2.5 t-z Curve

The t-z curve from the O-cell test and calibrated PLAXIS model are compared to theoretical conventional loading. Figure 6-14 includes t-z curves for points between strain gauges located at 35.3 feet and the top of the shaft at 8 feet. Figure 6-15 includes t-z curves for the points between 35.3 and 48.1 ft. and, Figure 6-16 includes t-z curves for the points between 48.1 and 57 ft.

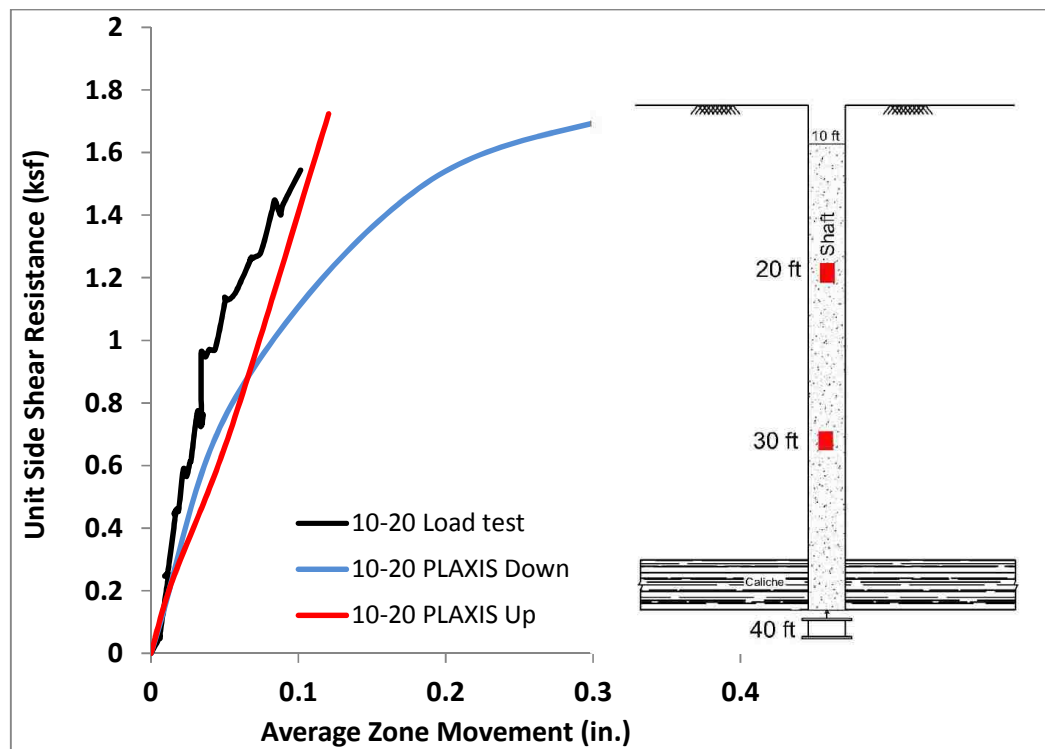


Figure 6-14: t-z Curve between 10 – 20 ft.

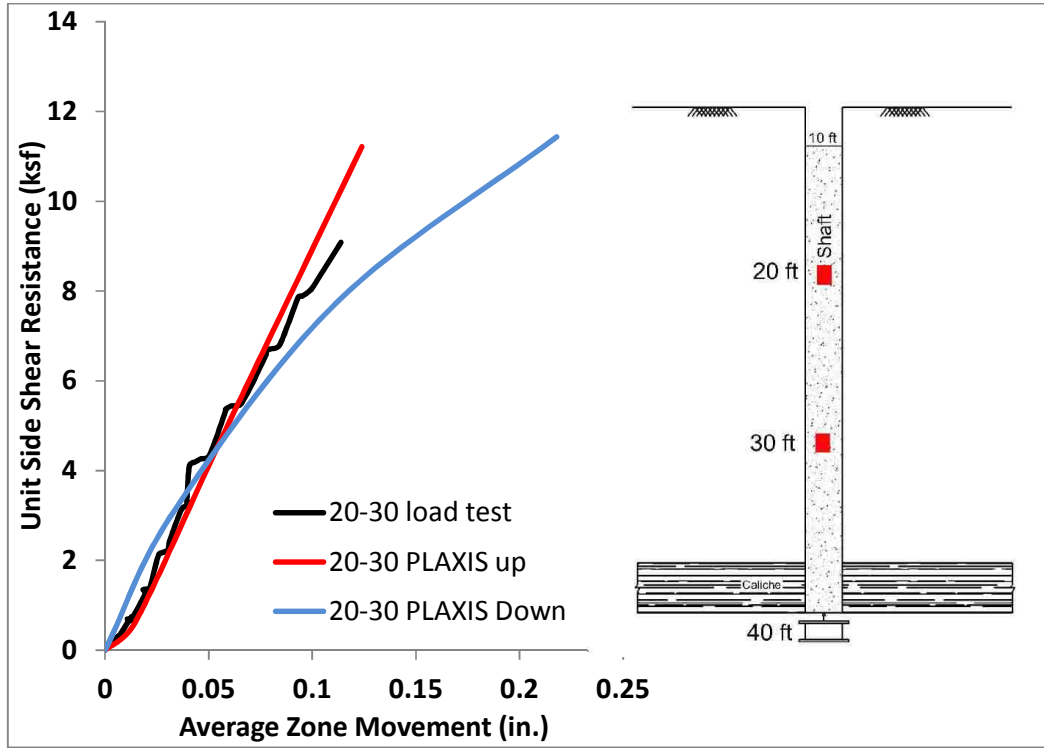


Figure 6-15: t-z Curve between 20-30 ft.

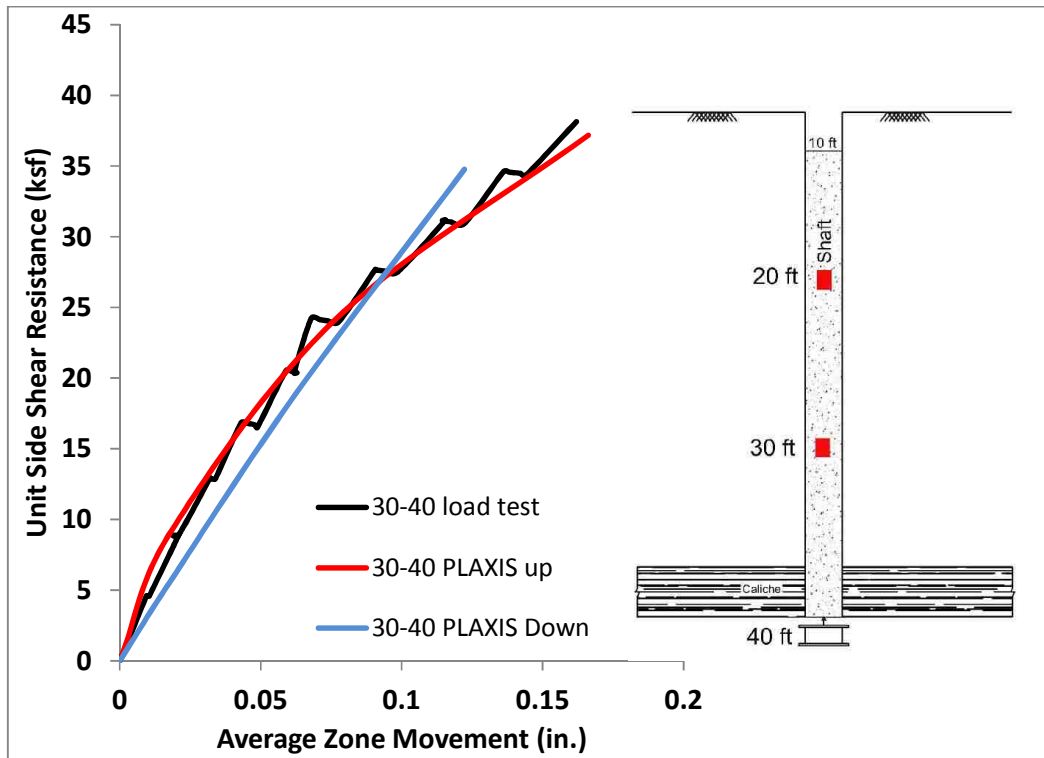


Figure 6-16: t-z Curve between 30-40 ft.

It can be perceived from Figure 6-14, Figure 6-15 and Figure 6-16, that the model follows the same load-settlement path in all strain gauge zones, whether it is an Osterberg test or a conventional loading. The geomaterial close to the ground surface are mobilized more during a conventional loading compared to when they were loaded from the bottom during O-cell test. However, being mobilized more is not associated with more loads since they already reached failure during the Osterberg test and their capacity is known. The calibrated PLAXIS model gives fairly close result to the O-cell test. The results show that when the O-cell is placed close to the caliche layer the difference between upward and downward loading is minimal.

6.1.2.6 Equivalent Load-Settlement Curve

The theoretical head-down load-settlement graph is re-constructed and compared with the equivalent load-movement curve traditionally obtained from O-cell test results. Figure 6-17 shows the load-settlement results for the traditional method proposed by Osterberg (1984) is comparable to when the shaft is loaded conventionally from the top. For a certain displacement points the associated load is a little more in the proposed method compared to what it is being used traditionally due to the presence of cemented geomaterial close to the ground surface.

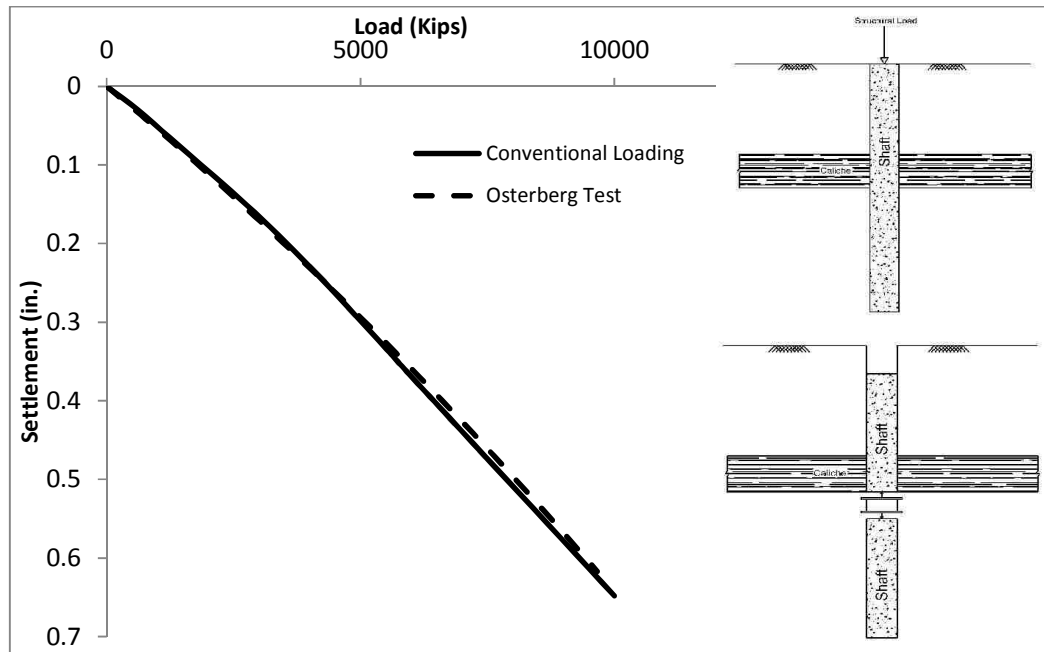


Figure 6-17: Equivalent Load Settlement Curve for Traditional Method and Proposed Method

6.1.3 Results and Discussion

Two extreme scenarios were analyzed and the results were presented in the previous sections. The difference between the two scenarios was simply the installation location of O-cell with respect to caliche layers during Osterberg test. In the first scenario, caliche layer was concentrated at a distant location from the O-cell location where in the second scenario caliche layer is right above the O-cell.

It could be perceived from the results that the caliche is not fully mobilized when the load cell is located very far from it. The load is dissipated through the soil layers and a very small residue is left to mobilize the caliche. Hence, the resistance developed for the caliche is for a small mobilization and does not represent the caliche capability fully. When the same load is applied from the top, the same caliche layer is mobilized more because it is closer to the load source. Therefore, higher shear resistance is developed during this loading scenario, as shown in Figure 6-19. It is now clear that

the existing caliche layer can carry more loads compared to what it is tested for. Theoretical elastic compression in top loaded test based on pattern of developed side shear stress is calculated using equation (6-1).

$$\delta_{\downarrow} = [(C_1)Q'_{\downarrow} + (1 - C_1)P] \frac{L}{EA} \quad (6-1)$$

And to model the elastic compression of the upper section of the pile above the point of application of load, is calculated using equation (6-2).

$$\delta_{\uparrow} = [(C_1)Q'_{\uparrow}] \frac{L}{EA} \quad (6-2)$$

Where, C_1 is the centroid of unit side friction values for the strain gauge zones in the upper shaft unit as seen on Figure 6-18. To estimate the top down elastic behavior, it is possible to subtract from the total for the section, as in equation (6-1), the elastic compression integrated already in the measured upward response, as in equation (6-2). Alternatively, it can be recomputed, but now the friction is effective from the top.

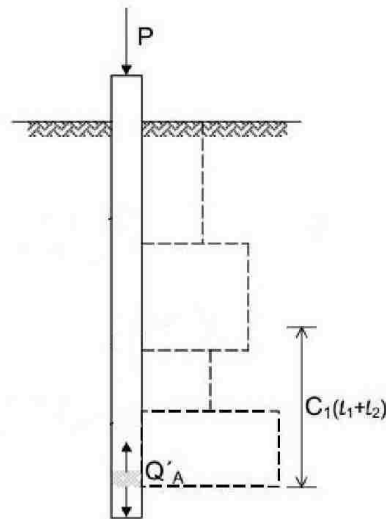


Figure 6-18: Developed Side Shear Resistance

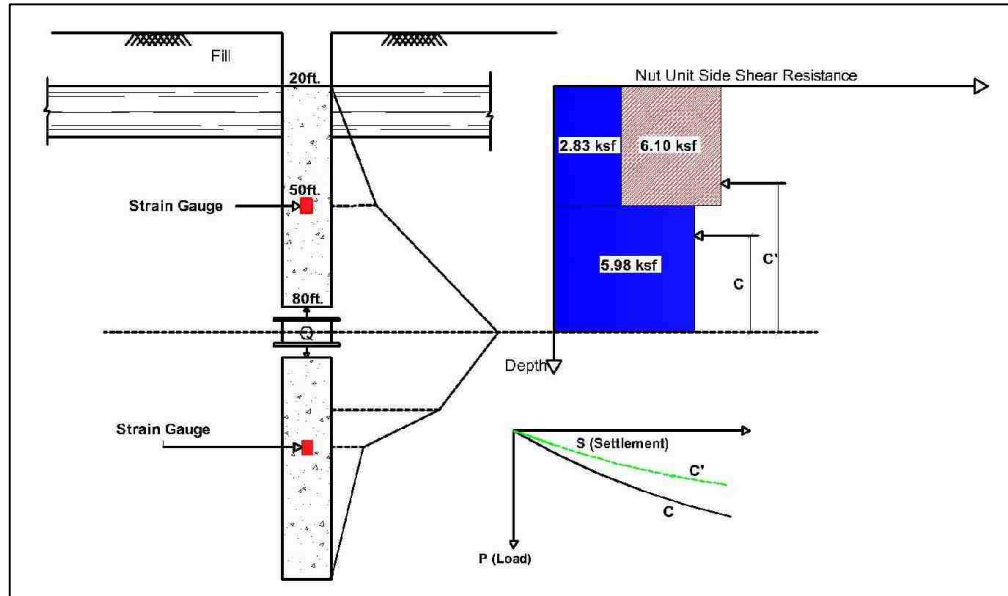


Figure 6-19: Unit Side Resistance and Load-settlement Comparison for O-cell test and Conventional Test (Case I)

During the Osterberg test, the unit side resistance that is developed between 20 and 50 ft. where the caliche exist is less than what is developed during the theoretical conventional loading of the shaft. The value of side resistance during a conventional load is at about 6 ksf which is almost twice what is developed during Osterberg test (3 ksf). Since caliche is located at a far distance from the O-cell, it is not mobilized enough to develop full capacity. During the head-down load a better behavior of caliche and its capacity can be observed through the developed side resistance value. The increase in caliche side resistance will affect the calculations for elastic shortening. By increasing the side resistance between 20 and 50 ft. the value of centroid for side resistance values “C” increases. By implementing the new “C” value in equations (6-1) and (6-2) and the precedent calculations it can be understood that the elastic shortening of the shaft decreases. As a results, the settlement in the equivalent top-down load-settlement curve decreases. For certain settlement more load can be used to design the shaft.

For the second case the caliche is very close to the O-cell and because of that, it is mobilized as much as the equipment allows us. The other soil layers above caliche also partially developed their failure and capacity load through the test. When the same load is applied from the top, soil layers in between the caliche and load fail and show some excessive movement but no extra side resistance is developed through this process. The transferred load eventually reaches caliche and develops the same unit side resistance as was developed during the Osterberg test. Since there is small to no changes in the side resistance during different loading orientations, the value of “C” does not change.

Accordingly, the load settlement graph for this shaft is the same for both loading orientation as shown in Figure 6-20.

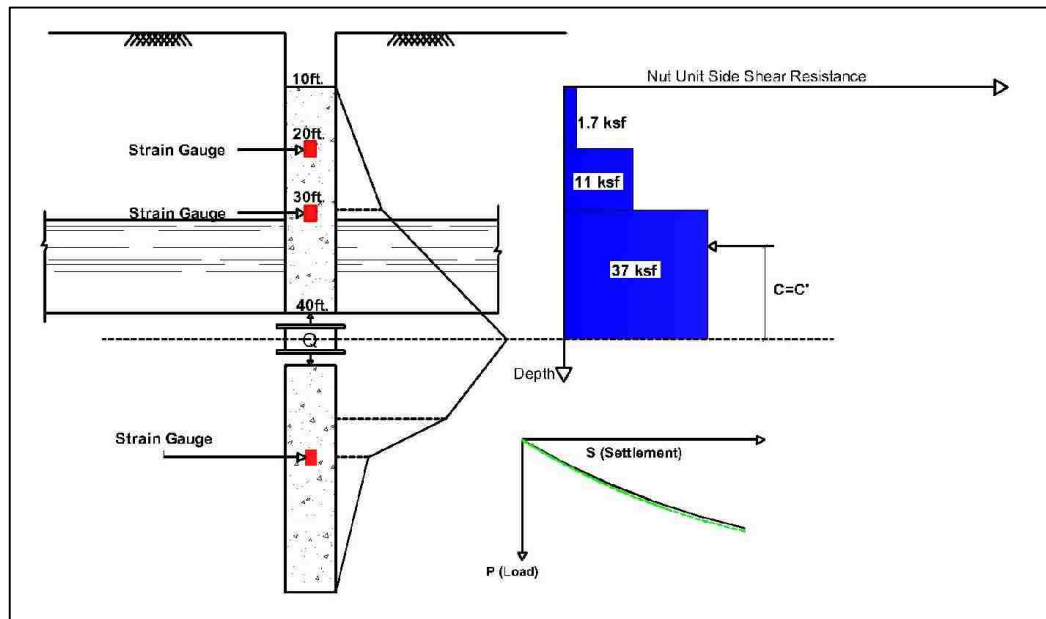


Figure 6-20: Unit Side Resistance and Load-settlement Comparison for O-cell test and Conventional Test (Case II)

7 CONCLUSIONS AND RECOMMENDATIONS

The findings in this thesis are:

- 1) It is concluded from the earlier FEM study that O-cell test result can provide different soil-pile interaction information as conventional head-down static loading test when the O-cell is installed in a relatively distant location to the most competent caliche.
- 2) The FEM computation indicates that the shaft resistance-movement curve for upward movement of the pile is fairly comparable with the downward shaft resistance-movement component of a conventional head-down test when the O-cell is installed very close to the caliche layer.
- 3) Selecting a proper installation location for O-cell increases the chance of failing caliche layers in side resistance. It is shown with a proper test design the side resistance of 25 ksf could be measured for caliche layers.
- 4) Caliche layers that are located close to the ground surface show an extra deflection during the Osterberg test that can be interpreted as flexural deflection. The reference beam readings is reversible during unloading when caliche is very close to the ground surface meaning the a portion of total deflection can be dedicated to elastic bending of caliche layer.

Based on this research effort, the following efforts should be taken to properly design an Osterberg load test in Las Vegas:

- 1- Perform borings and obtain samples at least every 5 feet close to the ground surface and 10 feet after 50 feet.

- 2- Coring and triaxial and unconfined compression tests for calculating the caliche capacity.
- 3- Calculate the ultimate side resistance values for all soil layers and caliche.
- 4- For caliche check the ultimate side resistance value with the pertinent empirical equations for rock.
- 5- Locate the most competent caliche in the soil profile and install the O-cell under the caliche layer.
- 6- Design the lower section of the shaft for downward loading in a way that the theoretical side resistance from lower section of the shaft is equal to the side resistance of the shaft from upper section + caliche
- 7- Before performing the test, the test should be modeled with PLAXIS 2D and the equivalent top-down behavior from Osterberg test results should be compared to conventional top-down load. If there is discrepancies between the two, the shaft length in the lower section should be adjusted to minimize the discrepancies.
- 8- Load test is performed and the results are used for design of production shaft.

7.1 Recommendations for Further Research

- 1) Ideally, side-by-side comparisons on identical test shafts constructed in the same soil profile containing caliche layer with similar characteristics and properties are needed to assess differences in upward and downward behavior of drilled shaft. It is expected that the potential differences, if any, will

eventually be identified and incorporated into interpretation methods for O-cell testing.

- 2) The bending of caliche should be investigated more thoroughly by acquiring more pertinent load test data. The data should include caliche at various location to understand the flexural capacity of caliche with respect to its location. It is expected that for deeper caliche layers the flexural behavior of caliche is less dominant compared to frictional behavior.
- 3) Proper distribution of strain gauges will help achieve a realistic load distribution along the shaft length. For strain gauge measurements to accurately represent the average distribution, it is recommended to place them no closer than three pile diameters above and below the cell.
- 4) The FEM analysis was performed with PLAXIS 8 during this study. The newer version of PLAXIS has more advanced constitutive models for rocks e.g. Drucker-Prager that can simulate the rock-socket behavior more realistic. Additionally, PLAXIS-3D could give more realistic results by simulating the whole project site using the borehole option provided in the latest version.
- 5) Core sampling and unconfined compression test should be performed on the caliche in Las Vegas to be able to correlate the field load test data to theoretical methods for estimating caliche capacity that are introduced in the literature.

APPENDIX A

Field and Laboratory Data

INTRODUCTION

A significant number of geotechnical investigations have been performed for various projects in Las Vegas mostly on the strip area which resulted in numerous borings and associated laboratory data. Some of the data that was acquired from laboratory and field tests are categorized and analyzed to be used as input for the modeling and analysis chapter.

GENERAL SOIL PROFILE IN LAS VEGAS

Las Vegas soil stratigraphy consist of 7 to 8 significant soil types including, clayey Sand (SC), silty sand (SM), lean clay with traces of caliche or gravel (CL), fat clay (CH), sand and gravel (GP, GM, GC) and cemented layers such as cemented sand and gravel or caliche. A review of the boring data indicates the caliche layers could be continuous or segregated depending on the location of site, depth and age of caliche layer. The clay covers a wide range starting from very soft to very hard clay which can be recognized by the blow counts and lab tests on clayey material in this region. Layers of silty and clayey sand were also observed in some depth; partially cemented sand, specially when they are mixed with clay can be observed in some locations.

LAB DATA

Soil testing results acquired for this study consist of, unit weight of caliche Atterberg Limits, unconfined compression, direct shear and triaxial tests. The results of laboratory test are discussed in the following subchapters.

ATTERBERG LIMITS (SOIL LAYERS)

Atterberg Limits test data (ASTM D4318) for different job sites is gathered and documented. For each type of soil the liquid limit, plastic limit and the plasticity index is documented. The variation of plasticity index values versus depth for each type of soil is shown in Figure A- 1.

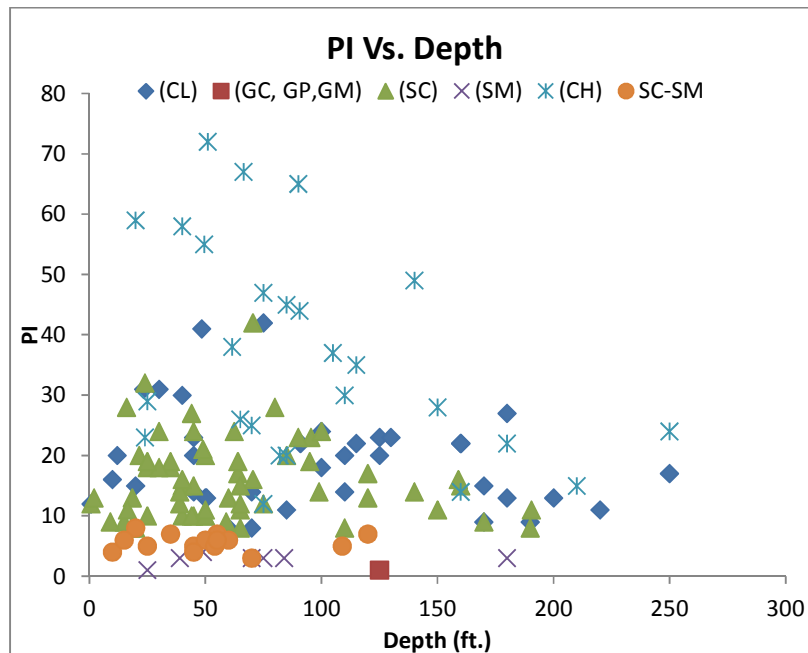


Figure A- 1: Plasticity Index vs. Depth for different Soil Types in Las Vegas

DIRECT SHEAR TESTS (SOIL LAYERS)

Direct shear test data (ASTM D3080) for different job sites was obtained and documented. Samples tested were obtained from ring samples. For each type of soil the friction angle and cohesion value is documented and a range of Mohr-Coulomb

strength parameters for each soil type is obtained. The variation of cohesion value vs. depth is shown in Figure A- 2.

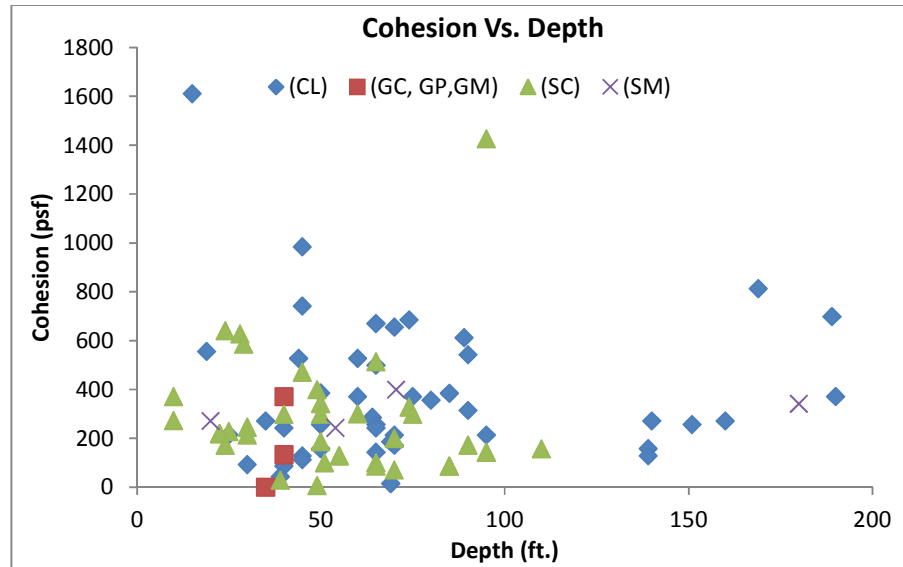


Figure A- 2: Cohesion vs. Depth for different Soil Types in Las Vegas

ATTERBERG LIMITS AND SOIL STRENGTH PARAMETERS CORRELATION

High quality undisturbed samples are difficult to obtain due to presence of caliche layers and cemented geomaterial so, the soil strength parameters are developed using correlations between plasticity index and friction angle (Terzaghi, 1996). For granular material and lean clay in the selected sites, the range of plasticity index (PI) and friction angle is shown in Figure A- 3.

Furthermore, to understand the probability of occurrence of different friction angle and cohesion values for different soil types, the normal distribution of these two values are calculated and shown in Figure A- 4 and Figure A- 5, respectively. From the normal distribution curved it could be understood that the most probable value for “Gravelly”, “Sandy” and “Clayey” Type material is about 30, 28 and 20 degrees respectively.

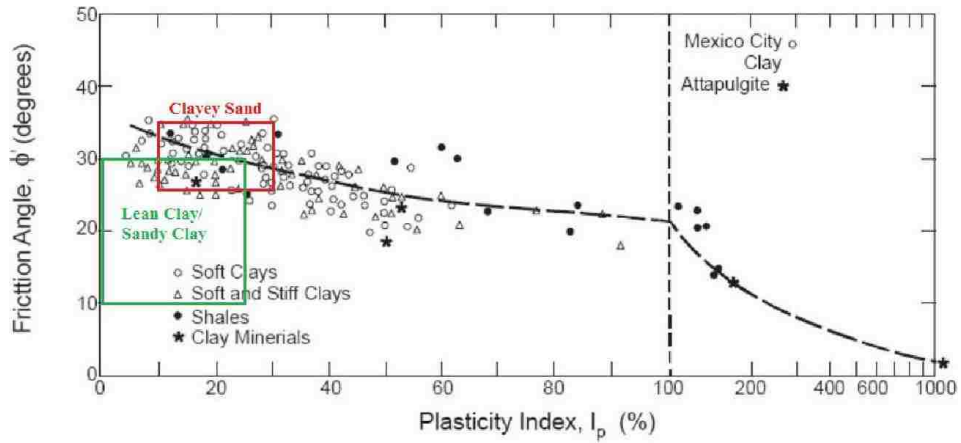


Figure A- 3: Relationship Between ϕ' and PI of Clay Soils (Terzaghi, 1996)

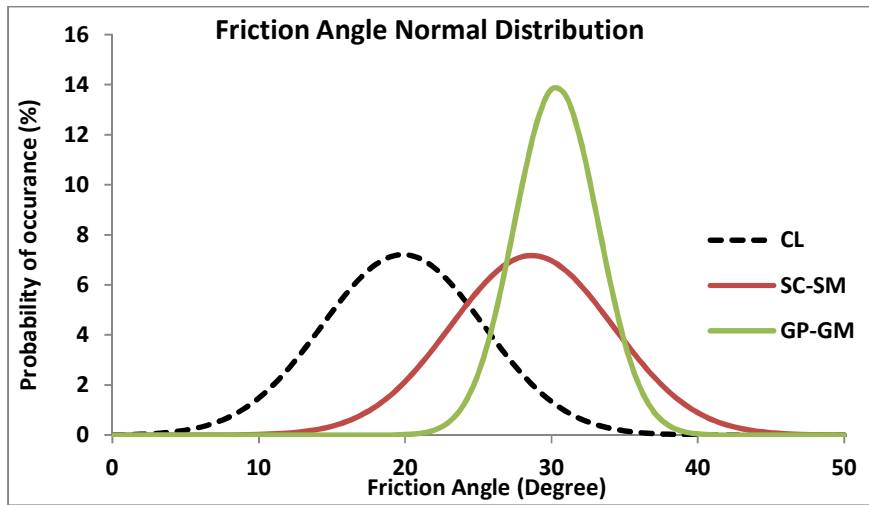


Figure A- 4: Normal Distribution of Friction Angle for Different Types of Soils in Las Vegas

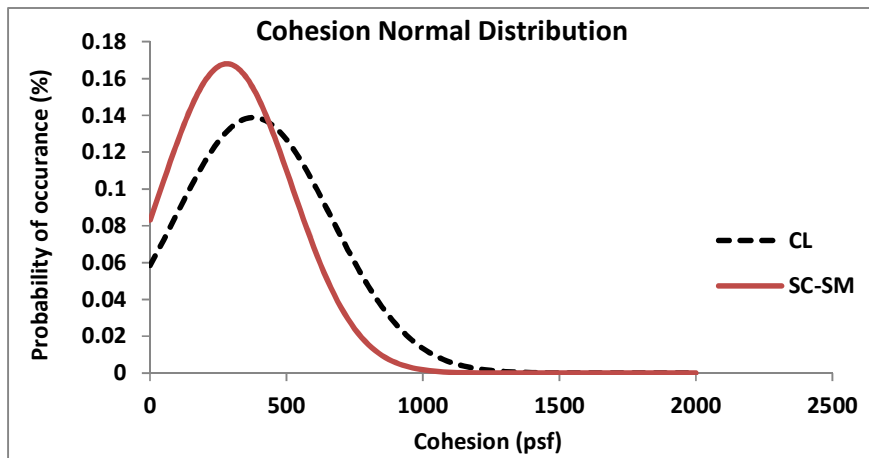


Figure A- 5: Normal Distribution of Cohesion values for Different Types of Soils in Las Vegas

A Mohr-Coulomb model as an elastic-plastic model is used to represent the clayey and silty sand soil types. The Mohr-Coulomb strength parameters are selected from a normal distribution over the available lab results in Las Vegas. The cohesion and friction angle values are then calibrated for the model to match the results from the field load test. The normal distribution shown in Figure A- 5 shows that the most probable values for “ c ” in a clayey sand and lean clay/fat clay soil types are between 200-300 and 400-500 psf, respectively. Additionally, the normal distribution shown in Figure A- 4 shows that the most probable value for “ ϕ ” in a clayey and silty sand and lean/fat clay soil types are between 28-30 and 18-22 degrees, respectively.

Additionally, the normal distribution shown in Figure A- 4, shows that the most probable value for “ ϕ ” in gravelly soil type is between 30-35 degrees. An average unit weight of $\gamma = 0.12 \frac{klb}{ft^3}$ and saturated unit weight of $\gamma_{sat} = 0.13 \frac{klb}{ft^3}$ is used for modeling the sand and gravel in this study.

UNIT WEIGHT (CALICHE)

Unit weight is the index that shows how dense a material is. Accordingly, to determine whether a caliche layer is competent for engineering purposes core samples from that layer should be collected and tested for classification purposes. Three triaxial tests were performed for I-15 and US-95 and the density vs. unconfined compression strength (UCS) is shown in Figure A- 6.

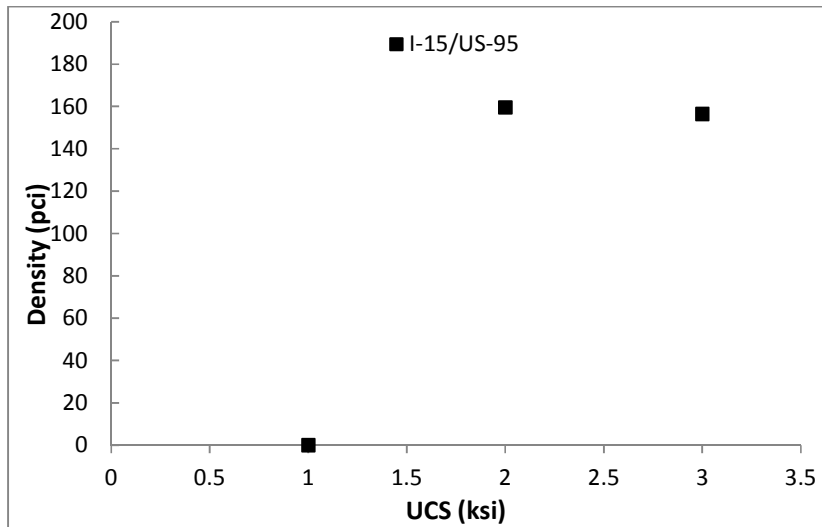


Figure A- 6: Density vs. UCS for Caliche core samples

The value of UCS for this set of data is more than 8 ksi. In the following sections a relatively good comparison is made to differentiate between different types of caliche specimen. UCSs of 8 ksi and more are usually categorized as hard to very hard caliche layers.

UNCONFINED COMPRESSION TEST (CALICHE)

Some data are reported on measured strength of the caliche, but Cibor (1983) reports a range of 576 ksf to 1,440 ksf (4,000 to 10,000 psi) for compressive strength of competent caliche in the Las Vegas Valley. Testing of caliche core samples is done according to unconfined compressive strength (UCS) testing (ASTM D2938). During the construction of a few projects rock cores of caliche material were obtained.

The values of UCS vs. core depths are shown in Figure A- 7. Most of the cores were taken from shallow depths down to 10 feet. For deeper specimen the value of UCS drops significantly compared to those from shallower depths.

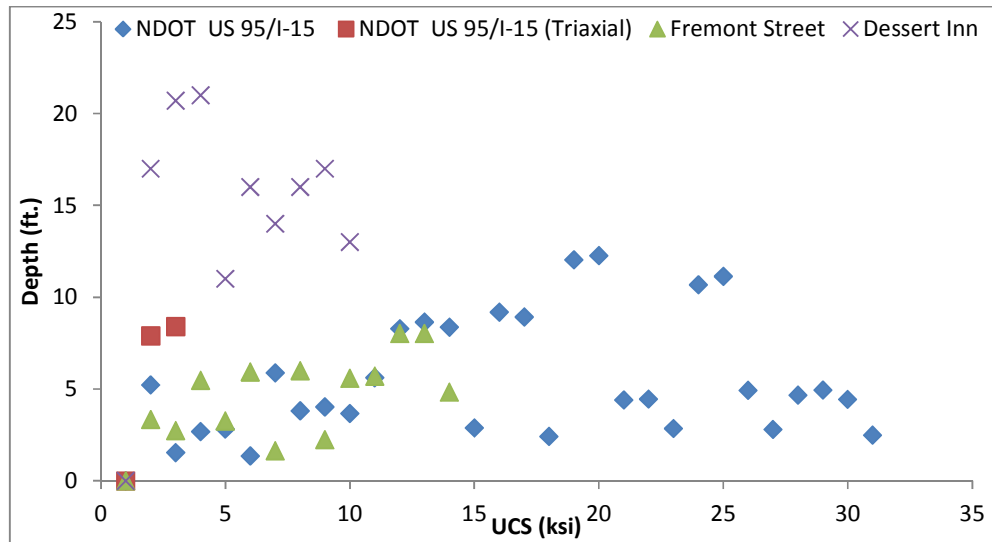


Figure A- 7: UCS vs. Depth for caliche core data (Kleinfelder, 1996; Kleinfelder, 2001; Western Technologies, 1994)

TRIAXIAL TESTING (CALICHE)

A few numbers of Triaxial tests were reported for core samples from caliche in Las Vegas (Kleinfelder, 1996; Western Technologies, 1994). Undrained triaxial and unconfined compressive strength tests on caliche samples to determine values for the density, ultimate strength (UCS), Young’s modulus and Poisson’s ratio. The tests were performed at a single confining pressure of 14 psi (Kleinfelder, 1996). All the specimen had a length to diameter ratio of more than 2 and according to the lab report they were all hand delivered in a good condition wrapped in plastic zip-lock bags for moisture preservation.

The results from the triaxial tests are presented in different formats. The first Set of data is the relationship between Young’s Modulus and Depth of core specimen is shown in Figure A- 8. For Project I-15/US-95 the values of specimen Young’s modulus are relatively high compared to those obtained from Fremont Project site. It could be understood that two different range of Young’s modulus could be assigned

to caliche cores using this graph. On the other hand, if the values of Young's Modulus are drawn vs. UCS of the caliche cores in Figure A- 9 and the graph shows a very good correlation between the two parameters that helps differentiate the caliche core samples obtained from these two projects.

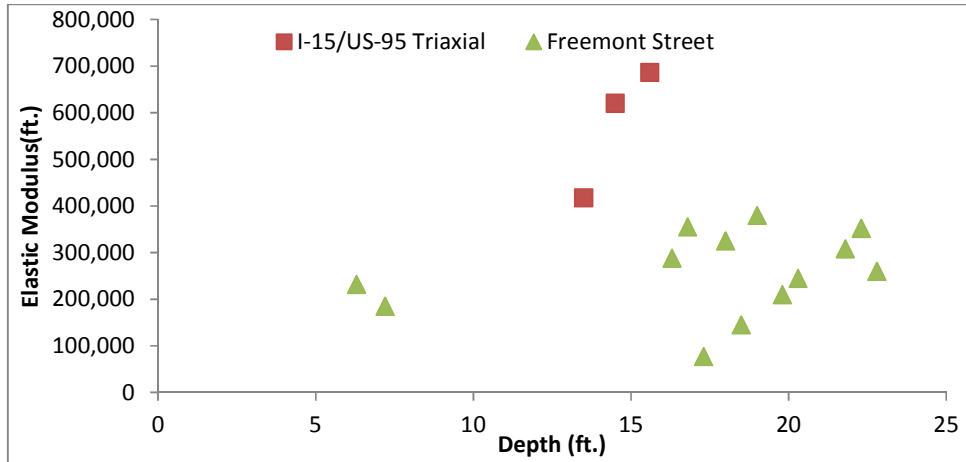


Figure A- 8: Young's Modulus vs. Depth

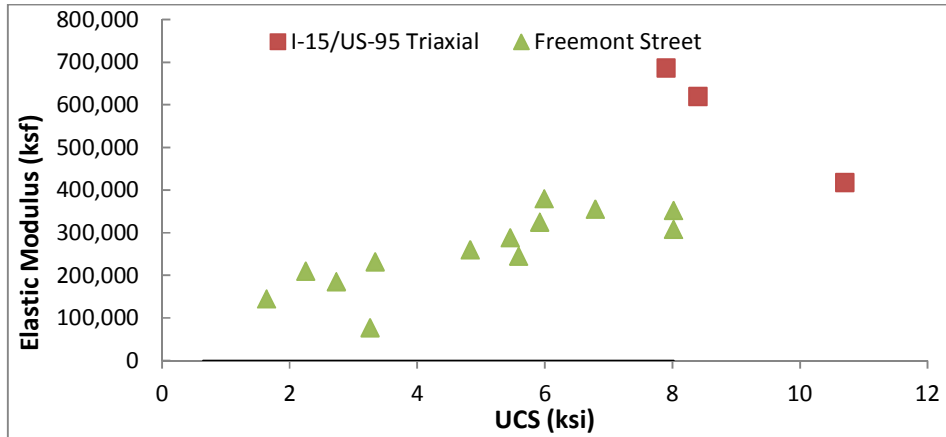


Figure A- 9: Young's Modulus vs. UCS

As shown in Figure A- 9, the UCS values from I-15/ US-95 are significantly higher than the ones obtained from Freemont Street project. Young's Elastic modulus values of specimen obtained from I-15/US-95 are much higher than the ones obtained from Freemont Street Project.

These values are compared to the empirical formula introduced by American concrete institute (ACI Committee, American Concrete Institute, & International Organization for Standardization, 2008).

$$E_c = 57000\sqrt{f'_c} \text{ (psi)} \quad (\text{A-1})$$

The Young's modulus obtained from equation (A-1) is always on the upper bound of the values measured from triaxial tests. Base on the envelope drawn in Figure A-10, until proven wrong from measurements and experiments, it could be concluded that the Young's modulus values for caliche core specimen should not exceed those obtained for concrete cores with the same UCS values.

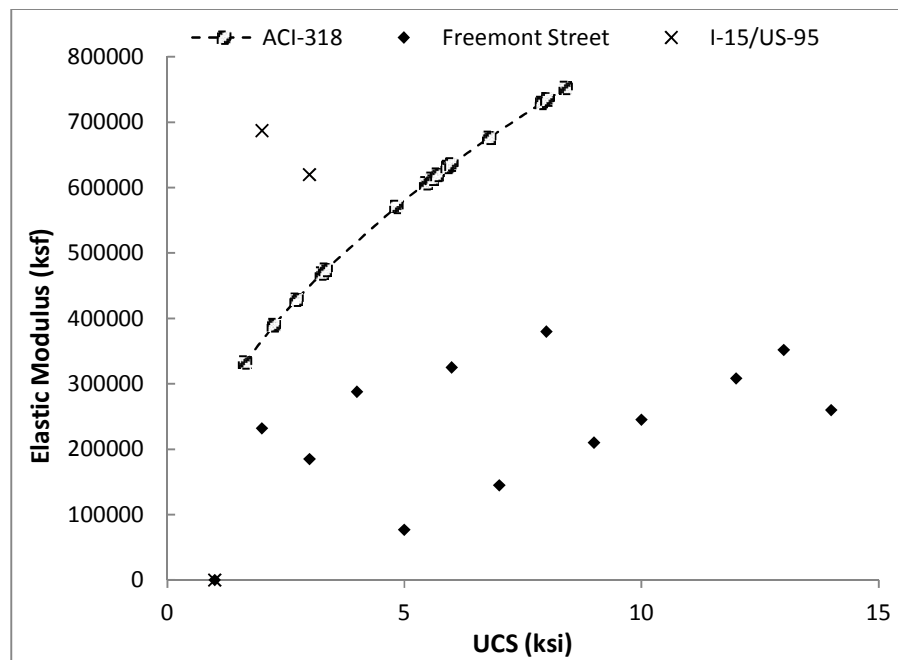


Figure A-10: Young's Modulus vs. UCS with ACI upper bound envelope

COHESION (CALICHE)

The unconfined compression tests on caliche layers are performed following ASTM D2938 for intact rock. The test is performed under a rapid loading and the

nature of the test is categorized under undrained shear strength. For undrained shear strength tests the cohesion is calculated from equation (A- 2).

$$C = \frac{q_u}{2} \quad (A- 2)$$

Where q_u is the unconfined compression strength of rock core with a length to diameter ratio of equal or greater than 2.

For caliche core tests in Las Vegas the cohesion values are drawn versus unconfined compression strength in Figure A- 11.

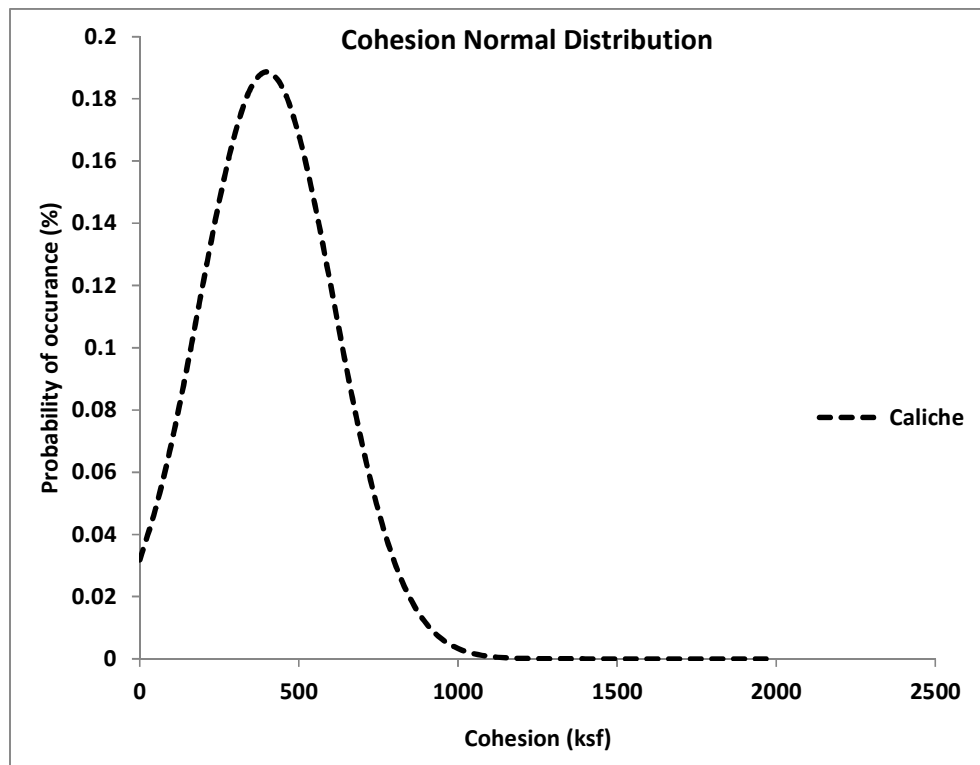


Figure A- 11: Normal Distribution of Cohesion for Caliche in Las Vegas

FIELD DATA

In-situ tests are used to estimate soil and rock properties that are used for both design and construction of drilled shafts. In-situ tests offer several benefits in comparison to laboratory tests because of a larger volume of material, thus providing more accurate measurement of soil or rock mass behavior. Limitations of in-situ testing include ill-defined boundary conditions and soil disturbance caused by advancing the test device, both of which can be difficult to evaluate quantitatively. Therefore, relationships between in-situ measurements and soil or rock properties are largely empirical (Brown et al., 2010). The Field data included in this chapter cover common in-situ tests including Standard Penetration Test (SPT), Pressuremeter test and Rock Quality Designation (RQD)

STANDARD PENETRATION TEST

The standard penetration test (SPT) is performed during the advancement of a soil boring to obtain a disturbed sample with the standard split spoon device and an approximate measure of the soil resistance. It is usually impossible to penetrate caliche layers due to their high density and strength. SPT sampling in caliche layers comes back in form of refusal numbers quite often. The test is a good identification of the presence of a caliche or cemented layers in the soil profile but it is not a good measurement to differentiate between various types and strength of caliche layers. Two completely different caliche layers could have the same SPT number but act completely different under loading condition. Other types of tests such as density tests, UCS or triaxial test are better indicators of caliche strength.

PRESSUREMETER TESTING AND ELASTIC MODULUS (SOIL)

The stiffness of a soil is represented by an engineering parameter termed a modulus. The elastic modulus is also the modulus that is most commonly measured from the results of the pressuremeter test. For the purposes of this study, the elastic modulus, which is the modulus of a soil in triaxial compression (Briaud, 2001), will be the modulus that is preferred because the elastic modulus is the modulus most typically used in standard deformation analyses.

A few pressuremeter tests are performed in Las Vegas based on (ASTM D4719). The results of this testing are shown in for each layer at a specific depth in Figure A- 12. Since the data is obtained from one project site there is high chance that these values may not be the same for other site locations in Las Vegas yet still this is the best direct test results for calculating elastic modulus of soil layers.

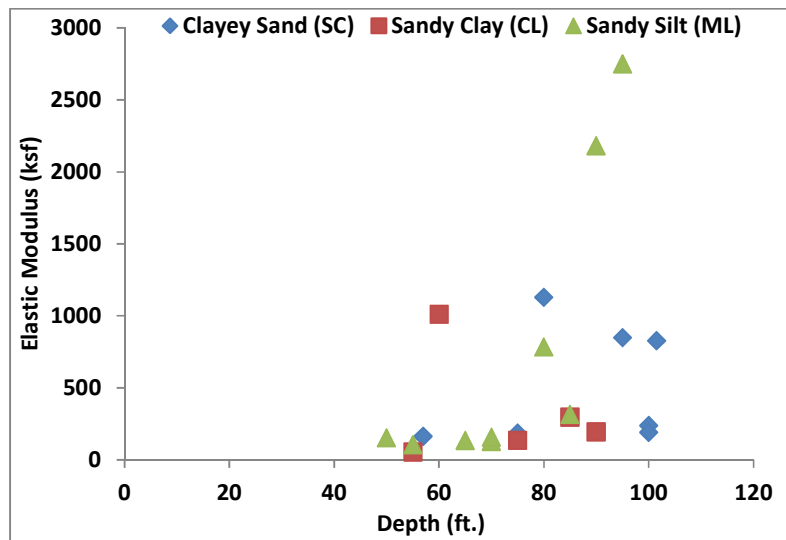


Figure A- 12: Elastic Modulus vs. Depth (Western Technologies, 2002)

Normal distribution of elastic modulus for different types of soil is also shown in Figure A- 13.

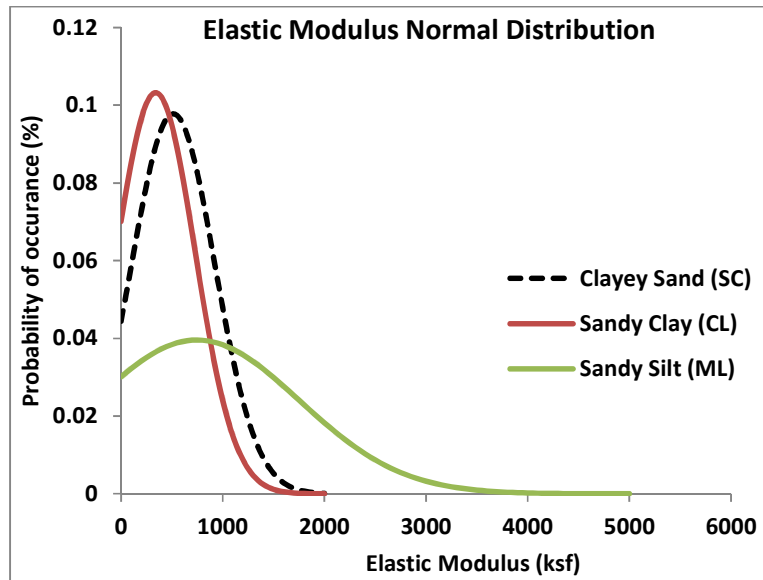


Figure A- 13: Normal Distribution of Elastic Modulus

Cemented deposits can be classified for quality using standard rock quality determination (RQD) techniques from rock mechanics.

RQD

Cemented deposits can be classified for quality using standard rock quality designation (RQD) techniques from rock mechanics. RQD is equal to the sum of the lengths of sound pieces of core recovered, 4 inches or greater in length, expressed as a percentage of the length of the core run (Deere & Deere, 1989) A widely used index of rock quality is the RQD (ASTM D6032), shown in Figure A- 14 and defined as:

$$RQD = \frac{\sum \text{Length of soundcore pieces} > 4 \text{ inches (100 mm)}}{\text{Total core run length}} \quad (\text{A- 3})$$

A general description of rock mass quality based on RQD is given in Table A- 1. Its wide use and ease of measurement make it an important piece of information to be gathered on all core holes. Taken alone, RQD should be considered only as an approximate measure of overall rock quality. RQD is most useful when combined

with other parameters that account for rock strength, deformability, and discontinuity characteristics.

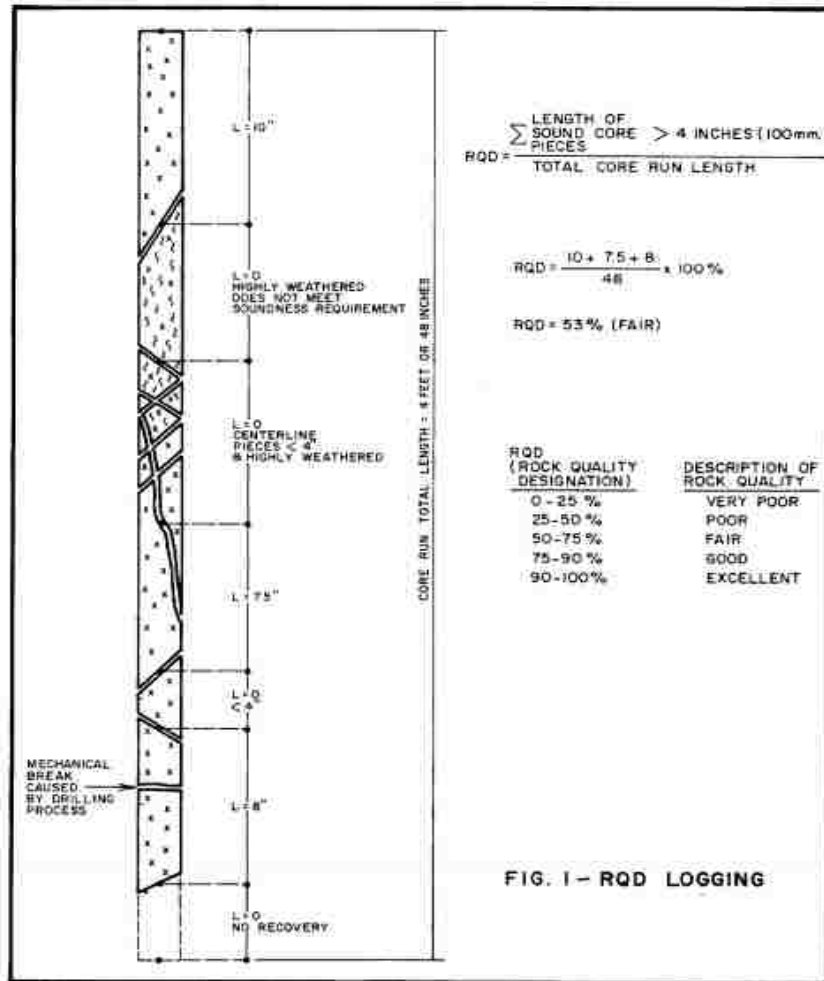


Figure A- 14: RQD Determination from Rock Core (Deere & Deere, 1989)

Table A- 1: Rock Quality Based on RQD (Brown et al., 2010)

Rock Mass Description	RQD
Excellent	90 - 100
Good	75 - 90
Fair	50 - 75
Poor	25 - 50
Very Poor	< 25

RQD is also used to estimate a side resistance reduction factor for shafts in fractured rock core segment lengths should be measured along the centerline or axis of the core, as shown in Figure A- 14. Only natural fractures such as joints or shear planes should be considered when calculating RQD. Core breaks caused by drilling or handling should be fitted together and the pieces counted as intact lengths. Drilling breaks can sometimes be distinguished by fresh surfaces. A set of data showing the relation between RQD and UCS values are shown in Figure A- 15.

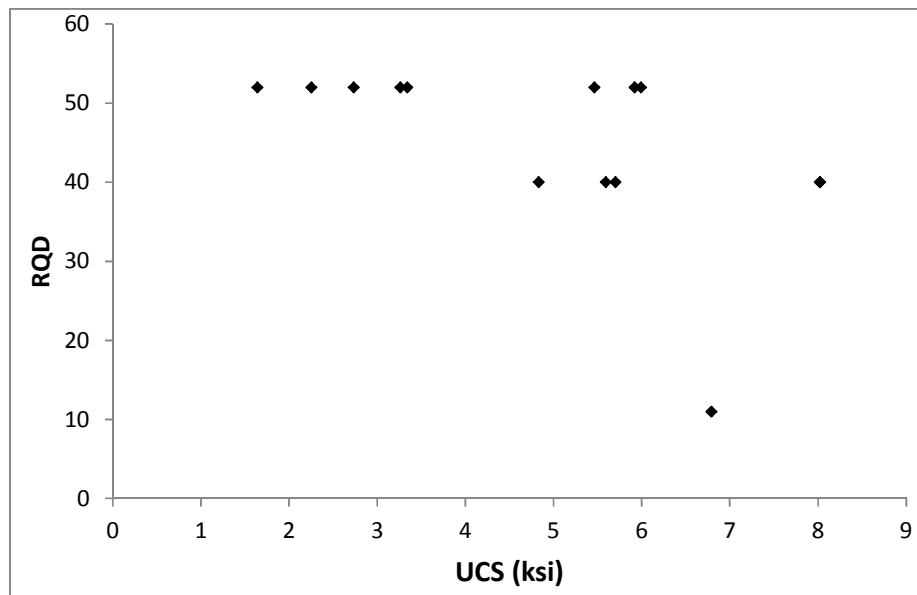


Figure A- 15: UCS vs. RQD in Caliche Core Data, Freemont Street Site (Western Technologies, 1994)

Since the relationship between UCS and RQD is obtained from one of the projects in Las Vegas, the lack of data does not allow us to see a pattern in this relationship. As shown for different values of UCS, similar RQD values could be obtained. The more RQD data from different project sites helps understand the relationship between the two parameters.

APPENDIX B

Young's modulus of the geomaterial is one of the most effective parameters for calculating elastic settlement in geotechnical problems. The Young's modulus values for existing geomaterial in Las Vegas are studied. There are numerous studies by other researchers that introduce a range of acceptable values for different geomaterial.

CLAYEY SAND – SILTY SAND (SC-SM)

The elastic modulus for sandy material has been studied by a few researchers and a range of acceptable values are provided in Table B- 1.

Table B- 1: Young's Modulus Values for Sandy Material

Researcher	Soil remark	Young's Modulus		
		Loose (ksf)	Medium (ksf)	Dense (ksf)
(Obrzud, 2010)	Uniform	210-620	620-1044	1044-1670
(U.S. Army Corps of Engineers, 1990)	-	200-500	-	500 - 2000
(Bowles, 1988)	-	210-522	-	522-1670

INCREASE OF STIFFNESS ($E_{\text{INCREMENT}}$)

In real soils, the stiffness depends significantly on the stress level, which means that the stiffness generally increases with depth. When using the Mohr-Coulomb model, the stiffness is a constant value. In order to account for the increase of stiffness with depth the $E_{\text{increment}}$ value should be used. This value is the increase of

stiffness with depth and it is calibrated based on the available field data shown in Figure B- 1. An average unit weight of $\gamma = 0.12 \frac{klb}{ft^3}$ and saturated unit weight of $\gamma_{sat} = 0.13 \frac{klb}{ft^3}$ is used for modeling the sandy material in this study.

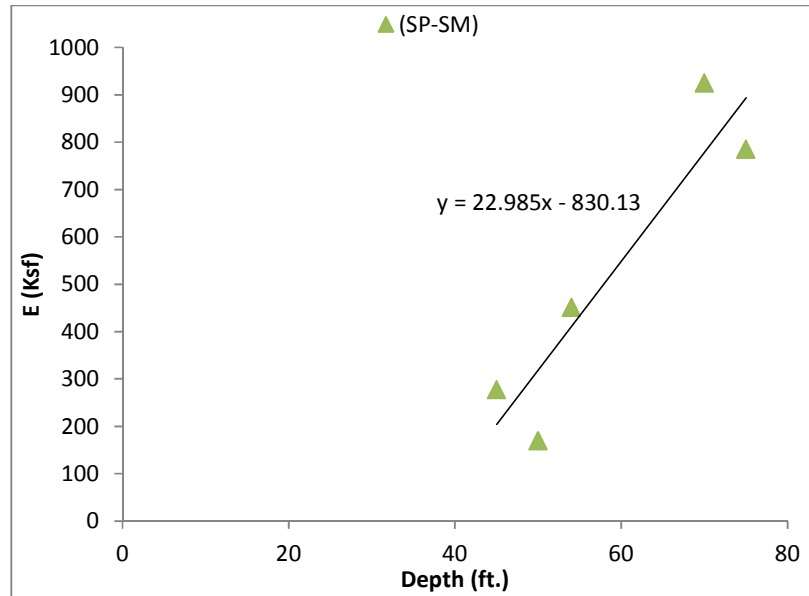


Figure B- 1: Elastic Modulus vs. Depth for Sandy Soil Types

The trend in Figure B- 1 shows that for sandy material the elastic modulus increase about 23 ksf per unit depth (ft.) but limited to the values presented in Table B- 1. For quarts sands the order of magnitude for dilatancy angle (ψ) is usually $\psi = \phi - 30^\circ$. For ϕ - values less than 30° , however, the angle of dilatancy is mostly zero (Bolton, 1986).

SANDY CLAY, LEAN CLAY AND FAT CLAY (CL-CH)

The elastic modulus for clayey material has been studied by a few researchers and a range of acceptable values are provided in Table B- 2.

Table B- 2: Young’s Modulus Values for Clayey Material

Researcher	Soil remark	Young’s Modulus			
		Soft (ksf)	Medium (ksf)	Stiff (ksf)	Hard (ksf)
(Kézdi, 1980; Obrzud, 2010; PRAT, BISCH, MILLARD, Mestat, & PIJAUDIER-CALOT, 1995)	Low to Medium Plasticity (CL)	11-104	104-167	167-625	625-1460
	High Plasticity (CH)	7-84	84-146	146-417	417-668
(U.S. Army Corps of Engineers, 1990)	-	100-400	400-1000	1000 - 2000	-
	Sandy Clay	500-4000			
	Clay Shale	2000-4000			
(Bowles, 1988)	-	104-522	315-1044	1044 - 2088	-
	Sandy Clay	525-5200			
	Clay Shale	3200-100,000			

INCREASE OF STIFFNESS ($E_{\text{INCREMENT}}$)

In order to account for the increase of stiffness with depth the $E_{\text{increment}}$ value should be used. This value is the increase of stiffness with depth and it is calibrated based on the available field data shown in Figure B- 2.

The trend in Figure B- 2 shows that for sandy material the elastic modulus increase about 28 ksf per unit depth (ft.) but limited to the values presented in Table B- 2.

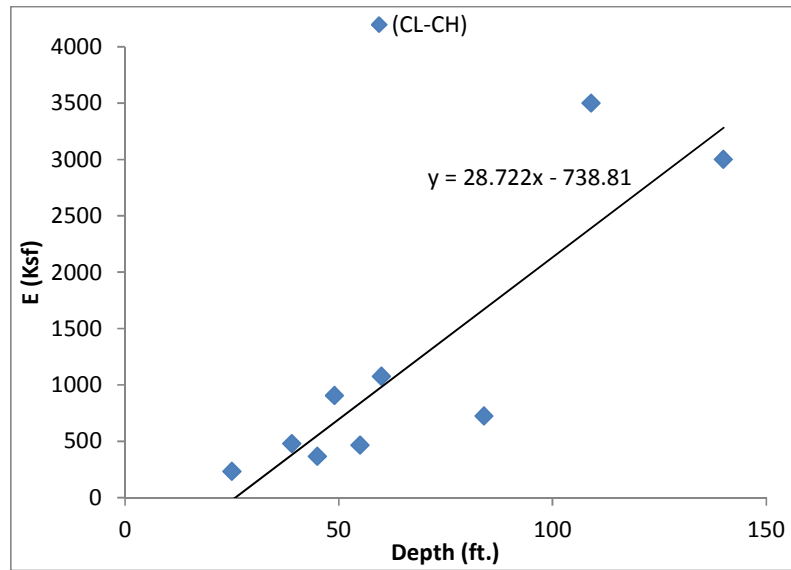


Figure B- 2: Elastic Modulus vs. Depth for Clayey Soil Types

INCREASE OF COHESION ($C_{\text{INCREMENT}}$)

Additionally, PLAXIS has the option for the input clay layers in which cohesion increases with depth. In order to account for the increase in cohesion with depth the $C_{\text{increment}}$ values may be used. It is the increase of cohesion per unit depth and can be obtained using the lab results for clayey material shown in Figure B- 3.

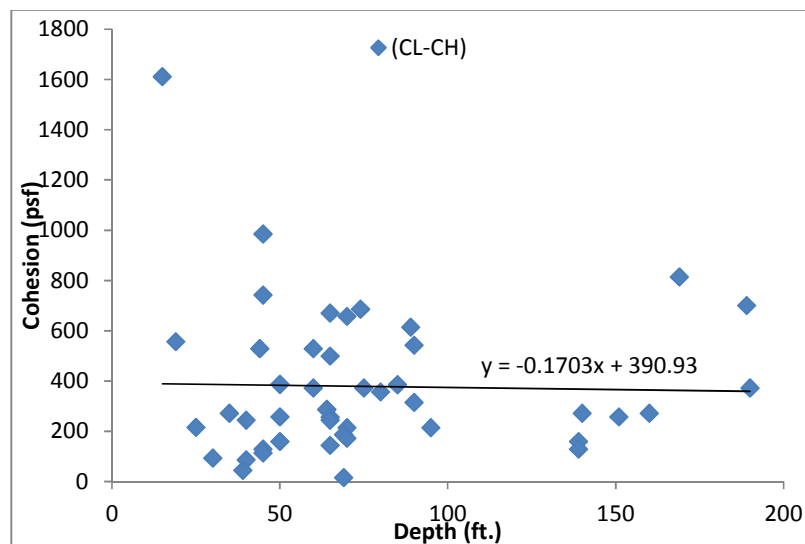


Figure B- 3: Variation in Clayey Soil Cohesion with Depth

It could be understood from Figure B- 3 that cohesion is relatively constant with depth for clayey material in Las Vegas. Accordingly, the value of $C_{\text{increment}}$ is selected to be zero “0” for clayey material in this research. Additionally, an average unit weight of $\gamma = 0.13 \frac{\text{klb}}{\text{ft}^3}$ and saturated unit weight of $\gamma_{\text{sat}} = 0.13 \frac{\text{klb}}{\text{ft}^3}$ is used for modeling the clayey material in this study.

SAND AND GRAVEL (GP, GM, GC)

The gravel material encountered in Las Vegas typically consists of sand and gravel with some clay or silt fines. This material is usually very dense in consistency with SPT N-values exceeding 50 to 100 blows per foot. Thus, for dense gravel, we can assign nominally high strength parameters and an elastic modulus. Typical values for the elastic modulus from different researchers are provided in Table B- 3.

Table B- 3: Young’s Modulus Values for Sand and Gravel

Researcher	Soil remark	Young’s Modulus		
		Loose (ksf)	Medium (ksf)	Dense (ksf)
(Kézdi, 1980; Obrzud, 2010; PRAT et al., 1995)	GW-SW	626-1670	1670-3340	3340-6683
	GM-SM	147-250	250-417	417-626
(U.S. Army Corps of Engineers, 1990)	-	2000-4000		
(Bowles, 1988)	-	1044-2088	-	2088-4177

There is not enough data for Sand and Gravel soil type to show an increasing trend with depth in Young's modulus. The value of Young's modulus is kept constant with depth.

CALICHE

A Mohr-Coulomb constitutive model is used to represent the caliche layers. The caliche layers usually act elastically under service load conditions and due to its brittle characteristic, caliche failure happens in tension cracks. The linear Mohr-Coulomb may not be the best representative model for caliche but it is easily applied and can be traced toward failure stages. Further calculation regarding caliche failure is performed using hand calculations to find the best constitutive model that can represent the failure of caliche. The triaxial tests indicate an elastic modulus similar to concrete. Based on ACI-318 correlations shown in APPENDIX A, Equation (A- 1) for evaluating the modulus of the caliche, one can make use of the expressions relating the unconfined compression strength to E for concrete.

The compressive strength of the rock forming the walls of discontinuities will impact shear strength and deformability. Rock compressive strength categories and grade vary from extremely strong (> 250 MPa grade R_6) to extremely weak (0.25 to 1 MPa grade R_0) (Sabatini, Bachus, Mayne, Schneider, & Zettler, 2002). For caliche, the range of UCS from triaxial tests came out to be between 14 to 75 MPa (2-11 ksi). According to Sabatini et al. (2002), caliche ranks as grade R3 and R4 based on its UCS values.

CSIR CLASSIFICATION

The ISRM (1978) procedures, combined with core recovery and RQD, helps characterizing rock and rock mass. The CSIR classification system is the commonly used in the US. The CSIR classification system considers (1) compressive strength of the intact rock; (2) RQD value; (3) joint spacing; (4) condition of the joints; and (5) groundwater conditions. The overall rating of the rock mass, termed the rock mass rating (RMR), is calculated as the sum of the individual ratings for each of the five parameters minus the adjustment for joint orientation (if applicable) (Sabatini et al., 2002).

For Las Vegas caliche RMR evaluation can be observed in Table B- 4. Based on the RMR value caliche can be categorized into good rock class.

Table B- 4: CSIR Classification of Caliche

A. CLASSIFICATION PARAMETERS AND THEIR RATINGS		
1	Strength of intact rock material	Uniaxial compressive strength 50 to 100 Mpa
	Relative Rating	
2	Drill core quality RQD	50%
	Relative Rating	
3	Spacing of joints	0.3 to 1 m
	Relative Rating	
4	Condition of joints	Slightly rough surfaces separation <1mm
	Relative Rating	
5	Ground water	Water under moderate pressure
	Relative Rating	
B. RATING AND ADJUSTMENT FOR JOINT ORIENTATIONS		
Strike and dip orientations of joint		0
C. ROCK MASS CLASSES DETERMINED FROM TOTAL RATINGS		
RMR Rating		64
Class No.		II
Description		Good Rock

ROCK DEFORMATION MODULUS VALUES

Typically, the settlement of a rock foundation will be controlled by the deformation modulus corresponding to the overall rock mass and will not be controlled by the deformation modulus of intact rock (Sabatini et al., 2002). According to the study performed by Bieniawski (1978), the following equation for rock mass modulus, E_M , exhibiting a RMR > 50 was developed:

$$E_M(GPa) = 2RMR - 100 \quad (\text{B- 1})$$

For Las Vegas Caliche the value of E_m comes out as 28 GPa ~ 576,000 ksf. The Young's modulus obtained from equation (B- 1) is very close to the young's modulus obtained from triaxial testings that were performed in Las Vegas. The elastic modulus for a good rock is an average of 600,000 ksf in this study and calibrated according to the field load test with an upper bound limited to equation (A- 1) from ACI-318 (2008). An average unit weight of $\gamma = 0.16 \frac{klb}{ft^3}$ and saturated unit weight of $\gamma_{sat} = 0.16 \frac{klb}{ft^3}$ is used for modeling the caliche in this study.

APPENDIX C

Boring Log for I-215/Airport Connector

LOG OF BORING NO. 06B-06									
CLIENT: Parsons Brinckerhoff Quade & Douglas					PROJECT: Interstate Route 215 / State Route 171				
BORING LOCATION: See Plot Plan			ELEVATION:		SITE: Airport Connector Interchange				
SOIL DESCRIPTION	CONSISTENCY	GRAPHIC	USCS SYMBOL	DEPTH (FT.)	SAMPLES			TESTS	
					SAMPLE	BLOWS/FT.	SMP. TYPE*	MOISTURE %	DRY DENSITY PCF
FILL - SANDY GRAVEL -w/ clay, lt. brown		[Cross-hatch pattern]	FILL	1					
CLAYEY SAND -w/ silt, wet, reddish brown	med. dense	[Diagonal lines]	SC	2					
SANDY CLAY -w/ gypsum, moist, brown	very stiff	[Vertical lines]	CL	4	19	SPT			
CLAYEY GRAVEL -w/ sand, moist, brown	dense	[Circular pattern]	GC	9	39	SPT			
SANDY CLAY -partially cemented, dry to sl. moist, lt. brown -w/ caliche lenses	very stiff to mod. hard	[Vertical lines]	CL	12					
CALICHE -dry, lt. brown	hard	[Horizontal lines]		14	50/0"	SPT			
Continued Next Page									
<small>THE STRATIFICATION LINES REPRESENT THE APPROXIMATE BOUNDARY LINES BETWEEN SOIL AND ROCK TYPES. IN-SITU, THE TRANSITION MAY BE GRADUAL.</small>					<small>*SAMPLE TYPES: R = Ring B = Bag CPT = Cone penetration test *SPT = Standard Penetration Test C = Core T = Shelby Tube</small>				
NOTES: Groundwater Measured @ 41 ft. after 24 hours HAMMER WEIGHT (lbs): 140						DATE DRILLED: 3-19-06		PAGE NUMBER: Page 1 of 7	
				PROJECT NO.: 64065013		PLATE: A-1			

THIS SUMMARY APPLIES ONLY AT THIS LOCATION AT THE TIME OF LOGGING. CONDITIONS MAY DIFFER WITH TIME OR AT OTHER LOCATIONS.

LOG OF BORING NO. 06B-06

CLIENT: Parsons Brinckerhoff Quade & Douglas		PROJECT: Interstate Route 215 / State Route 171						
BORING LOCATION: See Plot Plan		ELEVATION:		SITE: Airport Connector Interchange				
SOIL DESCRIPTION	CONSISTENCY	GRAPHIC	USCS SYMBOL	DEPTH (FT.)	SAMPLES		TESTS	
					SAMPLE	BLOWS/FT.	SMP. TYPE*	MOISTURE %
CALICHE -dry, lt. brown	hard			16				
CLAY -moist, reddish brown	stiff		CH	17				
CALICHE -dry, lt. reddish brown	hard			18				
				19	50/0"	SPT		
				20				
				21				
CLAYEY SAND -w/ gravel, sl. moist to moist, lt. reddish brown -w/ occ. partially cemented lenses	med. dense		SC	22				
				23				
				24		21	SPT	
				25				
				26				
-partially cemented, sl. moist	v.s.-m.h.			27				
-very moist, reddish brown	very stiff		CL	28				
				29				
-partially cemented, sl. moist, lt. reddish brown	v.s.-m.h.			29	8/6"	SPT		
				29	25/6"			
				30	50/3"			
Continued Next Page								
THE STRATIFICATION LINES REPRESENT THE APPROXIMATE BOUNDARY LINES BETWEEN SOIL AND ROCK TYPES. IN-SITU, THE TRANSITION MAY BE GRADUAL.				*SAMPLE TYPES: R = Ring B = Bag CPT = Cone penetration test *SPT = Standard Penetration Test C = Core T = Shelby Tube				
NOTES: Groundwater Measured @ 41 ft. after 24 hours				DATE DRILLED: 3-19-06		PAGE NUMBER: Page 2 of 7		
HAMMER WEIGHT (lbs): 140				PROJECT NO.: 64065013		PLATE: A-2		

THIS SUMMARY APPLIES ONLY AT THIS LOCATION AT THE TIME OF LOGGING. CONDITIONS MAY DIFFER WITH TIME OR AT OTHER LOCATIONS.

LOG OF BORING NO. 06B-06

CLIENT: Parsons Brinckerhoff Quade & Douglas		PROJECT: Interstate Route 215 / State Route 171									
BORING LOCATION: See Plot Plan	ELEVATION:	SITE: Airport Connector Interchange									
SOIL DESCRIPTION	CONSISTENCY	GRAPHIC SYMBOL	USCS SYMBOL	DEPTH (FT.)	SAMPLES		TESTS				
					SAMPLE	BLOWS/FT.	SMP. TYPE#	MOISTURE %	DRY DENSITY PCF	ORGANIC VAPOR METER	
CALICHE - partially cemented, dry to sl. moist, lt. reddish brown	very stiff to mod. hard			31							
				34	X	50/3"	SPT	11.2			
CLAY -w/ sand, tr. gravel, very moist, dark reddish brown	firm		CH	37							
				39	▲	6	SPT				
				40	▲						
				41							
				42							
SILTY, CLAYEY SAND - w/ gravel, wet, reddish brown	med. dense		SC-SM	43							
				44	▲	16	SPT	33.2			
				45	▲						
Continued Next Page											
THE STRATIFICATION LINES REPRESENT THE APPROXIMATE BOUNDARY LINES BETWEEN SOIL AND ROCK TYPES. IN-SITU, THE TRANSITION MAY BE GRADUAL.				*SAMPLE TYPES: R = Ring B = Bag CPT = Cone penetration test *SPT = Standard Penetration Test C = Core T = Shelby Tube							
NOTES: Groundwater Measured @ 41 ft. after 24 hours				DATE DRILLED: 3-19-06		PAGE NUMBER: Page 3 of 7					
HAMMER WEIGHT (lbs): 140				PROJECT NO.: 64065013		PLATE: A-3					

THIS SUMMARY APPLIES ONLY AT THIS LOCATION AT THE TIME OF LOGGING. CONDITIONS MAY DIFFER WITH TIME OR AT OTHER LOCATIONS.



LOG OF BORING NO. 06B-06

CLIENT: Parsons Brinckerhoff Quade & Douglas		PROJECT: Interstate Route 215 / State Route 171						
BORING LOCATION: See Plot Plan		ELEVATION:		SITE: Airport Connector Interchange				
SOIL DESCRIPTION	CONSISTENCY	GRAPHIC	USCS SYMBOL	DEPTH (FT.)	SAMPLES		TESTS	
					SAMPLE	BLOWS/FT.	SMP. TYPE*	MOISTURE %
SILTY, CLAYEY SAND -wet, reddish brown			SC, SM	46				
CLAYEY SAND -w/ occ. partially cemented lenses, wet, reddish brown			SC	47				
-w/ tr. caliche gravel				48				
				49		10	SPT	
				50				
-w/ clay lenses	med. dense			51				
				52				
				53				
				54		20	SPT	21.0
				55				
				56				
SANDY CLAY -very moist to wet, reddish brown			CL	57				
	firm to stiff			58				
-partially cemented, sl. moist, white				59		60	SPT	
	v.s.-m.h.			60				
Continued Next Page								
NOTES: Groundwater Measured @ 41 ft. after 24 hours			HAMMER WEIGHT (lbs): 140				DATE DRILLED: 3-19-06	PAGE NUMBER: Page 4 of 7
					PROJECT NO.: 64065013		PLATE: A-4	

THIS SUMMARY APPLIES ONLY AT THIS LOCATION AT THE TIME OF LOGGING. CONDITIONS MAY DIFFER WITH TIME OR AT OTHER LOCATIONS.

THE STRATIFICATION LINES REPRESENT THE APPROXIMATE BOUNDARY LINES BETWEEN SOIL AND ROCK TYPES. IN-SITU, THE TRANSITION MAY BE GRADUAL. *SAMPLE TYPES: R = Ring B = Bag CPT = Cone penetration test *SPT = Standard Penetration Test C = Core T = Shelby Tube

LOG OF BORING NO. 06B-06

CLIENT: Parsons Brinckerhoff Quade & Douglas		PROJECT: Interstate Route 215 / State Route 171						
BORING LOCATION: See Plot Plan	ELEVATION:	SITE: Airport Connector Interchange						
SOIL DESCRIPTION	CONSISTENCY	GRAPHIC	USCS SYMBOL	DEPTH (FT.)	SAMPLES		TESTS	
					SAMPLE	BLOWS/FT.	SMP. TYPE#	MOISTURE %
CALICHE -partially cemented, sl. moist, white	very stiff to mod. hard			61	▲			
CLAYEY SAND -w/ gravel, wet, reddish brown	med. dense		SC	62				
SANDY CLAY -very moist, reddish brown	very stiff		CL	64	▲	24	SPT	
CLAYEY SAND -very moist, reddish brown	med. dense		SC	65	▲			
CALICHE -partially cemented, sl. moist, white	very dense to mod. hard			69	▲	50/4"	SPT	
SANDY CLAY -very moist, reddish brown	firm to stiff		CL	70				
-w/ tr. caliche gravel				71				
SILTY CLAY -w/ sand, very moist, reddish brown	st.-v.st.		CL	74	▲	19	SPT	31.4
Continued Next Page				75	▲			
THE STRATIFICATION LINES REPRESENT THE APPROXIMATE BOUNDARY LINES BETWEEN SOIL AND ROCK TYPES. IN-SITU, THE TRANSITION MAY BE GRADUAL.				*SAMPLE TYPES: R = Ring B = Bag CPT = Cone penetration test *SPT = Standard Penetration Test C = Core T = Shelby Tube				
NOTES: Groundwater Measured @ 41 ft. after 24 hours				DATE DRILLED: 3-19-06		PAGE NUMBER: Page 5 of 7		
HAMMER WEIGHT (lbs): 140				PROJECT NO.: 64065013		PLATE: A-5		

THIS SUMMARY APPLIES ONLY AT THIS LOCATION AT THE TIME OF LOGGING. CONDITIONS MAY DIFFER WITH TIME OR AT OTHER LOCATIONS.

LOG OF BORING NO. 06B-06

CLIENT: Parsons Brinckerhoff Quade & Douglas		PROJECT: Interstate Route 215 / State Route 171							
BORING LOCATION: See Plot Plan		ELEVATION:		SITE: Airport Connector Interchange					
SOIL DESCRIPTION	CONSISTENCY	GRAPHIC	USCS SYMBOL	DEPTH (FT.)	SAMPLES		TESTS		
					SAMPLE	BLOWS/FT.	SMP. TYPE*	MOISTURE %	DRY DENSITY PCF
SILTY CLAY -w/ sand, tr. caliche gravel, very moist, reddish brown	stiff to very stiff		CL-ML	76	▲				
			77						
SANDY CLAY -w/ tr. caliche gravel, very moist, reddish brown to lt. reddish brown	stiff to very stiff		CL	79	▲	18	SPT		
			80	▲					
-w/ occ. partially cemented lenses	very stiff			81					
			82						
-w/ caliche, moist to very moist	very stiff			83					
			84	▲	40	SPT	18.8		
CLAYEY SAND -wet, reddish brown	med. dense		SC	85	▲				
			86						
SILTY SAND -wet, reddish brown	med. dense		SM	87					
			88						
CLAYEY SAND -wet, reddish brown	med. dense		SC	89	▲	11	SPT		
			90						
Continued Next Page									
THE STRATIFICATION LINES REPRESENT THE APPROXIMATE BOUNDARY LINES BETWEEN SOIL AND ROCK TYPES. IN-SITU, THE TRANSITION MAY BE GRADUAL.				*SAMPLE TYPES: R = Ring B = Bag CPT = Cone penetration test *SPT = Standard Penetration Test C = Core T = Shelby Tube					
NOTES: Groundwater Measured @ 41 ft. after 24 hours				DATE DRILLED: 3-19-06		PAGE NUMBER: Page 6 of 7			
HAMMER WEIGHT (lbs): 140				PROJECT NO.: 64065013		PLATE: A-6			

THIS SUMMARY APPLIES ONLY AT THIS LOCATION AT THE TIME OF LOGGING. CONDITIONS MAY DIFFER WITH TIME OR AT OTHER LOCATIONS.



LOG OF BORING NO. 06B-06

CLIENT: Parsons Brinckerhoff Quade & Douglas		PROJECT: Interstate Route 215 / State Route 171						
BORING LOCATION: See Plot Plan	ELEVATION:	SITE: Airport Connector Interchange						
SOIL DESCRIPTION	CONSISTENCY	GRAPHIC	USCS SYMBOL	DEPTH (FT.)	SAMPLES		TESTS	
					SAMPLE	BLOWS/FT.	SMP. TYPE*	MOISTURE %
SANDY CLAY - very moist, brown	firm to stiff		CL	91	25	SPT	13.0	
				92				
	stiff to very stiff		CL	93	8	SPT		
-moist to very moist, brown to lt. brown				94				
	med. dense		SC	95				
				96				
CLAYEY SAND -wet, brown	loose		SM	97				
				98				
SILTY SAND -wet, brown	firm		SC	99				
CLAYEY SAND -wet, brown				100				
SANDY CLAY -very moist, brown			CL	101				
Bottom Depth at Approximately 100.5 feet								
				102				
				103				
				104				
				105				
THE STRATIFICATION LINES REPRESENT THE APPROXIMATE BOUNDARY LINES BETWEEN SOIL AND ROCK TYPES. IN-SITU, THE TRANSITION MAY BE GRADUAL.				*SAMPLE TYPES: R = Ring B = Bag CPT = Cone penetration test *SPT = Standard Penetration Test C = Core T = Shelby Tube				
NOTES: Groundwater Measured @ 41 ft. after 24 hours				DATE DRILLED:	PAGE NUMBER:			
HAMMER WEIGHT (lbs): 140				3-19-06	Page 7 of 7			
				PROJECT NO.:	PLATE:			
				64065013	A-7			

THIS SUMMARY APPLIES ONLY AT THIS LOCATION AT THE TIME OF LOGGING. CONDITIONS MAY DIFFER WITH TIME OR AT OTHER LOCATIONS.

Boring Log for Palm

DATE DRILLED: 8-4-05		BORING NO. 1		ELEVATION: Not measured				
LOCATION: Palms Hotel & Casino								
MOISTURE CONTENT (% OF DRY WT)	DRY DENSITY (LBS/CU FT)	SAMPLE TYPE	SAMPLE BLOWS/FT.	DEPTH (FEET)	USCS GRAPHIC	SOIL DESCRIPTION	MOISTURE	CONSISTENCY
				1	SC	FILL-ASPHALT, TYPE II		
9.8	125	R	22	2		CLAYEY SAND-w/gravel, orange brown	damp	med. dense
				3				
				4	CL	SANDY CLAY-pale pink		very stiff
13.3	122	R	27	5				
				6				
				7				
				8	SC	CLAYEY SAND-gray		med. dense
				9				
13.5	119	R	22	10				
				11	CL	SANDY CLAY-w/gravel, pale brown	moist	very stiff
				12				
				13				
				14				

THIS SUMMARY APPLIES ONLY AT THIS LOCATION AND AT THE TIME OF LOGGING. CONDITIONS MAY DIFFER AT OTHER LOCATIONS AND MAY CHANGE AT THIS LOCATION WITH TIME. DATA PRESENTED IS A SIMPLIFICATION.

N- STANDARD PENETRATION TEST
 R- RING SAMPLE
 C- CORE: %RECOVERY%ROD
 B- BAG
 BN- BULL NOSE

NOTES: Water encountered at approximately 22.5 feet. Elevation not available.

DRIVING WEIGHT (LBS) 140

WESTERN TECHNOLOGIES INC.


PROJECT NO. 4125JD093

PROJECT: PALMS PLACE

BORING LOG

PLATE

A-3

DATE DRILLED: 8-4-05		BORING NO. 1 (Cont'd)		ELEVATION: Not measured				
LOCATION: Palms Hotel & Casino								
MOISTURE CONTENT (% OF DRY WT)	DRY DENSITY (LBS/CU FT)	SAMPLE TYPE	SAMPLE BLOWS/FT.	DEPTH (FEET)	USCS GRAPHIC	SOIL DESCRIPTION	MOISTURE	CONSISTENCY
16.4	112	R		52	CL	SANDY CLAY-w/gravel, lt. gray green-pale red	sl. damp	very stiff
				16				
				17				
				18		CEMENTED SAND & GRAVEL		hard
				19				
		R	50/0'	20				very hard
				21				
				22				
				23		CALICHE-brown	wet	
				24				
		R	50/0'	25				
				26				
				27				
				28				
				29				
N- STANDARD PENETRATION TEST R- RING SAMPLE C- CORE: %RECOVERY/%RQD B- BAG BN- BULL NOSE						NOTES: Water encountered at approximately 22.5 feet. Elevation not available.		
 WESTERN TECHNOLOGIES INC.						DRIVING WEIGHT (LBS) 140		PLATE
PROJECT NO. 4125JD093						PROJECT: PALMS PLACE BORING LOG		A-4

THIS SUMMARY APPLIES ONLY AT THIS LOCATION AND AT THE TIME OF LOGGING. CONDITIONS MAY DIFFER AT OTHER LOCATIONS AND MAY CHANGE AT THIS LOCATION WITH TIME. DATA PRESENTED IS A SIMPLIFICATION.

DATE DRILLED: 8-4-05 **BORING NO. 1** (Cont'd) ELEVATION: Not measured
 LOCATION: Palms Hotel & Casino


MOISTURE CONTENT (% OF DRY WT)	DRY DENSITY (LBS/CU FT)	SAMPLE TYPE	SAMPLE BLOWS/FT.	DEPTH (FEET)	USCS	GRAPHIC	SOIL DESCRIPTION	MOISTURE	CONSISTENCY
		R	50/0'	31			CALICHE-brown	wet	very hard
		R	50/0'	35			-brown-lt. gray		
		R	50/0'	40					
				42	CL		CLAY-w/gravel	moist	very stiff
				43					
				44					

THIS SUMMARY APPLIES ONLY AT THIS LOCATION AND AT THE TIME OF LOGGING. CONDITIONS MAY DIFFER AT OTHER LOCATIONS AND MAY CHANGE AT THIS LOCATION WITH TIME. DATA PRESENTED IS A SIMPLIFICATION.

N- STANDARD PENETRATION TEST
 R- RING SAMPLE
 C- CORE: %RECOVERY/%RQD
 B- BAG
 BN- BULL NOSE

NOTES: Water encountered at approximately 22.5 feet. Elevation not available.

DRIVING WEIGHT (LBS) 140

 WESTERN TECHNOLOGIES INC. PROJECT NO. 4125JD093	PROJECT:	PLATE
	PALMS PLACE BORING LOG	

DATE DRILLED: 8-4-05 **BORING NO. 1** (Cont'd) ELEVATION: Not measured
 LOCATION: Palms Hotel & Casino

MOISTURE CONTENT (% OF DRY WT)	DRY DENSITY (LBS/CC FT)	SAMPLE TYPE	SAMPLE	BLOWS/FT	DEPTH (FEET)	USCS	GRAPHIC	SOIL DESCRIPTION	MOISTURE	CONSISTENCY
37.5	82	R		29	46	CL	[Hatched]	CLAY-red brown-brown	moist	very stiff
					47					
					48			CALICHE-w/thin clay lenses, brown		very hard
					49	CL	[Hatched]	CLAY-w/gravel		very stiff
		R	50/0'		50			CALICHE-brown		very hard
					51					
					52					
					53					
					54					
					55	CL	[Hatched]	CLAY-brown	damp	very stiff
15.8	114	R		3/11	56					
					57					
					58					
					59					

THIS SUMMARY APPLIES ONLY AT THIS LOCATION AND AT THE TIME OF LOGGING. CONDITIONS MAY DIFFER AT OTHER LOCATIONS AND MAY CHANGE AT THIS LOCATION WITH TIME. DATA PRESENTED IS A SIMPLIFICATION.

- N- STANDARD PENETRATION TEST
- R- RING SAMPLE
- C- CORE: %RECOVERY/%RQD
- B- BAG
- BN- BULL NOSE

NOTES: Water encountered at approximately 22.5 feet. Elevation not available.

DRIVING WEIGHT (LBS) 140



WESTERN TECHNOLOGIES INC.

PROJECT NO. 4125JD093

PROJECT: PALMS PLACE
BORING LOG

PLATE
A-6

DATE DRILLED: 8-4-05 **BORING NO. 1** - (Cont'd) ELEVATION: Not measured
 LOCATION: Palms Hotel & Casino

MOISTURE CONTENT (% OF DRY WT)	DRY DENSITY (LBS/CU FT)	SAMPLE TYPE	SAMPLE	BLOWS/FT.	DEPTH (FEET)	USCS	GRAPHIC	SOIL DESCRIPTION	MOISTURE	CONSISTENCY
19.9	108	R		30	61	CL		CLAY-brown	moist	very stiff
					62					
					63					
					64					
24.8	103	R		13	65			-red brown		stiff
					66	SC		CLAYEY SAND-brown		
					67					
					68			CALICHE-lt. gray		very hard
					69					
		R		50/0	70					
					71					
					72					
					73					
					74					

THIS SUMMARY APPLIES ONLY AT THIS LOCATION AND AT THE TIME OF LOGGING. CONDITIONS MAY DIFFER AT OTHER LOCATIONS AND MAY CHANGE AT THIS LOCATION WITH TIME. DATA PRESENTED IS A SIMPLIFICATION.

- N- STANDARD PENETRATION TEST
- R- RING SAMPLE
- C- CORE: %RECOVERY/%RQD
- B- BAG
- BN- BULL NOSE

NOTES: Water encountered at approximately 22.5 feet.
 Elevation not available.

DRIVING WEIGHT (LBS) 140



WESTERN TECHNOLOGIES INC.

PROJECT NO. 4125JD093

PROJECT:

PALMS PLACE
BORING LOG

PLATE

A-7

DATE DRILLED: 8-4-05		BORING NO. 1 (Cont'd)		ELEVATION: Not measured				
LOCATION: Palms Hotel & Casino								
MOISTURE CONTENT (% OF DRY WT)	DRY DENSITY (LBS/CU FT)	SAMPLE TYPE	SAMPLE BLOWS/FT.	DEPTH (FEET)	USCS GRAPHIC	SOIL DESCRIPTION	MOISTURE	CONSISTENCY
19.4	109	R	50/0'			CALICHE-brown	moist	very hard
				91	CL	CLAY-w/gravel, reddish		very stiff
				92				
				93				
				94				
				95				
				96				
				97				
				98				
				99				
		R	50/0'			CALICHE-brown		very hard
				100	CL	CLAY-w/gravel		
				101				
				102		CALICHE		
				103				
				104				

THIS SUMMARY APPLIES ONLY AT THIS LOCATION AND AT THE TIME OF LOGGING. CONDITIONS MAY DIFFER AT OTHER LOCATIONS AND MAY CHANGE AT THIS LOCATION WITH TIME. DATA PRESENTED IS A SIMPLIFICATION.

N- STANDARD PENETRATION TEST
R- RING SAMPLE
C- CORE: %RECOVERY/%RQD
B- BAG
BN- BULL NOSE

NOTES: Water encountered at approximately 22.5 feet.
Elevation not available.

DRIVING WEIGHT (LBS) 140



WESTERN TECHNOLOGIES INC.

PROJECT NO. 4125JD093

PROJECT:

PALMS PLACE
BORING LOG

PLATE

A-9

DATE DRILLED: 8-4-05 **BORING NO. 1** (Cont'd) ELEVATION: Not measured
 LOCATION: Palms Hotel & Casino

MOISTURE CONTENT (% OF DRY WT)	DRY DENSITY (LBS/CU FT)	SAMPLE TYPE	SAMPLE BLOWS/FT	DEPTH (FEET)	USCS	GRAPHIC	SOIL DESCRIPTION	MOISTURE	CONSISTENCY
21.7	105	R	50/0'				CALICHE-brown	moist	very hard
				106					
				107	SC		CLAYEY SAND-w/gravel, brown		med. dense
				108					
				109					
		R	16	110					
				111			Bottom at 111 feet.		
				112					
				113					
				114					
				115					
				116					
				117					
				118					
				119					

THIS SUMMARY APPLIES ONLY AT THIS LOCATION AND AT THE TIME OF LOGGING. CONDITIONS MAY DIFFER AT OTHER LOCATIONS AND MAY CHANGE AT THIS LOCATION WITH TIME. DATA PRESENTED IS A SIMPLIFICATION.

N- STANDARD PENETRATION TEST
 R- RING SAMPLE
 C- CORE: %RECOVERY/%RQD
 B- BAG
 BN- BULL NOSE

NOTES: Water encountered at approximately 22.5 feet. Elevation not available.

DRIVING WEIGHT (LBS) 140



PROJECT NO. 4125JD093

PROJECT: PALMS PLACE
BORING LOG

PLATE
A-10

APPENDIX D

Table D- 1: Summary of Database Osterberg Load Test

No.	Project Name	Caliche Depth (ft.)	Caliche Thickness (ft.)	Shaft Diameter (in.)	Shaft Length (ft.)	O-cell Depth (ft.)	Top of The Shaft (ft.)	Maximum O-cell Load (kips)
1	Encore	18	3	48	106	50	20	6748
		24	10					
		39	3					
		47	6					
2	Westgate Tower	21	15	48	105	35	5	3964
		42	6					
		53	3					
		61	8					
3	City Center (1)	77	8	48	117	60	5	4722
		11	8					
		33	3					
4	City Center (2)	44	7	48	112	60	9	4287
		14	6					
		54	2					
5	Mandalay Bay	66	1	48	97	39	14	7086
		13	7					
		31	4					
		71	4					

6	Turnberry	23	7	42	105	39	24	3070
		34	5					
		56	3					
7,8	Dessert Inn-2 Tests	7	3	48	128	43	0	5476
		12	2					
		16	2					
		40	5					
		93	3					
9, 10	Venetian- 2 Tests	8	1	48	122	80 and 120	45	3077
		11	1					
		13	4					
		21	1					
		29	1					
11	Echelon (1)	30	10	36	100	55	30	1959
		55	8					
12	Echelon (2)	29	7	48	100	50	40	3544
		55	4					
		66	7					
		90	3					
		123	4					
146	4							
13	Echelon (3)	12	6	48	99	45	30	3684
		26	8					
		51	4					
		126	4					

14	Echelon (4)	12	6	48	99	45	30	5950
		26	8					
		51	4					
		126	4					
15	Fountain Bleau (1)	8	1	48	123	78	12	6164
		40	1					
		43	2					
16	Fountain Bleau (2)	36	51	48	123	65	10	6172
		51	1					
		60	2					
17	Palm	23	18	42	100	40	10	6128
		50	5					
		68	9					
18	P-1	10	1	48	62	57	8	3068
		13	1					
		52	4					
		65	4					
19	I-215/Airport Connector	13	9	48	103	80	19	3316
		30	6					
		60	2					
		69	1					
20	Trump	18	16	42	90	35	10	7358
		36	16					
		92	4					
21	Cendent	6	14	42	74	30	15	6400
22	Panorama III (1)	--	--	48	96	80	15	4800

23	Panorama III (2)	--	--	48	100	54	14	7202
24	P-2	4	5	48	80	42	8	2901
25	P-3	6	1	48	90	50	0	4098
		16	1					
26	P-4	--	--	36	79	41	1	1399 Tons
27	P-5	6	6	42	70	35	10	4088
		27	3					
		45	4					
28	P-6	--	--	42	73	27	4	4914
29	P-8	14	2	45	104	40	10	6365
		17	2					
		25	2					
		28	1					
		31	2					
		50	1					
		70	1					
30	P-9	19	2	42	90	50	15	2978
		35	3					
		55	7					

REFERENCE

- ACI Committee, American Concrete Institute, & International Organization for Standardization. (2008). Building code requirements for structural concrete (ACI 318-08) and commentary. Paper presented at the
- ARGEMA. (1992). In Tirant P. L. (Ed.), *Design guides for offshore structures: Offshore pile design*. Paris, France.: Association de Rechercheen Geotechnique Marine,.
- Barton, N. (1978). Suggested methods for the quantitative description of discontinuities in rock masses. *International Journal of Rock Mechanics and Mining Sciences*, 15(6), 319-368.
- Bieniawski, Z. (1978). Determining rock mass deformability: Experience from case histories. Paper presented at the *International Journal of Rock Mechanics and Mining Sciences & Geomechanics Abstracts*, , 15(5) 237-247.
- Bishnoi, B. (1968). *Bearing Capacity of a Closely Jointed Rock*,
- Blake, W. P. (1901). *The caliche of southern arizona: An example of deposition by the vadose circulation*
- Bolton, M. (1986). The strength and dilatancy of sands. *Geotechnique*, 36(1), 65-78.
- Bowles, J. E. (1988). *Foundation analysis and design*
- Briaud, J. (2001). Introduction to soil moduli. *Geotechnical News*, 19(2), 54-58.
- Brown, D. A., Turner, J. P., & Castelli, R. J. (2010). *Drilled shafts: Construction procedures and LRFD design methods* US Department of Transportation, Federal Highway Administration.
- Caltrans. (1998). Benicia-martinez bridge retrofit. Retrieved from <http://www.dot.ca.gov/hq/esc/tollbridge/Ben-Mar/0440U4/Photos/0440U4ProjectPhotos01.html>
- Canadian Geotechnical Society.,. (1985). *Canadian foundation engineering manual*. Vancouver: The Society.
- Carter, J., & Kulhawy, F. H. (1988). *Analysis and design of drilled shaft foundations socketed into rock* The Institute.
- Cibor, J. M. (1983). Geotechnical considerations of las vegas valley. Paper presented at the *Geological Environmental and Soil Properties*, 351-373.
- Coates, D. F. (1966). Rock mechanics principles. *Geoscience Abstracts*,

- Crapps, D., & Schmertmann, J. (2002). Compression top load reaching shaft bottom-theory versus tests. *Geotechnical Special Publication, 2*, 1533-1549.
- Deere, D. U., & Deere, D. W. (1989). *Rock Quality Designation (RQD) After Twenty Years.*,
- England, M. (1993). A method of analysis of stress induced displacement in soils with respect to time. *Deep Foundations on Bored and Auger Piles, BAPII Ghent, AA Balkema June*, , p241-246.
- Fellenius, B. H., Altaee, A., Kulesza, R., & Hayes, J. (1999). O-cell testing and FE analysis of 28-m-deep barrette in manila, philippines. *Journal of Geotechnical and Geoenvironmental Engineering, 125*(7), 566-575.
- Fleming, W. (1992). A new method for single pile settlement prediction and analysis. *Geotechnique, 42*(3), 411-425.
- Frye, J. C., & Leonard, A. B. (1967). Buried soils, fossil mollusks, and late cenozoic paleoenvironments. *Essays in Paleontology and Stratigraphy: Kansas Univ.Dept.Geol.Spec.Pub, 2*, 429-444.
- Hassan, K. M. (1994). *Analysis and Design of Drilled Shafts Socketed into Soft Rock*,
- Horvath, R. G., & Kenney, T. C. (1979). Shaft resistance of rock-socketed drilled piers. Paper presented at the *Symposium on Deep Foundations*, 182-214.
- Horvath, R. G., & University of Toronto. Dept. of Civil Engineering. (1978). *Field load test data on concrete-to-rock bond strength for drilled pier foundations* Department of Civil Engineering, University of Toronto.
- Hossain, S., Omelchenko, V., & Haque, M. A. (2007). Capacity of rock socketed drilled shafts in mid-atlantic region. Paper presented at the *Contemporary Issues in Deep Foundations*, 1-10.
- Kézdi, Á. (1980). *Handbook of soil mechanics. vol. 2. soil testing*. Elsevier Scientific Publishing Company.
- Kim, H., & Mission, J. L. C. (2010). Improved evaluation of equivalent top-down load-displacement curve from a bottom-up pile load test. *Journal of Geotechnical and Geoenvironmental Engineering, 137*(6), 568-578.
- Kleinfelder, I. (1996). *I-15/US 95 load test program*. (No. Project No. 31-215903-07A). Clark County, Las Vegas, Nevada.:
- Kleinfelder, I. (2001). *Geotechnical investigation, proposed desert inn hotel and casino*. (No. Project No. 31-34050). Clark County, Las Vegas, Nevada.:
- Kulhawy, F., & Carter, J. (1992a). Settlement and bearing capacity of foundations on rock masses and socketed foundations in rock masses. *Engineering in Rock Masses.Oxford, UK: Butterworth-Heinemann*, , 231-245.

- Kulhawy, F., & Carter, J. (1992b). Socketed foundations in rock masses. *Engineering in Rock Masses*, , 509-529.
- Kulhawy, F. H., & Goodman, R. E. (1980). Design of foundations on discontinuous rock. Paper presented at the *International Conference on Structural Foundations on Rock, 1980, Sydney, Australia*, , 1
- Kulhawy, F. H., & Phoon, K. (1993). Drilled shaft side resistance in clay soil to rock. Paper presented at the *Design and Performance of Deep Foundations@ sPiles and Piers in Soil and Soft Rock*, 172-183.
- Kulhawy, F. H., & Prakoso, W. A. (2007). Issues in evaluating capacity of rock socket foundations. *GEOTECHNICAL ENGINEERING*, 38(3), 169.
- Kulhawy, F. H., Prakoso, W. A., & Akbas, S. O. (2005). Evaluation of capacity of rock foundation sockets. Paper presented at the *Proceedings of the 40th United States Symposium on Rock Mechanics*,
- Kwon, O. S., Choi, Y., Kwon, O., & Kim, M. M. (2005). Comparison of the bidirectional load test with the top-down load test. *Transportation Research Record: Journal of the Transportation Research Board*, 1936(1), 108-116.
- Lattman, L. H. (1973). Calcium carbonate cementation of alluvial fans in southern nevada. *Geological Society of America Bulletin*, 84(9), 3013-3028.
- Lee, J., & Park, Y. (2008). Equivalent pile load-head settlement curve using a bi-directional pile load test. *Computers and Geotechnics*, 35(2), 124-133.
- Lee, W. T. (1905). *Underground waters of salt river valley, arizona* US Government Printing Office.
- LoadTest, I. (2007). *Report on drilled shaft load testing (osterberg method)
Echelon, las vegas, TS2*. (No. LT-9277-2). Las Vegas, NV: Terracon.
- Marion, G. M., Schlesinger, W., & Fonteyn, P. (1985). CALDEP: A regional model for soil CaCO₃ (caliche) deposition in southwestern deserts. *Soil Science*, 139(5), 468.
- McFadden, L. D., Wells, S. G., & Dohrenwend, J. C. (1986). Influences of quaternary climatic changes on processes of soil development on desert loess deposits of the cima volcanic field, california. *Catena*, 13(4), 361-389.
- McVay, M., Huang, S., & Casper, R. (1994). Numerical simulation of drilled shafts for osterberg, pullout, and axial compression loading in florida limestone. *Final Report, University of Florida*,
- McVay, M., Townsend, F., & Williams, R. (1992). Design of socketed drilled shafts in limestone. *Journal of Geotechnical Engineering*, 118(10), 1626-1637. doi:10.1061/(ASCE)0733-9410(1992)118:10(1626)

- Meigh, A., & Wolski, W. (1979). Design parameters for weak rocks. Paper presented at the *Proceedings of the 7th European Conference on Soil Mechanics and Foundation Engineering, Brighton*, , 5 59-79.
- Nam, M. S. (2004). *Improved Design for Drilled Shafts in Rock*,
- NAVFAC, D. M. (1982). Soil MechanicsU. S.Dep.Defence, *NAVFAC DM-7.1, Dep.Navy, Washington, DC* , 360.
- Obrzud, R. (2010). *The hardening soil model: A practical guidebook* Zace Services.
- O'Neil, M., & Reese, L. C. (1973). Behavior of bored piles in beaumont clay. *Journal of Geotechnical and Geoenvironmental Engineering*, 99(sm7)
- O'Neill, M. W., & Reese, L. C. (1999). Drilled shafts: Construction procedures and design methods.
- O'Neill, M., Townsend, F., Hassan, K., Buller, A., & Chan, P. (1996). *Load transfer for drilled shafts in intermediate geomaterials*. (No. FHWA-RD-95-172).Federal Highway Administration.
- Osterberg, J., & Pepper, S. (1984). A new simplified method for load testing drilled shafts. *Foundation Drilling*, 23(6), 9-11.
- Osterberg, J. O. (1998). The osterberg load test method for bored and driven piles: The first ten years. Paper presented at the *Proc., 7th Int. Conf. and Exhibition on Piling and Deep Foundations*, 1.28.
- Paikowsky, S. G. (2006). *Innovative load testing systems* Transportation Research Board of the National Academies.
- Pells, P., & Turner, R. (1980). Endbearing on rock with particular reference to sandstone. Paper presented at the *International Conference on Structural Foundations on Rock, 1980, Sydney, Australia*, , 1
- Pells, P., Rowe, R., & Turner, R. (1980). An experimental investigation into side shear for socketed piles in sandstone. Paper presented at the *Proceedings of the International Conference on Structural Foundations on Rock, Sydney*, , 1 291-302.
- Peng, L., Koon, A., Page, R., & Lee, C. (1999). Osterberg cell testing of piles. Paper presented at the *Proceedings of the International Conference on Rail Transit, Singapore, March*,
- PLAXIS, B. (2004). PLAXIS 2D version 8.2-finite element code for soil and rock analysis. *AA Balkema, Delft*,
- PRAT, M., BISCH, P., MILLARD, A., Mestat, P., & PIJAUDIER-CALOT, G. (1995). *La modélisation des ouvrages*

- Qudus, O., Osterberg, J., & Waxse, J. A. (2004). Drilled shaft value engineering delivers success to wahoo, nebraska bridge. Paper presented at the *GeoSupport 2004: Innovation and Cooperation in the Geo-Industry*,
- Reese, L. C., & O'Neill, M. W. (1988). *Drilled shafts: Construction procedures and design methods* Prepared for US Department of Transportation, Federal Highway Administration, Office of Implementation.
- Rodgers, A., Tkalcic, H., McCallen, D., Larsen, S., & Snelson, C. (2006). Site response in las vegas valley, nevada from NTS explosions and earthquake data. *Pure and Applied Geophysics*, 163(1), 55-80.
- Rosenberg, P., & Journeaux, N. L. (1976). Friction and end bearing tests on bedrock for high capacity socket design. *Canadian Geotechnical Journal*, 13(3), 324-333.
- Rowe, R., & Armitage, H. (1984). *The design of piles socketed into weak rock* Faculty of Engineering Science, University of Western Ontario.
- Rowe, R., & Armitage, H. (1987). A design method for drilled piers in soft rock. *Canadian Geotechnical Journal*, 24(1), 126-142.
- Russo, G., Recinto, B., Viggiani, C., & de Sanctis, L. (2003). A contribution to the analysis of osterberg's cell load test. Paper presented at the *Proceedings of 4th International Geotechnical Seminar on Deep Foundations on Bored and Auger Piles, Ghent, Belgium*, 331-338.
- Sabatini, P., Bachus, R., Mayne, P., Schneider, J. A., & Zettler, T. (2002). *Geotechnical Engineering Circular no.5: Evaluation of Soil and Rock Properties*,
- Schlesinger, W. H. (1985). The formation of caliche in soils of the mojave desert, california. *Geochimica Et Cosmochimica Acta*, 49(1), 57-66. doi:[http://dx.doi.org/10.1016/0016-7037\(85\)90191-7](http://dx.doi.org/10.1016/0016-7037(85)90191-7)
- Standard test methods for deep foundations under static axial compressive load. (2013). *American society for testing and materials, annual book of ASTM standards* (04.08th ed.,)
- Stone Jr, R. C. (2009). Analysis of a caliche stiffened pile foundation.
- Teng, W. C. (1962). FOUNDATION DESIGN..
- Terzaghi, K. (1996). *Soil mechanics in engineering practice* John Wiley & Sons.
- Theis, C. (1936). Possible effects of ground water on the ogallala formation of llano estacado [abs.]. *Washington Acad.Sci.Jour*, 26, 390-392.
- U.S. Army Corps of Engineers. (1990). *Engineering and design, SETTLEMENT ANALYSIS*. (No. Engineer Manual 1110-1-1904). Washington DC:

- Western Technologies, I. (1994). *Geotechnical exploration, fremont street experience*. (No. Project No. 4123JZ254). Las Vegas, Nevada.:
- Western Technologies, I. (2002). *Geotechnical evaluation, proposed le reve hotel & casino*. (No. Project No.4122JS038). Clark County, Nevada.:
- Williams, A., Johnston, I., & Donald, I. (1985). The design of socketed piles in weak rock. *Golden Jubilee of the International Society for Soil Mechanics and Foundation Engineering: Commemorative Volume*, , 247.
- Zhang, L. (1999). *Analysis and Design of Drilled Shafts in Rock*,
- Zuo, G., Drumm, E. C., Islam, M. Z., & Yang, M. Z. (2004). Numerical analysis of drilled shaft O-cell testing in mica schist. *Geotechnical Special Publication*, , 778-789.

CURRICULUM VITAE

Rouzbeh Afsharhasani
afsharha@unlv.nevada.edu

Education	Ph.D. Degree in Geotechnical Engineering <i>University of Nevada at Las Vegas (UNLV), Las Vegas, NV</i> Analysis and design of drilled shafts in soil profiles containing cemented geomaterial.	2014
	M.S. Degree in Earthquake Engineering <i>Sharif University of Technology (SUT), Tehran, Iran</i> Analysis and design of active and passive control systems in steel structures	2011
	B.S. Degree in Civil Engineering <i>Iran University of Science and Technology (IUST), Tehran, Iran</i>	2009

Career History & Accomplishments

Staff Professional, KLEINFELDER, Las Vegas. 2014 (May-Aug)
Project: All-Net Arena, Las Vegas Arena, Boulder City Bypass, Copper Mountain Solar, UHS Medical Hospital, NV Energy Substation

Responsibilities:

- Geotechnical Exploration and Report including design of a 10 ft. Mat foundation, + 50 ft. Retaining Wall and Drilled Shafts in Caliche for All-Net Arena resort
- Drilled Pier Load testing (Two O-cell Tests) Test, interpretation and QC
- for drilled shafts, Las Vegas Arena, MGM
- Load testing (Lateral and Axial) for Copper Mountain Solar
- Boulder City bypass preconstruction analysis

Soil Special Inspector, NOVA Geotechnical and Inspection Services, Las Vegas. 2013 (May-Aug)

Project: Summerlin Shopping Center

Responsibilities:

- Inspection on cut and fill for infrastructure embedment trenches
- Inspection on pile installation and creating associated boring logs
- Worked directly under the project manager, helping with documentation and reports

Staff Engineer, Tajeer Consulting Engineers, Tehran, Iran.
Project: Tabriz Police Department Theater

2010-2011

Responsibilities:

- Seismic evaluation of theater structure
- Structural design team focusing on the stability of the joints during earthquake
- Foundation design

Licenses

- Early P.E. exam (State of Nevada)
- E.I.T (License number: 0T7034)
- Certified Item-R (Drilled Piers) in Clark County, Nevada
- Soil special inspector (License number: 8186696)
- OSHA 10 hour construction safety certificate

Computer Skills

- FEM: MIDAS GTS NX, PLAXIS 2D and 3D, ABAQUS
- Geotechnical: SLOPE/W, SETTLE 3D, LPILE, ALLPILE, T-Z PILE
- Structure and earthquake: PERFORM 3D, SAP 2000
- Programing: MATLAB, Visual Basic
- Drawing: Civil 3D Auto Cad
- Microsoft Office

Publications

- M. Karakouzian, R. Afsharhasani and B. Kluzniak, **Elastic Analysis and Design of Drilled Shaft Foundations in Soil Profiles with Intermediate Caliche Layers**, 2015, IFCEE 2015, San Antonio, TX
- B. Kluzniak, M. Karakouzian, R. Afsharhasani, **CASE HISTORY: DRILLED SHAFT FOUNDATION SYSTEM IN CEMENTED SOILS**, LAS VEGAS, NEVADA, 2014, Atlanta, GA
- R. Stone, M. Karakouzian, R. Afsharhasani, **THE STIFFENING EFFECT OF A CALICHE LAYER ON PILE FOUNDATIONS**, 2013, Phoenix, AZ
- R. Afsharhasani, M. Ahmadizadeh, **Design of Optimal Passive Energy Dissipation Systems Using Active Control Theory**, 2011, Tehran, Iran